University of Wisconsin-Madison

Space Science and Engineering Center

Algorithm Theoretical Basis Document for the Geostationary Imaging Fourier Transform Spectrometer (GIFTS) Level 0-1 Ground Data Processing

Version 1.0 – August 2006

Corresponding author:

Robert Knuteson

1225 Dayton St.

Madison, WI 53706

robert.knuteson@ssec.wisc.edu

History of Revisions

Version 1.0: Prepared for August 9, 2006 GOES-R Risk Reduction Review

Technical editor—Jennifer O'Leary, UW-SSEC

1 Introduction

The Geostationary Imaging Fourier Transform Spectrometer (GIFTS) represents a revolutionary step in remote sensing of Earth's atmosphere that will demonstrate the technology and measurement concepts for future geostationary operational environmental satellites (GOES). As a technology demonstration for the Earth Observatory-3 (EO-3), NASA collaborated with several universities and industry leaders to create an engineering development unit (EDU) of the GIFTS sensor. The EDU was built and tested at Utah State University's Space Dynamics Laboratory (USU SDL) under management at NASA's Langley Research Center (LaRC). The University of Wisconsin-Madison's Space Science and Engineering Center (UW-SSEC) has contributed to this effort in three important ways:

1) UW-SSEC engineers designed, fabricated, and delivered the onboard precision calibration references for the GIFTS EDU;

2) UW-SSEC scientists are supporting NASA LaRC in the review of test results from the GIFTS EDU;

3) and UW-SSEC scientists and computer programmers are supporting NOAA in the creation of a software "pipeline" for the efficient and accurate ground data processing of the GIFTS data.

This document describes the theoretical basis of the algorithms that have been developed and are being implemented for ground processing of GIFTS data, both from Earth viewing simulations of GIFTS observations in orbit and from real data collected during the thermal vacuum testing of the GIFTS EDU. This work has been supported by NOAA to reduce the risk associated with the development of the next generation of GOES satellites. As risk reduction, this effort has been very successful in leading to the design and implementation of algorithms that take advantage of new computing technologies and can accommodate the large data volumes associated with these advanced instruments.

1.1 Purpose

This Algorithm Theoretical Basis Document (ATBD) describes the algorithms used to convert the raw interferogram measurements of the GIFTS sensor to calibrated and Earth geo-located radiances. This document will describe the inputs, pre-processing steps, processing algorithm descriptions, post-processing steps, and output along with practical considerations for the implementation. The purpose of this document is to provide a complete description and sufficient examples to allow software developers to implement the algorithms in one or more target environments. The original intent of the GIFTS program was to proceed from ground testing to an on-orbit demonstration of limited duration (e.g. 18 months). In that case, the UW-SSEC would

have provided the ground processing software of the data as part of the NOAA ground segment. The original intent of this approach has been maintained in the current software design by requiring the algorithm implementation to work with both the GIFTS EDU pre-launch test data and with simulated on-orbit data derived from models of the Earth's atmospheric radiation and a conceptual model of the sensor design.

1.2 Scope

This document describes the algorithms developed at UW-SSEC for ground data processing of 1) actual GIFTS data collected in pre-launch thermal vacuum testing of the EDU, and 2) synthetic GIFTS top of atmosphere (TOA) observations. The GIFTS Instrument Requirements Document (GIRD) contains a description of the relevant measurement requirements for the GIFTS system that the processing algorithms are designed to meet. The input to the algorithms described in this ATBD is assumed to be in the form of numerically-filtered interferograms of scene and calibration references. The output is a geo-located radiance that can be used in subsequent processing steps, including level 2 product generation. Details of the implementation design can be found in software design documentation and are outside the scope of this ATBD. The description of the algorithms that convert the level 1 measurements to geophysical units of temperature, water vapor, and winds are covered in the sounding and winds ATBDs.

1.3 Related Documents

Reference to GIFTS documents within this ATBD will be indicated by an italicized number in brackets, e.g., *[G-#]*.

[G-1] GIFTS-IOMI Mission System Requirements Document, v1.1, (13 March 2001)

[G-2] Measurement Concept Validation Plan (MCVP)

[G-3] GIFTS Instrument Requirements Document (GIRD)

[G-4] GIFTS Level 0-1 ATBD (this document)

[G-5] GIFTS/HES Sounding ATBD

[G-6] GIFTS/HES Winds ATBD

1.4 Definitions

AERI	Atmosphere Emitted Radiance Interferometer
AIRS	Atmospheric Infrared Sounder
ATBD	Algorithm Theoretical Basis Document
CIMSS	Cooperative Institute of Meteorological Satellite Studies
CONUS	Continental United States
EDU	Engineering Development Unit
EO-3	Earth Observing 3
FFT	Fast Fourier Transform
FPA	Focal Plane Array
FTIR	Infrared Fourier Transform Spectrometer
FTS	Fourier Transform Spectrometer
GIFTS	Geostationary Imaging Fourier Transform Spectrometer
GIRD	GIFTS Instrument Requirements Document
GOES	Geostationary Operational Environmental Satellite
HES	Hyperspectral Environmental Suite
IHOP	International H_2O Project
IOMI	Indian Ocean METOC Imager
KWAJEX	Kwajalein Experiment
LFPA	Large area format Focal Plane detector Array
McIDAS	Man-computer Interactive Data Access System
MCVP	Measurement Concept Validation Plan
NAST-I	NPOESS Airborne Sounder Testbed-Interferometer
NIST	National Institute for Standards and Technology
NMP	New Millennium Program

NPOESS	National Polar-orbiting Operational Environmental Satellite System
PCA	Principal Component Analysis
PLOD	Pressure Layer Optical Depth
SRF	Spectral Response Function
S-HIS	Scanning High-resolution Interferometer Sounder
UW-SSEC	Space Science and Engineering Center
TOA	Top of Atmosphere
USU SDL	Utah State University's Space Dynamics Laboratory
WRF	Weather and Research Forecast Model

2 Requirements and Background

This section contains a review of the higher level requirements that impact the design of the ground data processing algorithms, a summary of the GIFTS instrument measurement characteristics, and context information to provide a historical perspective for this sensor and algorithm development.

2.1 Requirements

The GIFTS ground data processing requirements are derived from the NASA-controlled GIFTS-IOMI Mission Systems Requirement Document and the GIFTS Instrument Requirements Document (GIRD). These documents contain requirements for instrument temporal, spatial, and spectral sampling that imply data rates and data volumes. The data rates and volumes determine requirements for the ground segment bandwidth, processing rates and storage capacity. With respect to ground data processing algorithms, the GIRD requirements on overall measurement accuracy and measurement approach are also relevant. As shown in Figure 1, the requirements in the GIRD for radiometric and spectral calibration serve to emphasize the overall need for measurement accuracy. The implied requirement on the ground data processing is to ensure that the output radiance product satisfies the overall measurement needs by appropriate use of the sensor observations. The block diagram in Figure 1 shows the top level GIFTS calibration error budget broken into two main contributions: radiometric and spectral calibration. Each box in these charts contains three pieces of information: the requirement (either from the GIRD or an equivalent implication), the budget allocation for that item, and the engineering current best estimate for that item. For example, the radiometric calibration requirement (labeled 1.1 in Figure 1) has a requirement of < 1K, a budget allocation of < 0.9 K, and an engineering best estimate of < 0.73K (LW) and < 0.54K (SMW). The engineering best estimate for the radiometric calibration requirement flows up from the lower level contributions shown in Figure 2. This example deals with the calibration budget contribution from uncertainties in the blackbodies as shown in the box labeled 1.1.1 in Figure 2. The blackbody calibration contribution budget allocation is < 0.5K and the engineering best estimates are <0.35K (LW) and <0.20K (SMW). The uncertainty estimates of the UW-SSEC blackbodies are described in much greater detail in Best et al. (2004; see Appendix 2). The uncertainty estimates in the calibrated radiance are obtained through a perturbation analysis of Equation 1 where the uncertainties of the blackbody emissivity and temperature are taken into account.

Eq. 1

$$N = \left(\frac{\tau_m}{\tau_t}\right)(B_H - B_C)Re\left(\frac{C_E - C_S}{C_H - C_C}\right) + B_S$$

The radiance (N) is derived from raw spectra of Earth (C_E), space (C_S), and the internal hot (C_H) and cold (C_C) blackbodies where B_i is the predicted radiance from the hot, cold, and space references. This term includes the effective emissivity of the blackbody cavity and the energy reflected off the blackbody from the environment.

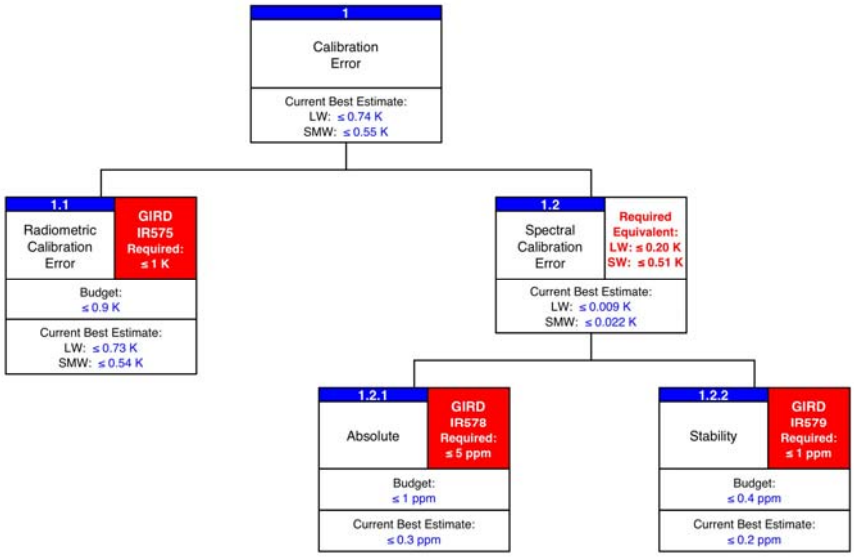

Figure 1: GIFTS top-level absolute calibration budget stating the radiometric and spectral requirements, the error budget allocation, and the current engineering best estimates.

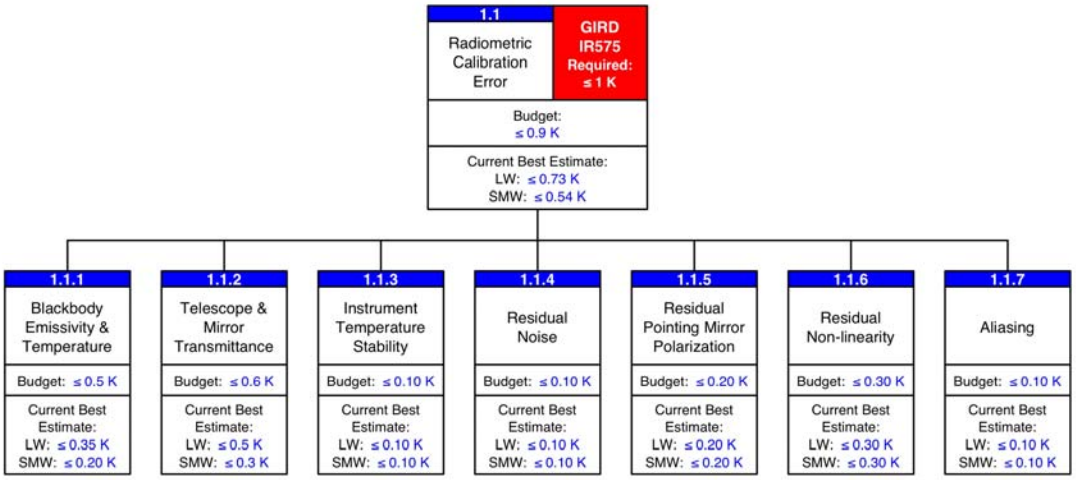

Figure 2: GIFTS radiometric calibration budget. The engineering estimates of the individual error contributors are combined (RSS) to obtain the total 3-sigma calibration error estimate.

The contribution to the total calibration budget caused by spectral calibration uncertainties is given in Figure 3. The requirement for absolute calibration is < 5 parts per million (ppm). Since we believe this requirement is too loose, we have assigned an error budget of < 1 ppm and have made an engineering best estimate on the absolute knowledge that is better than 0.3 ppm. The contributions to this absolute error estimate have been identified as coming mainly from the on-orbit determination using the positions of known atmospheric absorption lines such as that for carbon dioxide.

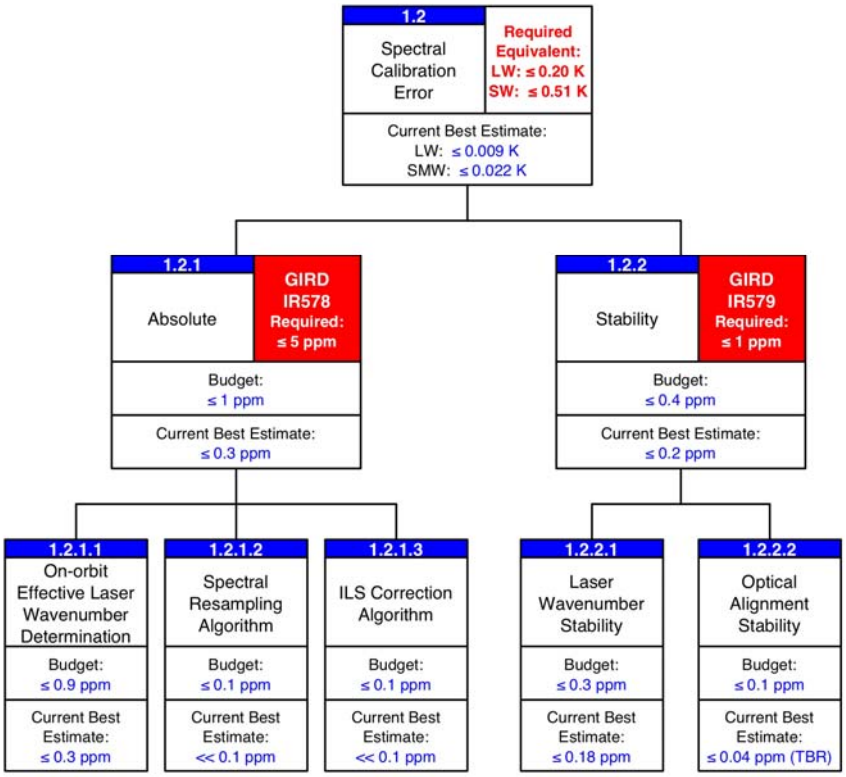

Figure 3: GIFTS spectral calibration budget and engineering best estimates. The spectral error budget is much tighter than the requirement in order to prevent errors in spectral knowledge from providing a significant contribution to the total calibration error budget. This is possible since the GIFTS makes use of a stable on-board laser combined with the FTS design which makes determination of the absolute spectral knowledge possible during flight using atmospheric absorption lines as a spectral reference. This approach has been demonstrated with UW-SSEC's Scanning-HIS aircraft instrument.

2.2 Instrument and Measurement Characteristics

The GIFTS instrument consists of large area format focal plane detector arrays (128 x 128) within a Fourier Transform Spectrometer (FTS) mounted on a geostationary satellite. (Dittberner et al. 2003; Gurka et al. 2003) The instrument provides observations of Earth infrared radiance spectra at high spectral resolution (as great as 0.6 cm $^{-1}$) and high spatial resolution (4-km x 4-km pixel). Depending on spectral resolution, GIFTS views a large area (512-km x 512-km) of the Earth within a 1 – 11 second time interval. Extended Earth coverage is achieved by step-scanning the instrument field of view in a contiguous fashion across any desired portion of the visible Earth. A visible camera provides daytime imaging of clouds at 1-km spatial resolution. Figure 4 shows a selection of GIFTS measurement modes.

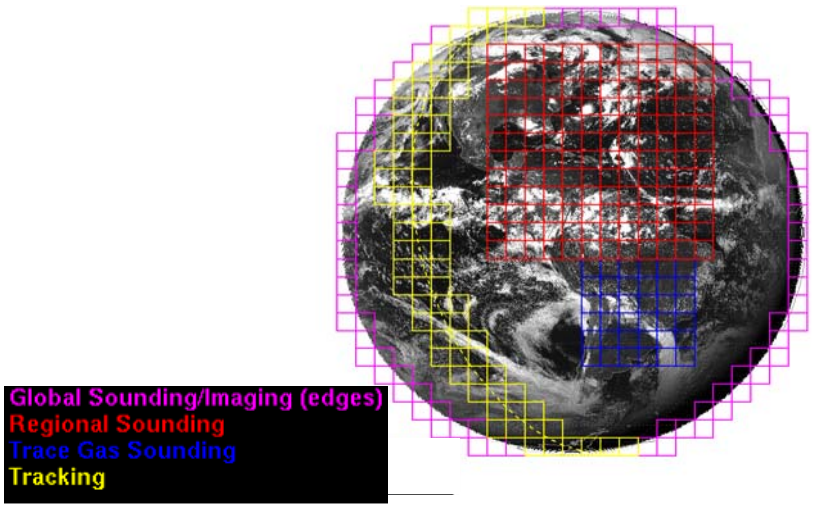

Figure 4: A selection of GIFTS measurement modes. Each box represents the 128 × 128 Large area format Focal Plane detector Array (LFPA).

The GIFTS uses two detector arrays to cover the spectral bands 685 to 1130 cm $^{-1}$ and 1650 to 2250 cm $^{-1}$, as shown in Figure 5, and a Michelson interferometer to obtain the spectrum of radiance within these bands. The spectral resolution of the measurements is sufficient to resolve, with 1-2 km vertical resolution, dynamic features of the atmospheric temperature and moisture profiles. The geostationary platform enables the tracing of fine scale features of the atmospheric water (cloud and vapor) distribution to permit the derivation of altitude resolved wind profiles.

GIFTS was selected for flight demonstration on NASA's NMP Earth Observing 3 (EO-3) Satellite Mission. (At the time of this writing, a specific space mission for GIFTS has not been defined so its geographical position is yet to be determined.)

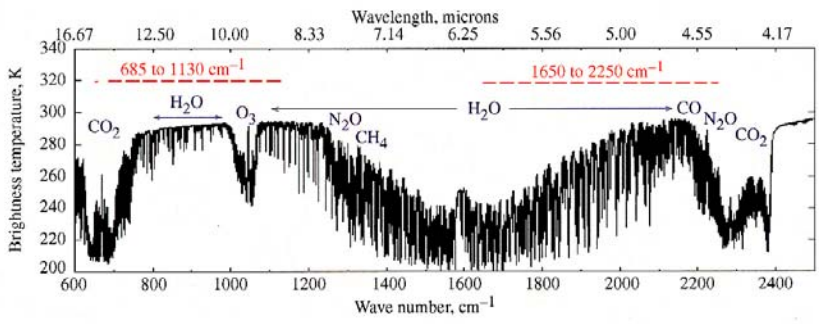

Figure 5: GIFTS spectral coverage with two detector arrays with spectral features of key radiatively active atmospheric trace gases.

Table 1 lists the area coverage, measurement frequency, spectral resolution, and geophysical measurement for example modes of operation for GIFTS. Quasi-continuous imagery of localized areas and minute-interval imagery of large-scale areas can be achieved. Full disk sounding coverage will be obtained within an hour at moderately high spectral resolutions (e.g., 1.2 cm^{-1}). Highest vertical resolution soundings and atmospheric chemistry measurements with GIFTS require 0.6 cm^{-1} spectral resolution and a longer stare time, thereby reducing the area coverage and/or frequency of observation relative to the imagery mode of operation.

Mode	**Resolution**		**Coverage**	
	Spectral	OPD	Area	Time*
Stare Mode	0.3–36cm^{-1}	0.014–1.744 cm	512 km	<1–11 sec
Regional Imaging	36 cm^{-1}	0.014 cm	6,000 km	3 min
Global Sounding	1.2 cm^{-1}	0.4 cm	10,000 km	< 1 hr
Regional Sounding and Chemistry	0.6 cm^{-1}	0.872 km	6000 km	< 20 min
***Assumes a constant data rate associated with Michelson mirror scan velocity of 0.145 cm/sec and 1 sec telescope pointing step time.**				

Table 1: Five example GIFTS operating modes

Nevertheless, GIFTS will cover a major portion of the visible disk with high vertical resolution soundings in less than 30 minutes. This feature is important for obtaining wind profiles from geostationary temperature and moisture sounding data. As part of UW's algorithm development, simulations of expected top of atmosphere (TOA) radiances are being used for algorithm development. An example simulation over the Earth disk is shown in Figure 6 below. A description of the simulation approach is included as an appendix. (Olson et al. 2004)

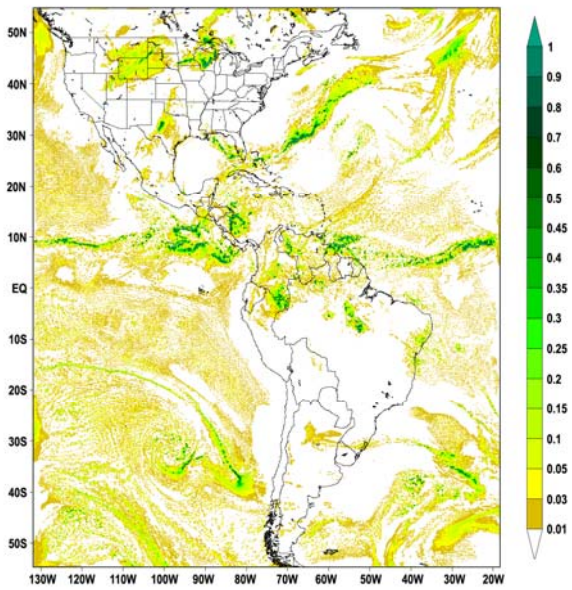

Figure 6: UW-CIMSS WRF simulation at 1400 UTC on 24 June 2003.

Since the design of the GIFTS Michelson interferometer provides a choice between spectral resolution and greater area coverage or higher temporal resolution, the instrument can obtain radiance data in up to ~6000 spectral channels plus a visible channel. By way of comparison, the current Geostationary Operational Environmental Satellite (GOES) sounder measures a total of 19 thermal bands and one visible light band. The GIFTS LW window region, from 850 to 950 cm^{-1}, contains temperature sounding channels and window channels for surface temperature and emissivity determination. The GIFTS shortwave band, from 1650 to 2250 cm^{-1}, includes the shortwave half of the 6.3 μm water vapor band and will be used for water vapor profile retrievals. This choice of spectral characteristics achieves all technological and scientific validation objectives of GIFTS as well as the sounding accuracy desired for a future operational sounding system.

The radiance spectra observed at each time step are transformed to high vertical resolution (1–2 km) temperature and water vapor mixing ratio profiles using rapid profile retrieval algorithms. These profiles are obtained on a 4-km resolution grid and then converted to relative humidity profiles. Images of the horizontal distribution of relative humidity for each atmospheric level, vertically separated by approximately 2 km, are constructed for each spatial scan. The sampling period will range from minutes to an hour, depending upon the spectral resolution and the area coverage selected for the measurement. Successive images of clouds and the relative humidity for each atmospheric level can be animated to reveal the motion of small-scale features, providing an estimate of the wind

velocity distribution as a function of altitude. The net result is a dense grid of temperature, moisture, and wind profiles that can be used for atmospheric analyses and operational weather prediction. Feature tracking can be performed for mixing ratio profiles of ozone and carbon monoxide, derived from their spectral radiance features observed by the GIFTS instrument, providing a direct measure of the transport of these pollutant and greenhouse gases.

2.3 Background

The U.S. National Oceanic and Atmospheric Administration (NOAA) operates GOES satellites for short-range warnings and nowcasting, and polar-orbiting environmental satellites (POES) for longer-term forecasting. GOES satellites continuously monitor the Earth from space in a geosynchronous orbit about 3,800 km (22,300 miles) above the Earth. A new generation of sensors is under development that will greatly increase the horizontal, vertical, and temporal sampling of the GOES sounder and provide a truly four-dimensional view of the Earth's atmosphere. NOAA's plan for a Hyperspectral Environmental Suite (HES) calls for the replacement of the current GOES instrumentation starting as early as 2013 (Dittberner et al. 2003; Gurka et al. 2003). The GIFTS sensor will serve as a valuable testbed for the evaluation of approaches to flight hardware and ground data processing in the years leading up to NOAA's operation HES. GIFTS uses a 2-D array of detectors to increase area coverage rates while providing dramatically higher vertical resolution by measuring the thermal infrared upwelling emission spectrum at high spectral resolution. The sensor calibration uses two internal high precision blackbody references in addition to an external view to space. The GIFTS ground data processing algorithms used to convert from instrument values (Level 0 data) to geo-located, calibrated radiances (Level 1 data) are under development at UW-SSEC.

Historically, UW-SSEC has contributed to the use of satellite observations for meteorological applications. The center has placed an emphasis on measuring atmospheric winds by tracking radiance features caused by the motion of clouds and water vapor. The development of the spin-scan cloud camera in the early 1960s led to the first global images from geostationary orbit as shown in Figure 7. UW-SSEC also developed the science algorithms and software for the processing of this geostationary satellite data stream. Figure 8 shows two pioneers of satellite data processing Verner Suomi and Robert Parent. The animation of a time series of geostationary images was used to track the motion of atmospheric features. The Man-computer Interactive Data Access System (McIDAS) was developed at UW-SSEC in the 1970s and 1980s, and has been used ever since in operational data processing of GOES satellites by NOAA. The GIFTS and HES concept is the natural next step in the

increasingly sophisticated exploitation of weather observations from geostationary orbit by providing enhanced vertical resolution to complement the high spatial and temporal sampling.

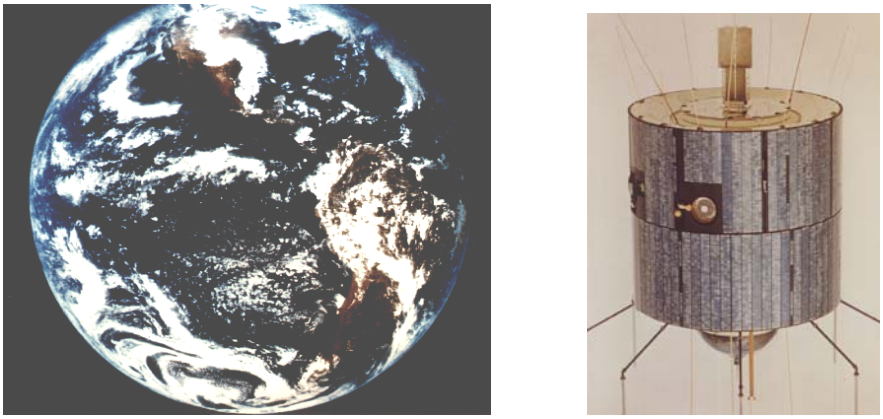

Figure 7: Full disk Earth (left) taken by ATS-3; ATS-3(right). The color full disk Earth image (left) shown was taken by ATS-3 (right) in 1966. Professor Verner Suomi's promotion of the use of geosynchronous orbit for tracking the motion of clouds to obtain wind information was captured in his famous phrase, "The clouds move, not the satellite!" The GIFTS and HES concept follows the natural technological progression toward this goal by allowing the time-dependent motion tracking of atmospheric constituents, e.g. water vapor, at many more atmospheric levels in the vertical than was previously possible.

Figure 8: Robert Parent (left) and Verner Suomi (right). UW-SSEC's involvement in the development of the hardware and software required to make images of the spin scan camera data lead to the development of McIDAS, which, after many generations, is still used extensively by NOAA in the processing of geostationary satellite imagery. Above, UW-Madison Professors Robert Parent (left) and Verner Suomi (right) are shown analyzing meteorological data using an early ground processing system (circa 1959).

UW-SSEC has also spearheaded the design and creation of absolute radiometric and spectral calibration for "warm" InfraRed Fourier Transform Spectrometers (FTIR). The accuracy and reproducibility of these calibration sources is sufficient to qualify these observations for use in atmospheric remote sensing applications (Revercomb 1988). The National Polar-orbiting

Operational Environmental Satellite System (NPOESS) program has adopted the principles of UW-SSEC's calibration sources for use with the NPOESS Cross-track Infrared Sounder. Even though GIFTS is a "cold" instrument, the same physical principles developed for UW-SSEC and NPOESS instruments will be applied to the calibration of the GIFTS radiances in order to take into account gain and offset changes in the instrument during normal operation. The GIFTS spectral coverage indicated in Figure 9 illustrates that the dynamic range of signals from terrestrial thermal infrared radiation spans hundreds of degrees. However, the demands of remote sensing of atmospheric effects are high since the signal of subtle changes in temperature and atmospheric humidity from the mean atmospheric state are only tenths of degrees (Smith, 2000). Achieving absolute calibration at the tenth of degree accuracy level is a goal that is within the reach of high spectral resolution IR remote sensing using precision on-board blackbody references with National Institute for Standards and Technology (NIST) traceability. This approach has been demonstrated at UW-SSEC in both the ground-based Atmospheric Emitted Radiance Interferometer (AERI) program and the aircraft-based High-resolution Interferometer Sounder (HIS) program (Knuteson, 2004a, b; Revercomb, 1988).

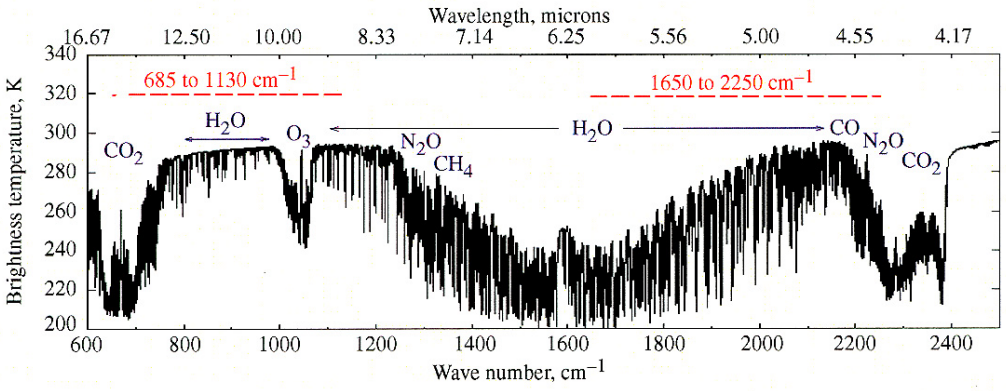

Figure 9: A calculation of the top of atmosphere radiance emitted by the standard atmosphere in units of equivalent brightness temperature (Kelvin). The dashed lines indicate the two spectral bands selected for the NASA GIFTS sensor. The longwave (LW) band covers the traditional "temperature sounding" region for the characterization of atmospheric temperature from the top of the atmosphere to the surface and includes the 8-12 μm IR window for the characterization of land surface and cloud top temperature and emissivity. The SWM band includes a non-traditional coverage of the shortwave side of the "6.3 μm water vapor sounding" region. The shortwave to midwave (SWM) band coverage (1650 to 2250cm^{-1}) was shown by analysis to be optimal for three reasons: 1) this region avoids the interference of "fixed" gases N_2O and CH_4 which degrade the water vapor sounding performance; 2) the shorter wavelength (fewer thermal photons) leads to better signal to noise performance for the detectors chosen; and 3) provides coverage of carbon monoxide thereby allowing the tracking of air pollution plumes from source to sink.

In both the AERI and HIS programs, FTIR spectrometers have been used in order to take advantage of the very high spectral frequency capabilities inherent in the FTS design. At the relatively high spectral resolutions (resolving power >1000) in the thermal infrared, the wavenumber sampling and instrument line shapes must be known to better than 1% accuracy or errors will be introduced in the comparison with forward model calculations that exceed the radiometric requirement. With an FTIR sensor, a single parameter determines the wavenumber sampling of each spectral band and all the spectral elements see the same field of view on the Earth. The FTS spectral parameter can be determined pre-launch but also in-flight by comparison to known spectral absorption lines across the spectral band of interest. In contrast, a grating spectrometer that uses individual detector elements at each spectral element requires extensive pre-launch testing to characterize the many individual unique spectral response function (SRF) shapes. Unfortunately the grating SRFs are impossible to confirm in-orbit to the desired accuracy. The excellent spectral knowledge and stability of the FTIR system was the primary motivation for the selection of FTS for the GIFTS sensor. The grating spectrometer implemented on the NASA Atmospheric InfraRed Sounder (AIRS) sensor has the further disadvantage that each detector has a slightly different field of view to the ground. This leads to spectral "artifacts" when viewing scenes that are not uniform temperature (over a 15 km region). This is illustrated in Figure 10 where spectral discontinuities are obvious in observations from the NASA AIRS grating spectrometer over tropical storm Isador, rendering the data effectively unusable near the eye of the storm. The GIFTS sensor avoids this problem by using a single detector to measure all the wavelengths of a spectral band simultaneously for each individual field of view to the Earth.

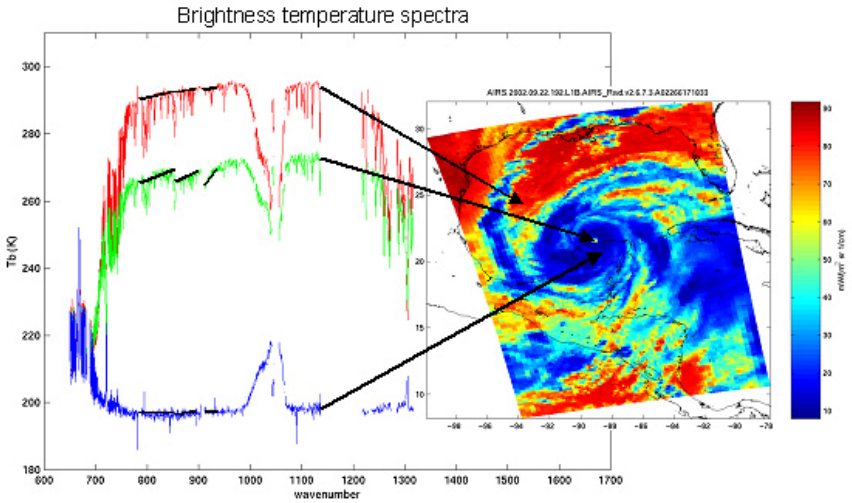

Figure 10: Brightness Temperature Spectra. Spectral artifacts in the 8-12 μm window region from a grating spectrometer are obvious from this observation from the NASA AIRS sensor on the Aqua platform. The AIRS observation that includes the eye of tropical storm Isadore (22 Sept 2002 @ ~19:12-

19:18 UTC) has large discontinuities (indicated by the black bars). This is not a physical atmospheric effect, rather it is caused by the fact that the thousands of individual AIRS detectors that record each spectral element have thousands of different fields of view to the Earth. This is a serious problem for the use of this data in scenes of mixed cloudiness. Notice that this spectral artifact disappears for fields of view that have little temperature contrast (either entirely warm or entirely cold). The FTIR design avoids this problem by using a single detector to record all the wavelengths in a spectral band simultaneously and an on-board metrology laser sampling system to provide a consistent wavenumber scale across each spectral band.

The ability to accurately calibrate high spectral resolution infrared observations is also important for the future of using observations from space-borne instruments to study global climate change (Goody & Haskins, 1998). The technology exists with precision blackbodies and FTS laser spectral sampling that approaches the tenth of a degree accuracy and stability. This level of accuracy and stability is desired for the detection of global climate change on decadal scales. Although this is outside the scope of the GIFTS sensor requirements, the GIFTS design shows the feasibility of high absolute accuracy in a practical implementation for sensors in geostationary orbit. The design makes use of two high precision cavity radiometers with high absolute emissivity (>0.998) and good long-term stability (diffuse paints). The cavity blackbodies used for GIFTS are built and calibrated at UW-SSEC based upon principles use in the AERI and HIS programs. The unique approach for GIFTS is to place these reference cavities aft of the Earth-viewing telescope with an "on-demand" flip in mirror to direct the IR emission from the blackbodies into the sensor. The successful design of these blackbodies for the GIFTS sensor is described in Best, et al. (2004; see Appendix Two). The high absolute accuracy of the onboard reference blackbodies compensates for the additional uncertainty from degradation of the telescope optics over time. A scheme for monitoring this telescope degradation that makes use of the internal reference views and views to deep space has been devised for the GIFTS sensor by SDL (Elwell et al., 2003). The main advantage of this approach is that the IR beam is much smaller beyond the telescope so a true high emissivity cavity design can be used for the blackbodies while keeping the volume, weight, and power requirements to a minimum. The GIFTS concept demonstrates how new technology developed by NASA can be combined with proven measurement concepts to provide a dramatic improvement in the ability to make the meteorological measurements needed for weather and climate in the future.

3 Algorithm Description

The input to the algorithm described in this document is assumed to be in the form of numerically filtered interferograms of scene and calibration references from the GIFTS sensor. The algorithms used in the data processing apply corrections for readout nonlinearity, a radiometric calibration using three references sources, spectral calibration and instrument line shape modification, and a spectral resampling to put the data on a common wavenumber scale. The output is a geo-located radiance which can be used in subsequent processing steps, including level 2 product production.

3.1 Input

3.1.1 Simulated Data

This section describes a simulation based on the specifications of the existing NASA GIFTS instrument. The 24-hour simulation of the full Earth disk is based upon a Weather Research and Forecasting (WRF) model run at 8 km resolution centered over the Western Hemisphere to provide internally consistent atmospheric profiles over a potential geostationary imaging area. The GIFTS forward radiative transfer model has been used to calculate the outgoing radiance spectra at the top of the atmosphere. Finally, a detailed mathematical model of the instrument is used to represent the resulting raw signal sent down from the satellite. Views of internal reference sources at hot and cold temperature and views of deep space are also simulated. The FullDisk simulation is stored in netCDF file format as multiple data cubes of signal interferograms and simulated noise. These data files are being used as input to the ground data processing software for algorithm development and testing. See Appendix Three for a full description of this simulation data.

3.1.2 Thermal Vacuum Measurements

Data files collected during the GIFTS thermal vacuum testing at USU SDL have been used as input to the GIFTS ground processing algorithms. These data files were created from the raw GIFTS data using a “spooler” at USU SDL that combines several data streams into a single Hierarchical Data Format file. The key elements of the data file are: the observed interferograms

after numerical filtering has been applied, the time of the observation and pixel element number, and the coincident measurements of the raw counts from the temperature sensors for the on-board reference (and space view) targets. Measurements have been made in all resolution modes with correspondingly variable sample times. Data from Cold Test 3 (Option period 2) is the primary input source for this ATBD description.

3.2 Preprocessing

3.2.1 Simulated Data

The simulated TOA radiances described in a previous section and the third appendix are converted into synthetic GIFTS interferograms prior to input into the ground processing algorithm. This pre-processing step is performed off-line due to the complex nature of the computations. The model used to create the GIFTS synthetic interferograms is described the third appendix. For the purposes of this description, we note that nonlinearity was not included in the simulation of GIFTS due to lack of information on instrument characteristics at the time the simulation was created. The effects of nonlinearity can be added to a later simulation study if this is desired. No other pre-processing steps are required beyond reading the data from the network common data format files containing the GIFTS synthetic interferograms.

3.2.2 Thermal Vacuum Measurements

The thermal vacuum test data acquired by SDL has all the characteristics (good and bad) of the real observations. Some of the bad characteristics (e.g. spikes in the interferograms, excessive noise in selected pixels, and phase anomalies) need to be detected in a preprocessing step to guard against the introduction of data values that would cause software applications to crash. For the use of the thermal vacuum test data collected in 2006 at USU SDL there is one particular correction that must be applied prior to application of the ground processing algorithms described below. This is a phase ambiguity resolution algorithm, which accounts for the fact that a numerical filter has been applied to the GIFTS interferograms. The filter keeps track of “fringe counting” from one interferogram to the next. This leads to a linear phase rotation of each interferogram relative to the next by a discrete integer value in phase (2 pi / n).

3.3 Nonlinearity Correction

3.3.1 Theory

The detectors used for the GIFTS instrument are photo-voltaic HgCdTe focal plane arrays (FPAs). The detector material is believed to be highly linear in its response to incident radiation. However, the FPA readouts do exhibit nonlinear characteristics for the range of voltages needed in the GIFTS application. UW-SSEC has developed a correction formula that uses a physical model for the known quadratic and cubic dependencies of the non-linearity of photo-conductive HgCdTe detectors. We intend to apply this approach also for the correction of nonlinearity of the GIFTS sensor data. Only the quadratic non-linearity term is described here explicitly, but the cubic and higher order terms follow in a straightforward manner from a Taylor expansion. The signal at the detector is modeled as the measured interferogram plus a DC level offset from zero. The corrected complex spectra for Earth, hot, cold, and space scenes is given by the equation

Eq. 2

$$C_{corr} = C_m + a_2 FT\left\{\left(I_m + V_m\right)^2\right\}$$
$$C_{corr} = C_m(1 + 2a_2 V_m) + a_2 FT\left\{\left(I_m\right)^2\right\}$$

where I_m is the measured interferogram, C_m is the Fourier transform of the measured interferogram, V_m is the modeled DC offset, and a_2 is the quadratic non-linearity coefficient. The symbol FT{} represents the Fourier transform of the argument. Note that the dominant correction term is proportional to the measured complex spectrum itself because the squared interferogram has only a small in-band contribution. However if a cubic contribution is required it also has an in-band contribution. Since the DC level is measured directly in the GIFTS instrument, the DC contribution is simply added to that of the interferogram to reconstruct the signal on the detector.

3.3.2 Methodology

The methodology used to determine the non-linearity coefficients is described here in brief. In principle, both the in-band and out-of-band signal could be used to determine the non-linearity coefficients. In practice, we can take advantage of the high precision external targets used in the thermal vacuum testing to determine the nonlinearity parameters that best fit the known external reference source emission. Fortunately, the out-of-band signal for the non-linearity provides an

independent determination of nonlinearity coefficients largely independent of the in-band signal. However, the out-of-band nonlinearity can only be observed with data that has not been numerically filtered. The combination of in-band and out-of-band nonlinearity signals has been used to obtain a best fit for the parameters of this model. Once the coefficents of the expansion are determined, the application of the correction is performed in a straightforward manner using FFTs and raising the reconstructed interferogram (and DC offset) to the order required in the polynomial expansion. The correction terms are applied to the original complex spectrum and the corrected complex spectrum is made ready for the linear radiometric calibration.

3.4 Radiometric Calibration

3.4.1 Background

The GIFTS design follows the general approach used or planned for other atmospheric sounding instruments for which high absolute accuracy is necessary. For radiometric calibration, GIFTS will periodically view one or more accurately characterized blackbody and cold space references during scheduled calibration sequences. The basic techniques needed to process data from an interferometer are the same as those needed for a more conventional radiometer (e.g., current NOAA sounders). In fact, these techniques yield more accurate results for an interferometer than a radiometer because interferometers lack the uncertainties associated with broadband spectral channels.

Noise in the IR signal is considered separately from calibration errors. We expect noise in the IR signal to be limited by detector noise. In other words, the interferometrically-generated noise will be less than photon- and thermally- generated random noise. Recent increased emphasis on calibration accuracy for ground-based (UW AERI instruments for Department of Energy (DOE) climate/radiative transfer work and the Planetary Imaging FTS Lab Instrument), airborne (UW HIS and Scanning HIS sounders; LaRC/MIT Lincoln Labs/UW NAST-I; Harvard INTESA), and spacecraft FTS instruments (SDL CIRRUS 1A; NPOESS CrIS interferometer design and demonstration units) will be reflected in the procedures used for this program.

Two options were considered for the GIFTS radiometric calibration implementation. One follows the traditional approach of using a large area external blackbody viewed with a flat pointing mirror that is also used to view cold space and the Earth (e.g., the current GOES imager and sounder or the GHIS Phase B design). The second option replaces the large area external

blackbody with a pair of internal small cavity blackbodies at different temperatures. There is a precedent for the use of a single blackbody approach in the Visible Infrared Spin-scan Radiometer Atmospheric Sounder (VAS). This document mainly focuses on discuss the internal blackbody approach, but the overall performance of both systems is compared and shown to meet advanced sounding requirements.

3.4.2 Internal Blackbodies

Radiometric calibration for the GIFTS instrument design is achieved by two small aperture internal reference blackbodies, viewed by a small 45° turning mirror located near the telescope field image. As illustrated in Figure 11, the blackbody design is a scaled version (linear dimensions reduced by a factor of 2.7) of the current UW AERI blackbodies and consist of a cone, cylinder, and inverted partial cone with an aperture of 2.5 cm.

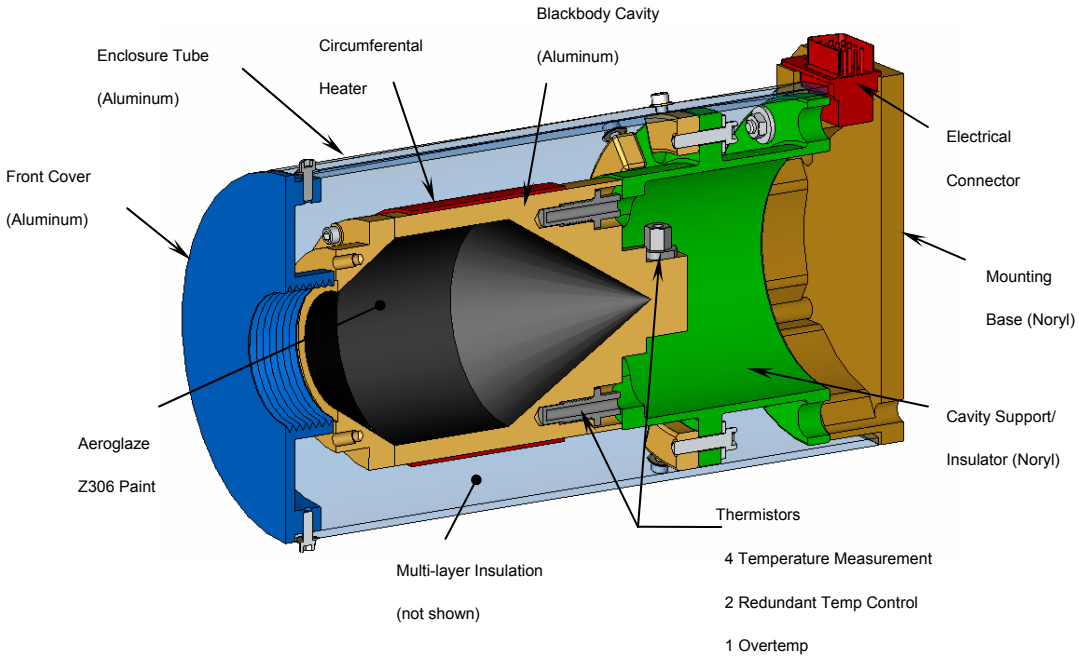

Figure 11: GIFTS Internal Blackbody cross-sectional view. This design follows from the UW-developed AERI blackbody, with a reduction in physical size by a factor of 2.7.

The cavity surface for the GIFTS blackbodies will most likely be Chemglaze Z306, as is used for the AERI blackbodies, though a specular surface will also be considered. With Chemglaze Z306, the cavity spectral emissivity ranges between 0.993 and 0.996 with an absolute uncertainty of < 0.002. The cavity is supported structurally and isolated thermally from the case by the Cavity Structural Support. Radiative coupling between the cavity and case is minimized by the use of multi-layer insulation. Each cavity has a redundant set of four YSI Super-stable thermistors that

are used for both temperature measurement (fully characterizing the cavity gradients), and temperature control. Heater wire wound around the cavity allows each reference blackbody to be run at or above ambient temperature. For GIFTS, one blackbody will be maintained at about 300 K and the other will be thermally coupled to the telescope structure that is expected to operate at 265 K. The GIFTS blackbody temperature uncertainties are expected to be ~0.07 K. The AERI blackbody performance has been demonstrated by comparison with a NIST maintained blackbody reference showing agreement to better than 0.05 K for temperatures from 293 to 333 K.

Currently, Monte Carlo ray trace analysis is being conducted to help characterize the spatial distribution of radiance at the aperture of the cavity. This analysis includes both surface paint reflectivity characteristics and cavity temperature gradients. The ray trace analysis is also being used to bound the uncertainty in cavity radiance resulting from specified uncertainties and distributions of surface emissivity.

3.4.3 Radiometric Calibration Uncertainty Analysis

This section describes the relationships that are used to determine the GIFTS radiometric calibration uncertainty. Assume that we represent the complex, uncalibrated spectrum for incident radiance N by:

Eq. 3

$$C = \left[N\tau_t + B_t \left(1 - \tau_t\right) \right] R_f + C_f$$

where τ_t is the transmission of the telescope (and external pointing mirror, if included): B_t is the Planck emission at the temperature of the telescope; R_f is the complex responsivity of the portion of the instrument behind the telescope; and C_f is the complex offset from the same portion of the instrument behind the telescope. The term in the square brackets is the radiance incident on the turning flat, assuming there is no scattering from the telescope mirror. Similarly, the uncalibrated spectra for the internal hot and cold blackbodies can be represented as

Eq. 4

$$C_H = B_H R_f + C_f \text{ and } C_C = B_C R_f + C_f$$

where the radiance emitted by the blackbodies is represented by B_H and B_C. Differencing the equations in 4 shows that the complex responsivity is given by

Eq. 5

$$R_f = \frac{C_H - C_C}{B_H - B_C}$$

Therefore, the responsivity excluding the telescope can be monitored without changing the instrument pointing. Careful control of the detector temperature and use of low temperature-coefficient electronics should make the responsivity a very stable quantity.

Now, since the space view raw spectrum is given by Equation 3 with the scene radiance N replaced by B_s (which consists of space emission and any warmer tail of the field of view), differencing an Earth view C_E at time t_E and a space view C_S spectrum interpolated to time t_E yields the relationship

Eq. 6

$$N = \frac{1}{\tau_t} Re\left(\frac{C_E - C_S}{R_f}\right) + B_s = \frac{1}{\tau_t}(B_H - B_C) Re\left(\frac{C_E - C_S}{C_H - C_C}\right) + B_s$$

where Equation 5 has been used to eliminate the complex responsivity and where *Re* stands for the real part of the complex spectral ratio. The subtraction of the background noise assumes that instrument emissions have not changed significantly between the space view and the Earth view. In practice, the space views must be performed frequently enough that temporal interpolation can approximate the required simultaneity with only small errors.

If the telescope transmission were known, Equation 6 would be the basic calibration relationship. In fact, the transmission will be measured both from piece-part reflectivity measurements and

from full aperture blackbody observations on the ground. This means that the telescope transmission will be known at the start of the mission. The equation is very similar to that for a full aperture hot blackbody calibration approach for which the cold blackbody raw spectrum in the denominator would be replaced by the space-view spectrum, C_S .

However, we do not need to rely on the stability of the telescope transmission in flight. The transmission will be determined by differencing the space and the cold blackbody views, and using the measured temperature of the telescope optical elements.

Eq. 7

$$C_S - C_C = \left[(1-\tau_t)B_t + \tau_t B_s - B_C\right]R_f$$

Solving for the transmission and using Equation 5 to eliminate the responsivity yields

Eq. 8

$$\tau_t = 1 - \frac{1}{B_t} Re\left(B_C + \frac{C_S - C_C}{R_f}\right) = \frac{B_t - Re\left(B_C + \frac{C_S - C_C}{R_f}\right)}{B_t - B_s}$$

$$= 1 - \frac{1}{B_t}\left[B_C + (B_H - B_C) Re\left(\frac{C_S - C_C}{C_H - C_C}\right)\right] = \frac{B_t - B_c - \left(B_H - B_C\right) Re\left(\frac{C_S - C_C}{C_H - C_C}\right)}{B_t - B_s}$$

It should be necessary to perform this observation infrequently. Despite the infrequency with which this value is calculate, the cold view should be performed close in time to the space view to ensure that the instrument backgrounds accurately cancel. For a high telescope transmission, however, precise temperature values for the optical elements are not necessary to reduce the uncertainties that arise from low telescope transmission.

Note that in both Equations 6 and 7, the ratio of differences of complex spectra automatically eliminates the phase of the raw spectra (Revercomb et al. 1988). As for an external blackbody calibration, phase correction is not needed and in fact, should be avoided.

To summarize this approach, the emission from the telescope is removed by subtracting the space view from the Earth view, and the responsivity (excluding the telescope transmission) is provided by the internal blackbody views. The telescope transmission is both determined pre-launch and monitored from the calibration views in flight. Both time interpolation of the space views and telescope temperature measurements are used to assure accurate subtraction of telescope emission while minimizing the required frequency of space views.

3.4.4 Expected Radiometric Accuracy

Figure 12 shows, for ν = 1000 and 2000 cm^{-1}, the GIFTS baseline calibration radiometric accuracy compared to the external blackbody approach, assuming the same parameter uncertainties for both, except for the emissivity uncertainty of the external blackbody (increased to 0.005 to account for its lower cavity enhancement factor). At each scene temperature, the calibration accuracy is the root sum square (RSS) combination of several system uncertainties. This includes uncertainties due to temperature and emissivity for each of the blackbodies, the structure temperatures affecting reflection from the blackbodies, and the telescope mirror reflectivity. Also included is the contribution from the time variation of the telescope temperature between the space and Earth views. For the case where the transmission is known, we have assumed that ground-based testing with a large external blackbody has determined the transmission of the telescope to within 0.2%. Table 2 presents the input parameters and uncertainty magnitudes that were used in the uncertainty analysis model to generate the GIFTS calibration accuracies presented in Figure 12. Figure 13 illustrates the individual error contributions at ν = 2000cm^{-1} due to the temperature stability parameters and uncertainty magnitudes shown in Table 2. Even including the uncertainty due to the characterization of the telescope transmission in-flight, the expected calibration accuracy is well within the nominal 1 K requirement for accurate atmospheric sounding. The short wavelengths are not used for the cold scene temperatures of the upper atmosphere.

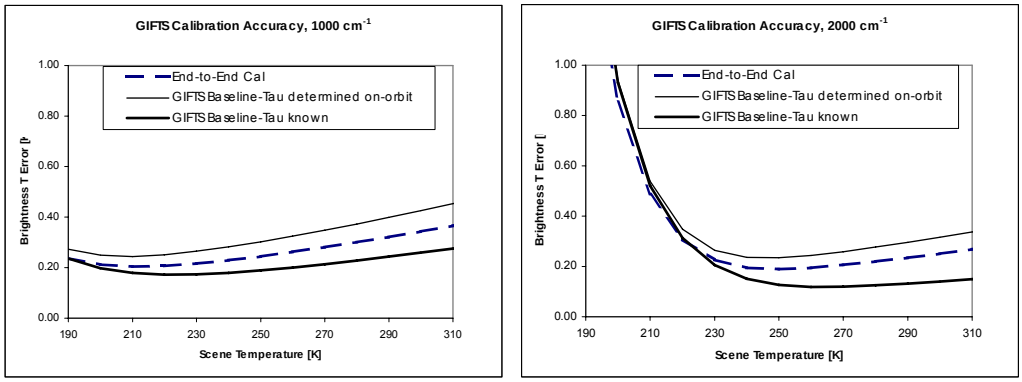

Figure 12: GIFTS calibration accuracy at wavenumbers of 1000 cm^{-1} (left) and 2000 cm^{-1} (right). The three cases plotted for each wavenumber represent the baseline GIFTS design where the telescope reflectivity is known from pre-launch characterization, a worst case assumption using only on-orbit determination of telescope reflectivity, and the external large area blackbody option (labeled "End-to-End Cal").

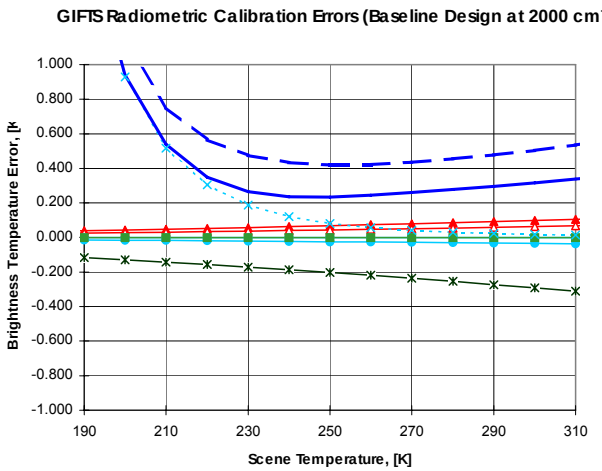

Figure 13: GIFTS radiometric calibration errors at 2000 cm^{-1} wavenumbers by individual contributor. The additive and RSS accumulation of the errors are shown (dashed and solid line respectively). The RSS curve in this figure is plotted as "GIFTS Baseline-Tau determined on-orbit" on the right side of Figure 12.

Input Parameters		
wn	Wavenumber	2000 cm^{-1}
tau	Telescope (2) elements and blackbody mirror transmission	0.913
Thbb	Hot blackbody temperature	300 K
Tcbb	Cold blackbody temperature	265 K
Tspace	Temperature of space	4 K
Ttel	Telescope temperature	265 K

Tstr	Temperature of structure reflecting into BB's	265K
Ehbb	Emissivity of hot blackbody	0.996
Ecbb	Emissivity of cold blackbody	0.996
Parameters Used For Temperature Stability		
Etel	Telescope emissivity	0.087
TauTot	Total transmission through instrument	0.205
TtelΔ	Change in telescope temp between Earth and space views	0.5 K
Uncertainty Magnitudes		
ΔThbb	0.07 K	
ΔTcbb	0.07 K	
ΔEhbb	0.002 K	
ΔEcbb	0.002 K	
ΔTstr	5 K	
Δtau	0.0086 RSS	
ΔTtel	2 K	

Table 1: Calibration uncertainty analysis parameters

3.4.5 Practical Application

Radiometric calibration of the GIFTS spectrometer has the same considerations as that of any radiometer. Key factors include the accuracy of onboard references, thermal stability over calibration cycles, and linearity after correction. The calibration method is summarized in Equation 9. This is a modified version of the Revercomb et al. (1988) equation to include the ratio of the transmission of the flip in mirror (labeled "m") to the fore optics telescope, which is labeled "t" (Knuteson et al., 2004b).

Eq. 9

$$N = \left(\frac{\tau_m}{\tau_t}\right)(B_H - B_C)Re\left(\frac{C_E - C_S}{C_H - C_C}\right) + B_S$$

The radiance (N) is derived from raw spectra of Earth (C_E), space (C_S), and the internal hot (C_H) and cold (C_C) blackbodies where $B_{H,C,S}$ is the predicted Planck radiance from the hot, cold, and space references including the effective emissivity of the blackbody cavity and the energy reflected off the blackbody from the environment, assumed here to be 265 K.

Uncertainty of the reference source temperature and emissivity will lead to uncertainty in the calibrated radiances. The space view is assumed to be known exactly so no error is introduced. However, measured characteristics of the UW-SSEC blackbody can be used to estimate a 3-sigma (not-to-exceed) error bound. These parameter uncertainties are summarized in Table 3. The uncertainty estimates in the calibrated radiance are obtained through a perturbation analysis of Equation 9 where the uncertainties of the blackbody emissivity and temperature are taken into account.

On-orbit Calibration Parameter	Nominal value	Assumed Uncertainty
Hot BB Temperature	300 K	0.1 K
Cold BB Temperature	265 K	0.1 K
Hot BB Emissivity	(see Fig. 13)	0.001
Cold BB Emissivity	(see Fig. 13)	0.001
Space View Temperature	2.76 K	0.0
Space View Emissivity	1.0	0.0

Table 3: On-orbit calibration parameter uncertainties assumed in this analysis (3-sigma)

Simulated GIFTS interferograms were used as input to the modified Revercomb et al. (1988) calibration equation given in Equation 9. Details of the GIFTS simulation model have been previously described in Huang et al. (2000). The complex spectra resulting from the FFT of the simulated interferograms is shown in Figure 14 as magnitude and phase spectra for each of the four scene views; Earth, hot blackbody, cold blackbody, and deep space. A linearly varying phase has been included in the simulation to force the FFT of the interferograms to have both a real and imaginary component. The responsivity, which is the inverse of the calibration slope, is shown in Figure 15 for each of the two simulated GIFTS spectral bands. This value is the cutoff assumed for the simulated GIFTS optical pass bands. The GIFTS simulation is not intended to be completely realistic, but merely to serve as an example of the type of data that will be available from the instrument in flight. The simulation is suitable for illustrating the expected radiometric calibration accuracy of a typical Earth scene. Figure 16 shows the result of application of the calibration equation to the raw complex spectra; the real part of the equation is shown as a brightness temperature spectrum while the imaginary part (not shown) is zero to within the noise level.

A perturbation analysis has been performed using these simulated GIFTS observations. The analysis illustrates the uncertainty in the calibration error expected in this typical clear sky scene due to uncertainties about the internal calibration reference sources. Figure 17 shows the brightness temperature error as a function of wavenumber induced by varying the blackbody temperature and emissivity by the amounts shown in Table 4. Figure 18 shows the same perturbation analysis as a function of scene brightness temperature.

To illustrate the imaging capability of the GIFTS sensor, an Earth scene data cube (128x128 fields of view) was simulated and the same calibration error analysis was applied to each field of view. The result is shown in Figure 19 as images of the scene brightness temperature in the LW window and the estimated calibration error at the same wavelength. Note that the colder scenes have slightly smaller errors than the warmer scene pixels. This is further illustrated in the 3-D plot of Figure 20 where the error closely follows the cloud scene temperature.

The GIFTS error budget for the contribution of the internal calibration errors is 0.5 K (3-sigma) out of a total requirement of <1K for all radiometric calibration errors. The current engineering best estimate is < 0.35 K in the LW and < 0.20 K in the short to midwave bands. The examples shown here are consistent with those previous estimates. Moreover, the analysis shown in this paper for a specific simulation dataset is consistent with the general perturbation analysis described in Knuteson, et al. (2004b).

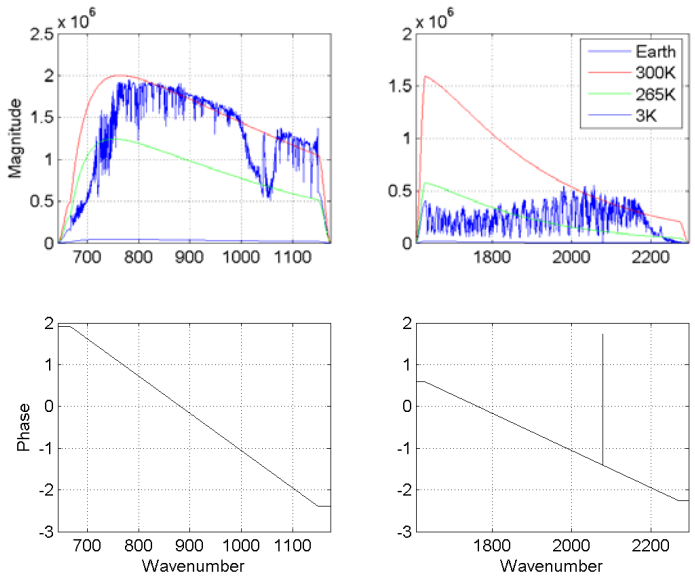

Figure 14: Simulated GIFTS interferograms have been Fourier transformed to show the magnitude and phase of the uncalibrated complex spectra used in this noise analysis.

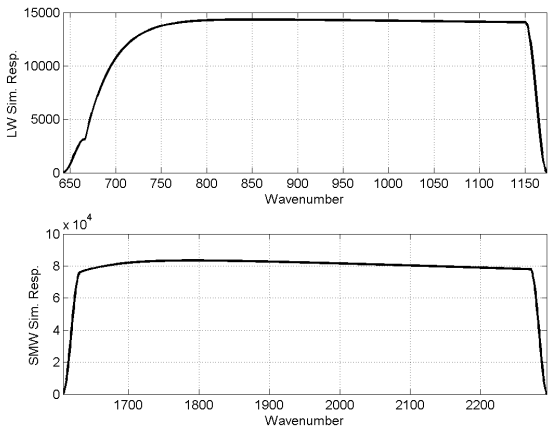

Figure 15: Simulated GIFTS responsivity magnitudes. The above graphs show simulated GIFTS responsivity magnitudes computed from the ratio of the difference of simulated internal blackbody views to the difference of planck radiances at 300 K and 265 K. These simulated responsivities are not intended to mimic the real GIFTS instrument except in defining the approximate spectral cutoffs for the LW and SWM bands.

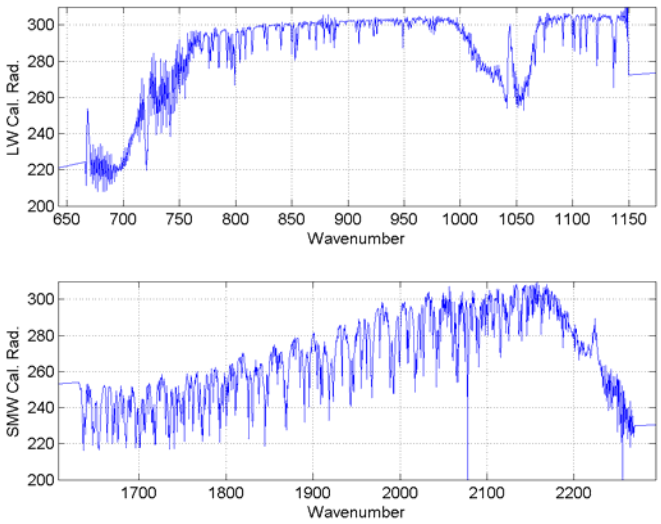

Figure 6: Calibrated GIFTS radiances from sample scenes. Above are calibrated GIFTS radiances obtained after applying Equation 9 to simulated GIFTS interferograms for a warm scene (Central Oklahoma, IHOP case) and simulated views of internal (hot and cold) and external (space) views. Telescope transmission is assumed known in this simulation.

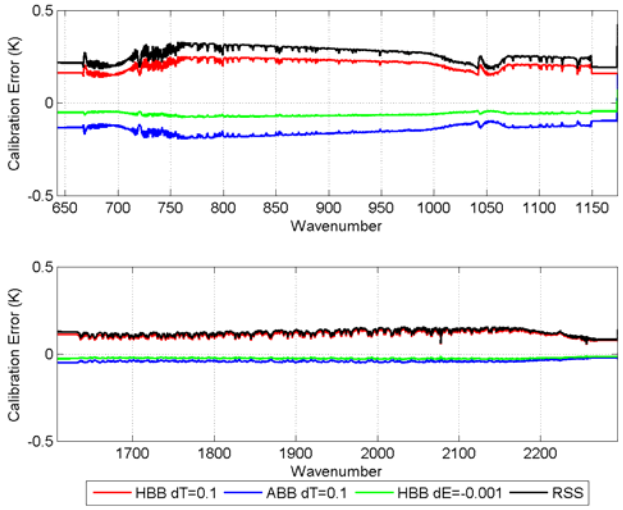

Figure 17: Internal blackbody calibration error. The internal blackbody calibration error of LW and SWM GIFTS bands are shown as an error spectrum for the calibrated scene shown in Figure 6 and using the uncertainties shown in the figure legend. The GIFTS error budget for the contribution of the internal calibration errors is 0.5 K (3-sigma).

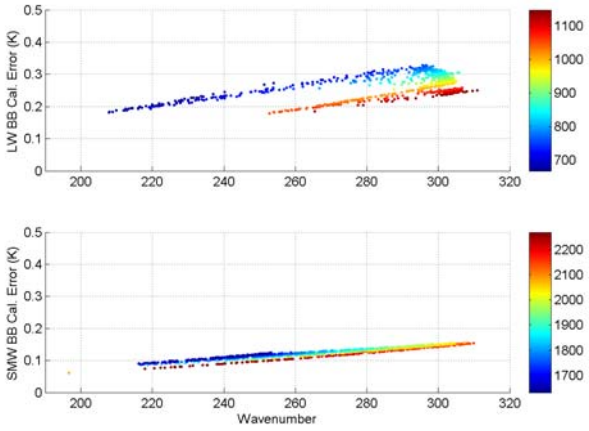

Figure 18: Scatterplot of internal blackbody calibration error. The internal blackbody calibration error of LW and SWM GIFTS bands are shown as scatterplot for the calibrated scene shown in Figure 16 and using the uncertainties given in Table 4. The points are color coded based upon the wavenumber scale as indicated in the colorbar to the right of each panel.

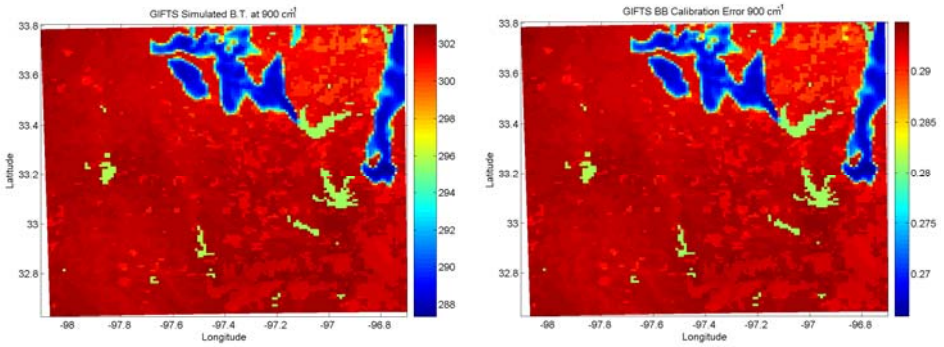

Figure 19: Brightness temperature for simulated GIFTS dataset. A brightness temperature image of a simulated GIFTS Earth scene (left panel) is shown for the center of the LW band (900 cm^{-1}). The internal blackbody calibration error at 900 cm^{-1} is shown in the right-hand panel as an image using the uncertainties given in Table 4. The variation in window scene temperature is caused by presence of clouds in the simulation. All units are in Kelvin.

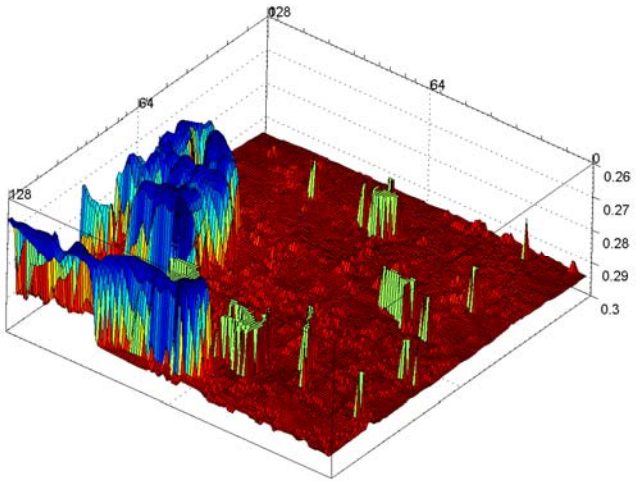

Figure 20: 3-D surface plot of blackbody calibration error data. Same blackbody calibration error data as the right hand panel of Figure 19, but shown here as a three-dimensional surface plot. The internal blackbody calibration error at 900 cm^{-1} varies across the scene due to the presence of clouds in the simulation. The "peaks" in the surface represent a decrease in the error in the absolute calibration of the GIFTS radiances for the colder cloudy scenes. All units are in Kelvin.

3.5 Instrument Line Shape and Spectral Calibration

3.5.1 Background

The spectral calibration used for GIFTS will build on principles from ground-based and aircraft FTS systems (AERI, HIS, S-HIS, and NAST-I) designed with a single on-axis FOV. The spectral characteristics of these instruments can be defined by an Instrument Line Shape (ILS) and a spectral sampling interval. The observed spectrum is the atmospheric spectrum convolved with the ILS and sampled at equally spaced points starting at zero wavenumbers and ignoring radiometric calibration errors and noise.

The accuracy of the spectral sampling scale is maintained by the stable laser used to trigger sampling at equal intervals of Optical Path Difference (OPD). Because the wavenumber samples are known to be equally spaced as well, the calibration of this spectral scale is determined for an entire broad spectral band by the determination of the proper wavenumber for any single spectral feature in the band. We use the comparison of observed atmospheric spectra to line-by-line radiative transfer calculations based on observed atmospheric state parameters to determine the

proper wavenumber scale. This calibration process transfers the very accurate positions of prominent spectral line features in the HITRAN database to the observed spectral scale. We define an effective laser wavenumber parameter to describe this scale. Once the effective laser wavenumber for a given instrument is known, interpolation techniques can be used to rigorously transform the spacing to a standard wavenumber scale allowing standardization of the spectra from different instruments. This is routinely performed for the multiple AERI instruments deployed for the DOE Atmospheric Radiation Measurement Program.

The ILS for these existing FTS systems is determined by the maximum OPD sampled (X) and the range of field angles through the interferometer that contribute to the signal, which is defined by an effective half-angle, b, for an on-axis field stop. By design, b is kept small to limit the influence of the finite field-of-view of the instrument. To first order, the ILS centered at wavenumber 0 is a sinc function

Eq. 10

$$ILS(-(0)) = \sin[2((-(0)X))]/[2(-(0)X)]$$

However, for accurate radiometry, it is important to make sure that the FOV is carefully aligned about the central axis of the interferometer and that an effective b is determined. Again, we use comparisons with specific regions of calculated atmospheric spectra to refine our nominal values of b (based on optical design). The finite FOV effect on ILS for the AERI, HIS and NAST instruments is negligible for the LW band, but can be significant in the shortwave band. Procedures to remove the relatively small effects of ILS wavenumber dependence (0) are routinely applied to the data from AERI, Scanning HIS and NAST-I.

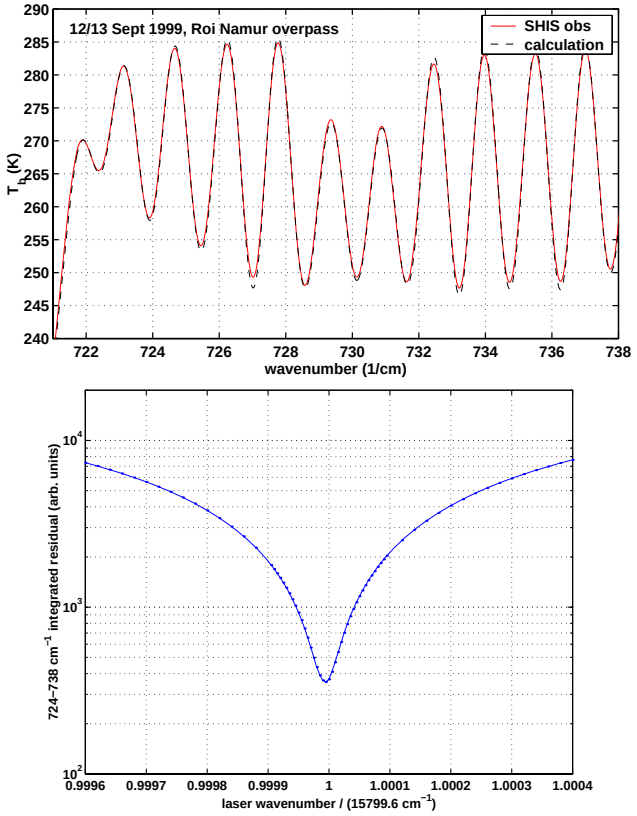

Figure 21: Spectral scale calibration example for S-HIS from NASA KWAJEX experiment. The top panel shows a comparison of observed S-HIS data to a line-by-line calculation for a clear sky overpass of Roi Namur on 12 September 1999 flight for several carbon dioxide spectral lines. The bottom panel shows integrated residuals (observed and calculated) for the 724 to 738 cm^{-1} region with the effective S-HIS laser wavenumber (and resulting S-HIS wavenumber scale) perturbed by various amounts ranging from -0.04 to +0.04 percent.

The upper panel in Figure 21 shows a comparison of measured and calculated S-HIS spectra for the 722-738 cm^{-1} spectral region from a clear sky flight on 12 September 1999. This spectral region has been chosen for spectral calibration, because of the high accuracy of the measured spectral line parameters of the dominant CO_2 absorption lines in this region. The bottom panel of Figure 21 shows integrated residuals (observed minus calculated) for this spectral region versus the unitless quantity of the effective laser wavenumber divided by the expected laser wavenumber of 15799.6 cm^{-1}. There is a well defined minimum in this curve, establishing the S-HIS laser wavenumber (and spectral calibration) to better than 1 part in ~ 2 x 10^5.

3.5.2 Approach

The major difference between GIFTS and single-FOV instruments is that each pixel of its imaging detector array has a different wavenumber scale. This effect is a predictable result of the different paths the beams focused on each pixel travel though the interferometer. While the central pixel is nominally the same as the single FOV instruments discussed above, off-axis detectors are irradiated by beams passing through the interferometer at non-zero mean angles. A non-zero mean angle causes the OPD for any given position of the interferometer Michelson mirror to be reduced by the cosine of the off-axis angle.

This OPD scale variation with pixel location is illustrated in Figure 22, which shows a simulated interferogram for the GIFTS LW band with a uniform scene. For the LW FPA, the double-sided interferogram is sampled at 2048 points. The exact OPD sampling positions, however, vary for each pixel depending on the mean off-axis angle, θ, and the single pixel half-angle, b. The magnified portion of the interferogram illustrated in Figure 5 shows the 0.66 cm region enhanced by the equal spacing of 15 (m CO_2 lines. Three individual OPD points from an on-axis interferogram (0.6637, 0.6654, 0.6671 cm) are also shown for every pixel along the diagonal from the center to a corner pixel of the detector array.

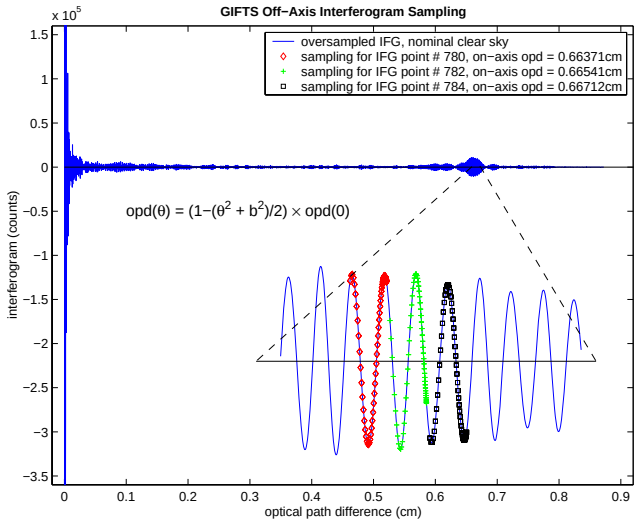

Figure 22: Illustration of the OPD sampling variations due to off-axis beams. The off-axis pixels sample the interferogram at smaller OPDs (compared to the on-axis beams), according to the given equation for OPD(θ). For three different on-axis sample points, the range of off-axis sampling points (from the near-center pixels to the corner pixels of the focal plane array) are shown in the blowup. (See text for more details).

Note that all of the points fall on the same continuous interferogram. For a uniform scene, the only significant difference is a small change in the OPD sampling interval. In other words, the differences are the same as those caused by differences in the effective laser wavenumbers for different instruments, and can be rigorously eliminated by interpolation to a standard scale.

This behavior is realized for the geostationary-orbiting GIFTS because of the extremely small range of angles contributing to each individual detector pixel (< 1 mrad in the interferometer). As a result, the variation of ILS across the array is extremely small and can be ignored without introducing significant errors. As shown in Figure 23, the ILS is essentially a pure sinc function and exhibits extremely small ILS differences between the on-axis and extreme-diagonal pixels.

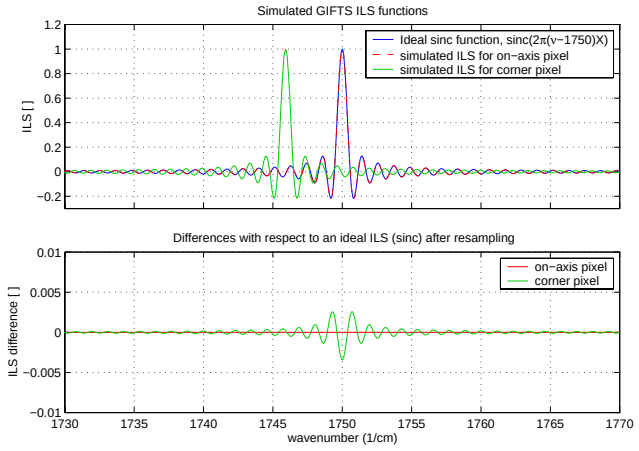

Figure 23: Comparison of ILS. Top panel: comparison of an ideal sinc ILS function centered at 1750 cm^{-1} with simulated GIFTS ILS functions for an on-axis pixel and for a corner pixel (the ideal sinc and the simulated on-axis ILS are indistinguishable in this panel). The shift in the corner pixel ILS is only apparent due to (incorrectly) plotting it on the on-axis sampled wavenumber scale. The bottom panel shows the difference between the corner and on-axis pixel ILS functions from the ideal sinc function after resampling, but without any attempt to correct for the finite detector size effects.

Another way of depicting the small variation of the ILS is to show the small self-apodization in the interferogram domain caused by the finite FOV effect. Figure 24 shows that at the extremes of OPD for the GIFTS primary sounding and chemistry mode, the self-apodization variation out to 1750 cm^{-1} is very small—less than 1% over the array. In fact, because of the very small angles involved for GIFTS, the deviations from a pure sinc-function ILS are significantly smaller than for the aircraft and ground-based instruments discussed above. Figure 25 shows that the peak

brightness temperature effect of ignoring ILS variations is less than 0.15 K for a typical Earth scene.

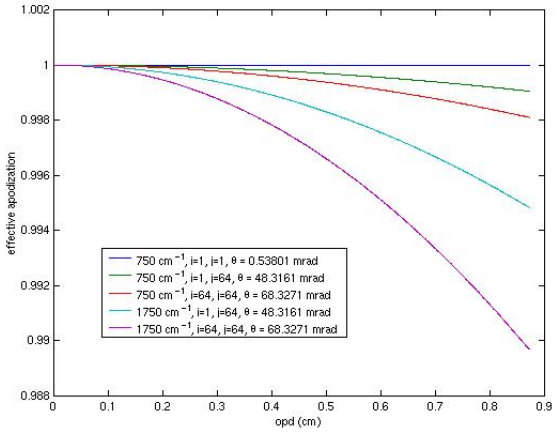

Figure 24: Effective apodization functions due to finite detector size at 750 and 1750 cm^{-1} for various pixel locations. Curves appear in the same order (from top to bottom) as they appear in the legend. In this figure, and in Figure 25, i and j denote the pixel location within the 128 × 128 FPA, where for example i, j = (1,1) is near the center of the FPA, and i, j = (64, 64) is the pixel in the upper right hand corner of the FPA.

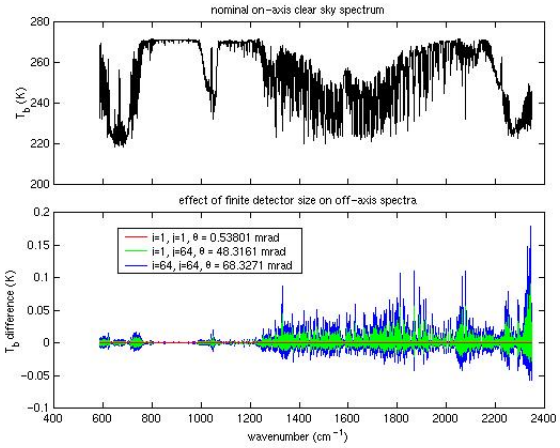

Figure 25: Peak brightness temperature effect of ignoring ILS variations. The top panel depicts a nominal clear sky spectrum and the bottom panel shows the magnitude of the finite detector size self-apodization effect in brightness temperature for three FPA pixel locations. In the bottom panel, the i, j = (1,1) curve is the dark curve near zero, the i, j = (1,64) has a slightly larger magnitude, and the i, j = (64, 64) curve has the largest magnitude.

In summary, the imaging Fourier transform spectrometer system used in GIFTS has a well-understood ILS and wavenumber scale variation with pixel location. These spectral properties depend on a few well-defined instrument parameters that need to be characterized; specifically, the effective wavenumber of the laser used for the detector trigger and the geometry of the focal plane relative to the interferometer axis. Therefore, the spectral calibration for GIFTS can be thought of as very similar to that for a single detector FTS. By observing a localized spectral feature with the central pixel, the effective laser wavenumber can be determined for the central pixel and variations for the other pixels predicted from the known detector and optical geometry. In practice, the spectral scale calibration will be determined for each detector pixel during ground testing with a gas cell before launch. Consistency of these measurements with the known geometry will be verified. Moreover, precise measurements of the ILS will also be obtained from the same gas cell tests.

3.6 Spectral Resampling

3.6.1 Wavenumber Sampling Methods

Once the spectral calibration (i.e. wavenumber sampling scale) is determined for each of the GIFTS FOV, the calibrated radiance spectrum can be resampled from the original sampling interval to a pre-specified reference wavenumber scale (Tobin et al. 2003). The resampling can be performed accurately in software using a double FFT and linear interpolation of an oversampled spectrum. An alternative approach using a convolution rather than an FFT to resample the spectra has been evaluated for any potential performance advantages. The result of the wavenumber resampling operation will be that all of the GIFTS spectra have a common wavenumber scale independent of their location in the focal plane array. This is essential for the routine comparison of observations and radiative transfer calculations needed in the production of Level 2 products (e.g. temperature and humidity profiles).

The double FFT method requires the fast fourier transform of the original spectrum (with a power of two number of points, N=2(n-1)) to the interferogram domain where additional zeros are added to the end of the interferogram (“zero padding”). For the GIFTS focal plane arrays used in this analysis, the number of points in the spectrum are taken to be n=1025 (LW), and 2049 (SMW). Zeros are added to produce a symmetric interferogram containing M*N points where M*N is a power of two. Transforming this expanded interferogram back to the spectral domain provides an

oversampled spectrum that can be used to interpolate to the desired spectral sampling. Equation 11 illustrates this method where the original radiance spectrum S is interpolated to the final resampled spectrum S'. In Equation 11, FFT and IFFT are the Fast Fourier Transform and its inverse, and L() is the linear interpolation operator from the oversampled wavenumber scale v'' to the desired final spectral scale v'. The double FFT method (with linear interpolation) is of order M'*N log (M'*N) + M*N floating point operations (FLOPs) where M' = M+1 to account for the original forward FFT. The FLOP estimate is valid only when a power of two is used in the inverse FFT. Powers of two are the most efficient use of FFTs, though prime factor algorithms are also an option.

Eq. 11

$$
\begin{aligned}
&I = FFT(S, N) \\
&I'(i) = I(i), i = 1, n; \\
&I'(j) = 0, j = n+1, M*(n-1) \\
&S'' = IFFT(I', M*N) \\
&S' = L(S'', v'', v')
\end{aligned}
$$

The sinc resampling (or F-matrix) method can also be used to transform the original spectrum S to the desired resampled spectrum S' defined in Equation. 12 as the matrix multiplication (from CrIS ATBD; BOM-CrIS-0067).

Eq. 12

$$
\begin{aligned}
&S' = F \cdot S, \\
&\textit{where} \\
&F = \frac{dv}{dv'} \cdot \frac{\sin c((v - v')/dv')}{\sin c((v - v')/(N dv'))}
\end{aligned}
$$

In Equation 12, F is an nxn matrix, S and S' are 1xn column vectors, the sinc function is defined to be sin(x)/x, and N = 2(n-1). The generation of the F-matrix is computationally expensive, but it can be precomputed and stored for later use as long as the GIFTS spectral calibration is stable

over time. The application of the sinc resampling method is a simple matrix multiplication and has order n^2 floating point operations for a full rank matrix.

The GIFTS focal plane arrays contain 128x128 (16384) pixel elements, each of which represents a complete GIFTS spectrum (one spectrum per spectral band). Due to the fact that the laser trigger is aligned with the interferometer optical axis, the spectral calibration of the GIFTS sensor varies as a function of off-axis pixel angle from near the center of the focal plane arrays. Correcting for this effect using the double FFT plus linear interpolation method requires only that the initial wavenumber sampling scale be known for each pixel element. Once this original scale is known the actual computational time required to perform the FFT method is independent of which pixel is being corrected. There is no preferred order of processing the pixel elements. In contrast, the F-matrix approach suggests that concentric "rings" of detector elements should be grouped together in the data processing to take advantage of precomputed F-matrices. This is because the full F-matrix is too expensive to generate for each of the individual 16384 pixel elements in each spectral band. Since the F-matrix approach will require a more sophisticated data management approach for efficient implementation, it is important to quantify the computational advantages (if any) of this approach over the double FFT method.

3.6.2 Accuracy versus Efficiency

In order to compare the numerical performance of the two spectral resampling methods, we first investigate the theoretical number of floating point operations for each method. As stated previously, the number of operations of the FFT method with linear interpolation is proportional to M'*N log (M'*N) + M*N where M'=M+1, N=2(n-1), and n = 1025 (LW), 2049 (SMW). The expansion factor M is a parameter that can be adjusted to increase algorithm efficiency by reducing algorithm accuracy. Note that M*N must be a power of two for this estimate of FLOPs to be valid. Figures 26 and 27 illustrate the tradeoff between algorithm accuracy and number of zeros used in the inverse FFT transform for a c-language implementation of the double FFT method with linear interpolation (using FFTW for the FFT).

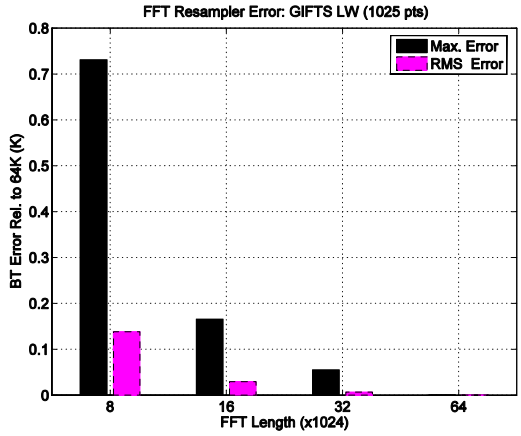

Figure 26: FFT resampler maximum and root mean square error for the GIFTS LW band where the 64K length is taken to be exact (zero error).

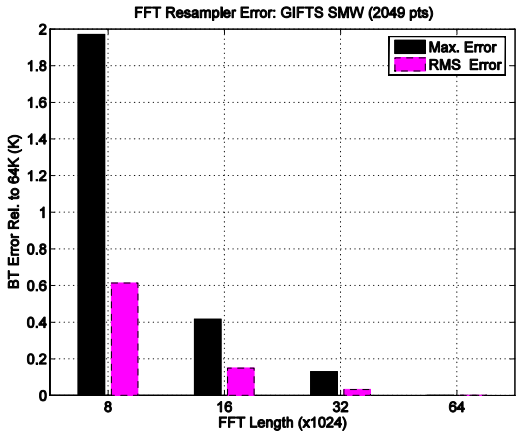

Figure 27: FFT resampler maximum and root mean square error for the GIFTS SMW band where the 64K length is taken to be exact (zero error).

The sinc resampler method has significant overhead associated with the generation of the full F-matrix for a given initial wavenumber scale. After the F-matrix is generated, application of the full matrix is of order n^2 floating point operations. A comparison of the theoretical number of floating point operations for the two methods is shown in Figure 28 for a range of M values in the double FFT method. Figure 28 was computed using n=1025, which is appropriate for the GIFTS LW band. Note that the double FFT method has an overall constant scale factor that is difficult to estimate theoretically. For that reason both methods have been implemented in c-language and test runs were performed as a function of pixel number. The results are shown in Figures 28 and 29 for the sinc resampler and double FFT methods respectively.

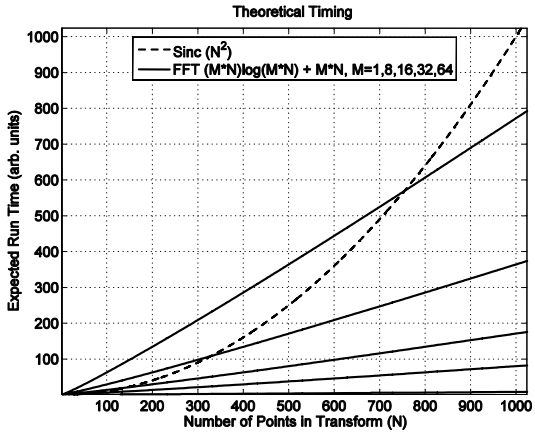

Figure 28: Theoretical execution time for Sinc resampler (N2) versus FFT resampler (M*N log(M*N)+M*N. Note FFT estimate is valid only for powers of two.

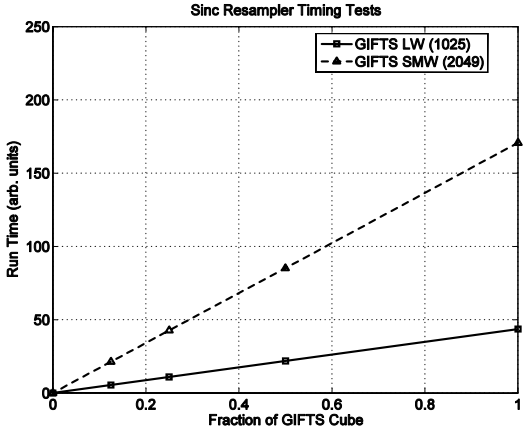

Figure 29: Sinc resampler execution time as a function of the number of spectra processed (full GIFTS cube has 128 x 128 pixel elements).

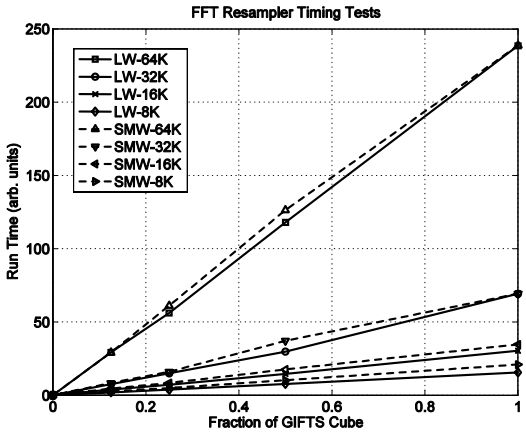

Figure 30: FFT resampler execution time as a function of the number of spectra processed (full GIFTS cube has 128 x 128 pixel elements).

3.6.3 Conclusions

UW-SSEC has performed timing tests using prototype implementations of two competing algorithms for the task of resampling the GIFTS spectra in each band to a common wavenumber scale. The conclusions of this analysis are given below:

(1) The computational performance of the FFT resampling method using a 16K FFT is roughly comparable to the full F-matrix sinc resampler for the GIFTS LW band. However, in the GIFTS SMW band the FFT 32K FFT is about three times faster than the full F-matrix method with similar accuracy.

(2) When the complications of the data management of the large F-matrices is taken in to account and the need to precompute the F-matrices, it would be hard to justify the use of sinc resampling using the full F-matrix approach for the GIFTS task.

(3) However, there is still the possibility that the F-matrix can be reduced in one dimension by zeroing out off-diagonal matrix elements while still meeting the accuracy requirements. Investigation of this "near diagonal" F-matrix approach is under evaluation.

3.7 Geo-Location and Navigation

The GIFTS uses a LFPA (128 × 128 grid) in a Fourier Transform Spectrometer (FTS) to enable the simultaneous gathering of high spectral resolution (as great as 0.6 cm^{-1}) and high spatial resolution (4-km × 4-km pixel size) Earth infrared radiance spectra over a large geographical area (512 km × 512 km). An additional visible low light level camera provides quasi-continuous imaging of clouds at 1-km spatial resolution. Extended Earth coverage is achieved by step scanning the instrument field of view in a contiguous fashion across any desired portion of the visible Earth. See Figure 31. The center point and rotation axis of each FPA will be geolocated at the time of the zero path difference (ZPD) crossing of the measurement. The angles of each FPA pixel relative to the center of the array are known from pre- and post-launch characterization and are expected to remain fixed. Navigation errors caused by pointing inaccuracies will lead to both a rotation and translation of the image cube for which a correction is required. The details of this correction approach remain to be defined because at the time of writing of this document, the satellite platform was still to be decided.

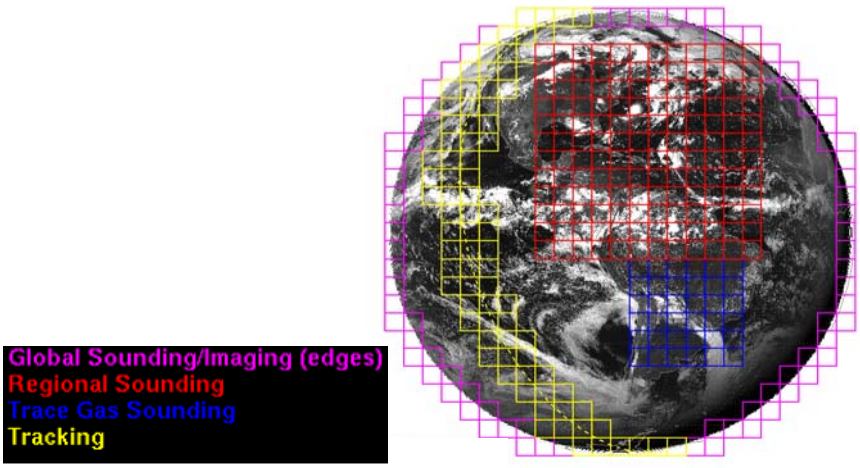

Figure 31: A selection of GIFTS measurement modes. Each box represents the 128 × 128 Large area format Focal Plane detector Array (LFPA).

3.8 Post-processing

The following tasks are anticipated to be performed at the end of the processing chain while important intermediate products are still accessible, these tasks include the following;

- Instrument responsivity (gain) estimates using internal and space views.
- Total Noise Equivalent Spectral Radiance (NESR) estimate from calibrated reference source views and a breakdown into spectrally random and correlated components.
- Noise and phase error estimates from the imaginary part of the complex calibrated spectra.
- Spectral stability estimation using a standard reference scale (calculation).

3.9 Output

This section lists the primary outputs of the level 0-1 ground processing algorithm developed for the GIFTS sensor; 1) Time, 2) Spatial Location, 3) Spectral scale, and 4) Spectral Radiances. Additional metadata and quality flags are described elsewhere.

Time. The time associated with the GIFTS calibrated radiance is that taken from the observation time as the Michelson moving mirror passes through zero path difference. The time interval varies depending on the observation mode from about 11 seconds for regional sounding mode down to about 1 second for regional imaging mode.

Spatial Location. Each pixel of the 128x128 focal plane array is assigned a latitude and a longitude on the Earth sphere. Details of the geolocation are discussed elsewhere.

Spectral Scale. The spectral scale of the radiances is provided in wavenumbers (1/cm) between fixed limits for each focal plane array (LW and SMW). The output of every pixel of each FPA are resampled to a common wavenumber scale. The wavenumber scale used as a reference has a constant $\Delta\nu$. The exact value of the wavenumber scale interval is defined in the final test documentation. Band limits for the LW and SMW focal plane arrays will be adjusted to control the output data range based upon signal to noise considerations.

Spectral Radiances. The final output radiances are in units of $mW/(m^2\ sr\ cm^{-1})$. The radiance value at each spectral element has been radiometrically calibrated using on-board and space reference sources. A nonlinearity correction has been applied prior to radiometric calibration. The spectral calibration assignment has been made and the spectrum resampled to a common reference wavenumber scale. The result is a radiance measurement which can be compared with calculated top of atmosphere radiances using a simple sinc function (idealized FTS).

4 Quality Flags

This section is reserved for the description of algorithms used to create quality metrics to be applied to the Level 1 radiances. These quality metrics are intended to be made available with the radiance datasets to allow the user to make an assessment of the data quality. The full set of quality metrics has yet to be determined but should include the following;

- Pixel mask indicating useable pixel elements in each focal plane array.
- Spike indicator and the success of attempted repair (if any).
- Noise specification limits test to indicate if an observation is out of spec.
- Calibration phase test, with limits check on the imaginary part of the calibrated spectrum.
- Radiance limits check with physical constraints.

Appendix 1: Level 0-1 Algorithm Description for GIFTS

Robert Knuteson, Fred Best, Ralph Dedecker, Ray Garcia, Sanjay Limaye, Erik Olson,

Henry Revercomb, and David Tobin

Space Science and Engineering Center, University of Wisconsin-Madison

The Geosynchronous Imaging Fourier Transform Spectrometer (GIFTS) instrument, under development for the NASA New Millennium Program, will serve as a valuable test bed for the evaluation of approaches to flight hardware and ground data processing in the years leading up to NOAA's operational Hyperspectral Environmental Suite (HES). The GIFTS sensor makes use of a 2-D array of detectors to increase area coverage rates while providing dramatically higher vertical resolution by measuring the thermal infrared upwelling emission spectrum at high spectral resolution. The sensor calibration makes use of two internal high precision blackbody references in addition to an external view to space. The GIFTS ground data processing algorithms used to convert from instrument values (Level 0 data) to geo-located, calibrated radiances (Level 1 data) are under development at the University of Wisconsin Cooperative Institute for Meteorological Satellite Studies (UW-CIMSS). These algorithms include geo-location, non-linearity correction, calibration, and correction for off-axis effects. This paper provides a description of the Level 0-1 GIFTS algorithms and their performance characteristics.

Introduction

The U.S. National Oceanic and Atmospheric Administration (NOAA) operates geostationary operational environmental satellites (GOES) for short-range warning and nowcasting, and polar-orbiting environmental satellites (POES) for longer term forecasting. GOES satellites provide continuous monitoring from space in a geosynchronous orbit about 35,800 km (22,300 miles) above the Earth. The current generation of GOES satellites contain separate imager and sounder instruments. The sounder is used to remotely sense the atmospheric thermodynamic state, e.g. atmospheric stability and total column water vapor. A new generation of sensors are under development that will greatly increase the horizontal, vertical, and temporal sampling of the GOES sounder and provide a truly four-dimensional view of the Earth's atmosphere. NOAA's plan for a Hyperspectral Environmental Suite (HES) calls for the replacement of the current GOES instrumentation starting as early as 2013 (Dittberner et al. 2003; Gurka et al. 2003). Meanwhile, NASA's New Millennium Program Earth Observing 3 (NMP EO3) mission is the first step in improving the U.S. geostationary weather observing system. The NMP EO3 mission features the Geosynchronous Imaging Fourier Transform Spectrometer (GIFTS), an instrument that incorporates new technologies to implement an innovative atmospheric measuring concept proposed by Dr. William L. Smith of NASA's Langley Research Center (Smith et al. 2000). The NASA GIFTS research instrument will serve as a valuable test bed for the evaluation of approaches to flight hardware and ground data processing in the years preceding the implementation of NOAA's operational Hyperspectral Environmental Suite.

This paper provides an overview of the algorithm theoretical basis document (ATBD) that is being written by the University of Wisconsin Cooperative Institute for Meteorological Satellite Studies (UW-CIMSS) describing the science algorithms required in the ground processing of GIFTS data. The scope of this document is limited to the algorithms needed for the conversion of raw instrument counts (Level 0 data) to calibrated radiances (Level 1 data). The geo-location approach is described in Limaye et al. (2004) while the science algorithms for higher level products (2+) are described in Huang et al. (2004).

Instrument Description

The GIFTS instrument is an imaging Fourier Transform Spectrometer (FTS) designed to provide significant advances in water vapor, wind, temperature, and trace gas profiling from geostationary orbit. Imaging FTS offers an instrument approach that can satisfy the demanding radiometric and spectral accuracy requirements for remote sensing and climate applications, while providing the massively parallel spatial sampling needed for rapid high spatial resolution coverage of the Earth disk, as well as more frequent coverage of selected regions. The GIFTS baseline design uses focal plane detector arrays to cover two broad spectral regions; a longwave infrared band (685–1129 cm^{-1}) and a midwave/shortwave band (1650–2250 cm^{-1}). Each focal plane array contains a grid of 128 × 128 elements for a total of 16,384 fields of view with a nominal field of view diameter of 4 km at the sub-satellite point. Details of the initial instrument design are described in Bingham et al. (2000).

Algorithm Descriptions

The GIFTS sensor will sample the interferogram from each detector as a function of optical path delay and numerically filter the data in real-time to reduce the data rate before transmission to the ground-based X-band receiver. The sensor will obtain views of the onboard calibration references and deep space at regular intervals interleaved with the observations of Earth scenes. The ground reception facility will decode the telemetry stream and pass the GIFTS sensor data in real-time to a ground data processing facility. The GIFTS Level 0 to 1 ground data processing is anticipated to include the following tasks: i) Fourier transform of the GIFTS interferograms, ii) application of a non-linearity correction to the sensor data, iii) radiometric calibration, iv) spectral calibration, v) instrument line shape correction, and vi) spectral resampling to a common wavenumber grid.

Fourier Transform

One of the first operators applied to the GIFTS sensor data will be a Fourier transform to convert the measured interferograms into complex spectra. Since the measured interferograms (real) have been numerically filtered and decimated on-board using a complex function, the Level 0 interferograms are a series of complex numbers as a function of point number. A complex Fourier transform and data folding will be performed to convert the complex interferograms to complex spectra corresponding to a wavenumber scale that will be assigned in the spectral calibration process. There are a number of fast Fourier transform algorithms that could be used for this operation and the actual choice of FFT algorithm is deferred to the implementation stage. It is important to note, however, that the same FFT algorithm must be used throughout the Level 0 to 1 processing to avoid numerical inconsistencies. One of the implementation decisions will be whether to "zero fill" or truncate the measured interferograms to a convenient number of points to optimize computational efficiency.

Non-linearity Correction

The precise treatment of non-linearity is pending the collection of GIFTS ground test data using flight detectors. The expectation is that the GIFTS detector material should be highly linear in the range of photon fluxes used, but the electronics readout of the focal plane array can introduce a small signal non-linearity. The non-linearity correction algorithm to be used for the GIFTS interferometric data is based on the successful application of this technique to MCT detectors on the UW-CIMSS ground-based AERI

instrument and the UW-CIMSS Scanning-HIS instrument (Revercomb et al. 1998). The signal coming out of the detector readout is composed of an interferogram plus a scene dependent DC offset . The quadratic non-linearity can be modeled as the true signal plus an additional term made up of an unknown coefficient times the square of the sum of the true signal plus the DC level. In the spectral domain, this quadratic non-linearity has two terms; the first is slowly varying in wavenumber with a peak near zero wavenumber while the second term is linear in the uncalibrated spectrum. This non-linearity signature is quite different from that of conventional radiometers and means that the non-linearity coefficents can be determined independently from other calibration errors. The application of a non-linearity correction involves the reconstruction of the readout signal from the numerically filtered interferogram and the application of the quadratic correction. Higher order corrections can be applied if needed.

Radiometric Calibration

The top-level GIFTS calibration requirement is to measure brightness temperature to better than 1 K, with a reproducibility of ±0.2 K. A calibration concept has been developed for the GIFTS instrument configuration (Best et al. 2000). For in-flight radiometric calibration, GIFTS uses views of two on-board blackbody sources (300 K and 265 K) along with cold space sequenced at regular, programmable intervals. The temperature difference between the two internal blackbody views provides the sensor slope term in the calibration equation, while the deep space view corrects for radiant emission from the telescope by establishing the offset term. The blackbody references are cavities that follow the University of Wisconsin (UW) Atmospheric Emitted Radiance Interferometer (AERI) design, scaled to the GIFTS beam size (Best et al. 1997).

Two options were considered for the GIFTS radiometric calibration implementation. One follows the traditional approach of using a large area external blackbody viewed with a flat pointing mirror that is also used to view cold space and the earth (e.g., the current GOES imager and sounder). The second option replaces the large area external blackbody with a pair of internal small cavity blackbodies at different temperatures. Here we mainly discuss the internal blackbody approach, but the overall performance of both systems is compared and shown to meet advanced sounding requirements.

Assume that we represent the complex, uncalibrated spectrum for incident radiance by

(1)

$$C = \left[N\tau_t + B_t\left(1-\tau_t\right)\right] R_f + C_f$$

where is the transmission of the telescope (and external pointing mirror, if included), is the Planck emission at the temperature of the telescope, is the complex responsivity of the portion of the instrument behind the telescope, and is the complex offset arising from the same portion of the instrument behind the telescope. The term in the square brackets is the radiance incident on the turning flat, assuming there is no scattering from the telescope mirror. Similarly, the uncalibrated spectra for the internal hot and cold blackbodies can be represented as

(2)

$$C_H = B_H R_f + C_f \text{ and } C_C = B_C R_f + C_f$$

where the radiance emitted by the blackbodies is represented by B_H and B_C. Differencing the equations in (2) shows that the complex responsivity is given by

(3)

$$R_f = \frac{C_H - C_C}{B_H - B_C}$$

Therefore, the responsivity excluding the telescope can be monitored without changing the instrument pointing. Careful control of the detector temperature and use of low temperature-coefficient electronics should make the responsivity a very stable quantity.

Now, since the space view raw spectrum is given by Equation 1 with the scene radiance N replaced by B_s (which consists of space emission and any warmer tail of the field of view), differencing an earth view C_E at time t_E and a space view C_S spectrum interpolated to time t_E yields the relationship

(4)

$$N = \frac{1}{\tau_t} Re\left(\frac{C_E - C_S}{R_f}\right) + B_s = \frac{1}{\tau_t}(B_H - B_C) Re\left(\frac{C_E - C_S}{C_H - C_C}\right) + B_s$$

where Equation 3 has been used to eliminate the complex responsivity and where *Re* stands for the real part of the complex spectral ratio. The subtraction of the background assumes that instrument emissions have not changed significantly between the space view and the earth view. In practice, the space views must be performed frequently enough that temporal interpolation can approximate the required simultaneity with only small errors. When the telescope transmission is known, Equation 4 is the basic calibration relationship. In fact, the transmission will be measured both from piece-part reflectivity measurements and from full aperture blackbody observations on the ground, so it will be well known at the start of the mission. The equation is very similar to that for a full aperture "hot" blackbody calibration approach for which the cold blackbody raw spectrum in the denominator would be replaced by the space view spectrum C_S. The telescope transmission can also be determined in flight using internal blackbody and space views as described in Best et al. (2000). Note that in Equation 4, the ratio of differences of complex spectra automatically eliminates the phase of the raw spectra (Revercomb et al. 1988). As for an external blackbody calibration, phase correction is not needed and in fact, should be avoided. The details of algorithm implementation are deferred to a future paper.

Figures 1 and 2 show the GIFTS baseline calibration radiometric accuracy compared to the external blackbody approach, assuming the same parameter uncertainties for both, except for the emissivity uncertainty of the external blackbody (increased to 0.005 to account for its lower cavity enhancement factor). At each scene temperature, the calibration accuracy is the root sum square (RSS) combination of several system uncertainties, including those due to temperature and emissivity for each of the blackbodies, the structure temperatures affecting reflection from the blackbodies, and the telescope mirror reflectivity. Also included is the contribution from the time variation of the telescope temperature between the space and earth views. For the case where the transmission is known, we have assumed that ground based testing with a large external blackbody has determined the transmission of the telescope to within 0.2%. Table 1 presents the input parameters and uncertainty magnitudes that were used in the uncertainty analysis model to generate the GIFTS calibration accuracies. Even including the uncertainty due to the characterization of the telescope transmission in-flight, the expected calibration accuracy is well within the nominal 1 K requirement for accurate atmospheric sounding. The estimates shown in Figures 1 and 2 are derived from specifications presented at the GIFTS preliminary design review and will be updated following the critical design review. The optimal methodology for the determination of telescope transmission on-orbit continues to be a subject of ongoing research.

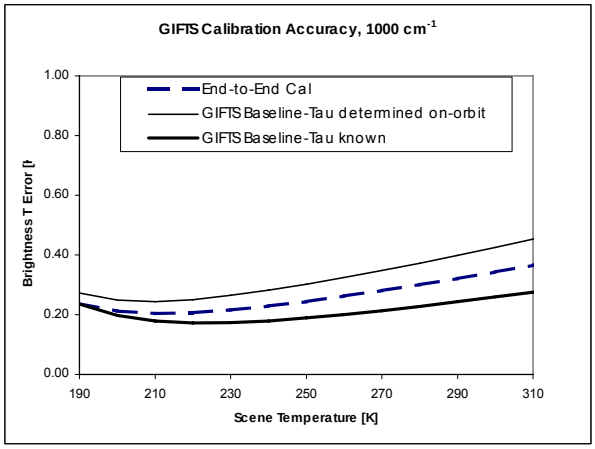

Figure 1. Calibration uncertainty estimate at 1000 cm-1 comparing a large aperture external "End-to-End" calibration target to the GIFTS baseline design which uses two high emissivity targets located behind the telescope. Tau is the telescope transmission.

Input Parameters		
wn	Wavenumber	See figures.
tau	Telescope (2) elements and blackbody mirror transmission	0.913
Thbb	Hot blackbody temperature	300 K
Tcbb	Cold blackbody temperature	265 K
Tspace	Temperature of space	4 K
Ttel	Telescope temperature	265 K
Tstr	Temperature of structure reflecting into BB's	265
Ehbb	Emissivity of hot blackbody	0.996
Ecbb	Emissivity of cold blackbody	0.996
Parameters Used For Temperature Stability		
Etel	Telescope emissivity	0.087
TauTot	Total transmission through instrument	0.205
TtelΔ	Change in telescope temp between earth and space views	0.5 K
Uncertainty Magnitudes		
ΔThbb	0.07 K	
ΔTcbb	0.07 K	

ΔEhbb	0.002 K
ΔEcbb	0.002 K
ΔTstr	5 K
Δtau	0.0086 RSS
ΔTtel	2 K

Table 1. Calibration uncertainty analysis parameters.

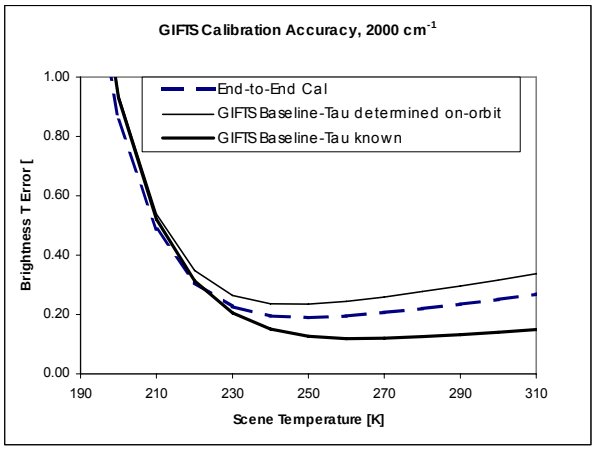

Figure 2. Same as Figure 1 but at 5 microns.

Spectral Calibration

The spectral calibration used for GIFTS will build upon the experience of ground-based and aircraft FTS systems (AERI, HIS, S-HIS, and NAST-I) designed with a single on-axis field-of-view (FOV) (Revercomb et al. 1998, Cousins and Smith 1997). The spectral characteristics of these instruments can be defined by an Instrument Line Shape (ILS) and a spectral sampling interval. The observed spectrum is the atmospheric spectrum convolved with the ILS and sampled at equally spaced points starting at zero wavenumber.

The spectral sampling scale is maintained very accurately by the stable laser used to trigger sampling at equal intervals of Optical Path Difference (OPD). Because the wavenumber samples are known to be equally spaced as well, the calibration of this spectral scale is determined for an entire, broad spectral band by the determination of the proper wavenumber for any single spectral feature in the band. We use the comparison of observed atmospheric spectra to line-by-line radiative transfer calculations (based on observed atmospheric state parameters) to determine the proper wavenumber scale. This calibration process transfers the very accurate positions of prominent spectral line features in the HITRAN database to the observed spectral scale (Rothman et al. 1998). An effective laser wavenumber parameter is used to describe this scale.

An example of the spectral scale calibration process is shown for observations of upwelling infrared radiance from the UW S-HIS aircraft instrument during the NASA KWAJEX experiment. Figure 4 shows a comparison of measured and calculated S-HIS spectra for the 722–738 cm-1 spectral region from a clear sky flight of the NASA DC-8 aircraft on 12 September 1999. This spectral region has been chosen for spectral calibration, because of the high accuracy of the measured spectral line parameters of the dominant CO_2 absorption lines in this region. Figure 4 shows integrated residuals (observed minus

calculated) for this spectral region versus the unit-less quantity of the effective laser wavenumber divided a reference wavenumber value. There is a well defined minimum in this curve, which can be used to determine the S-HIS spectral calibration. From an analysis of many similar cases collected over the DOE ARM site in north central Oklahoma (Tobin et al. 2003), the S-HIS effective laser wavenumber (and spectral calibration) has been determined with an accuracy of ~1 part in a million. Similar accuracy is expected for the GIFTS spectral calibration.

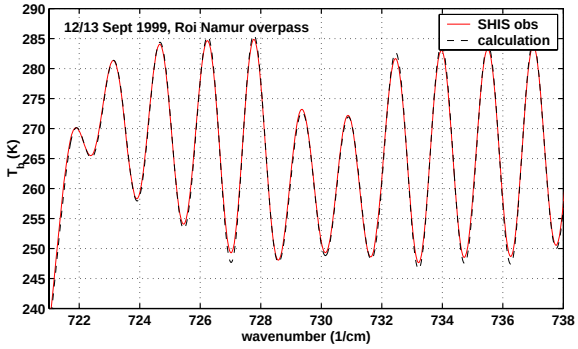

Figure 3. Observations of the regularly spaced CO2 emission lines in the upwelling infrared radiance obtained by the UW Scanning HIS instrument are compared to a line-by-line calculation based upon a coincident radiosonde temperature and water vapor vertical profile and the HITRAN spectroscopic database.

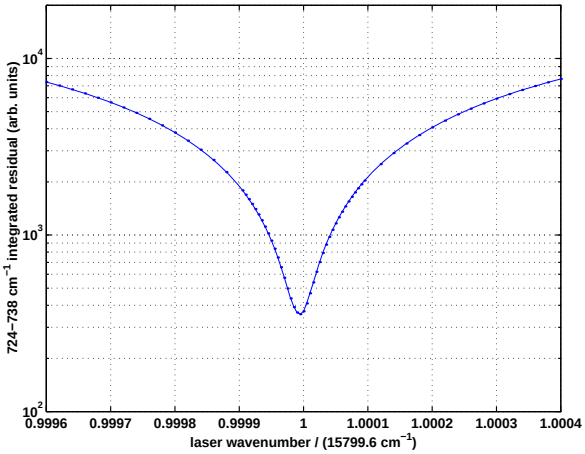

Figure 4. Fitting the residuals (observed-calculated) in the 724 to 738 cm^{-1} region for the effective S-HIS laser wavenumber by adjusting the observed wavenumber scale in the range of -0.04% to +0.04%.

The major difference between GIFTS and these single-FOV instruments is that each pixel of its imaging detector array has a different wavenumber scale. This effect is a very predictable result of the different angles traversed through the interferometer by the beams focused on each pixel. While the central pixel is nominally the same as the single FOV instruments discussed above, off-axis detectors are irradiated by beams passing through the interferometer at non-zero mean angles. A non-zero mean angle causes the OPD for any given position of the interferometer Michelson mirror to be reduced by the cosine of the off-axis angle.

This OPD scale variation with pixel location is illustrated in Figure 5, which shows a simulated interferogram for the GIFTS longwave band with a uniform scene. For the longwave FPA, the double sided interferogram is sampled at 2048 points. The exact OPD sampling positions, however, vary for each

pixel depending on the mean off-axis angle, and the single pixel half-angle, b. The magnified portion of the interferogram illustrated in Figure 5 shows the 0.66 cm region enhanced by the equal spacing of 15 (m CO2 lines. Three individual OPD points from an on-axis interferogram (0.6637, 0.6654, 0.6671 cm) are also shown for every pixel along the diagonal from the center to a corner pixel of the detector array. Note that all of the points fall on the same continuous interferogram. For this uniform scene, the only significant difference is a small change in the OPD sampling interval. In other words, the differences can be rigorously eliminated by interpolation to a standard reference wavenumber scale.

The on-orbit spectral calibration process for GIFTS will make use of comparisons of observations with detailed radiative transfer calculations in order to assign a wavenumber scale to each field of view in each of the two GIFTS focal plane arrays. The plan for resampling of the GIFTS spectra to a common wavenumber grid is described in a subsequent section.

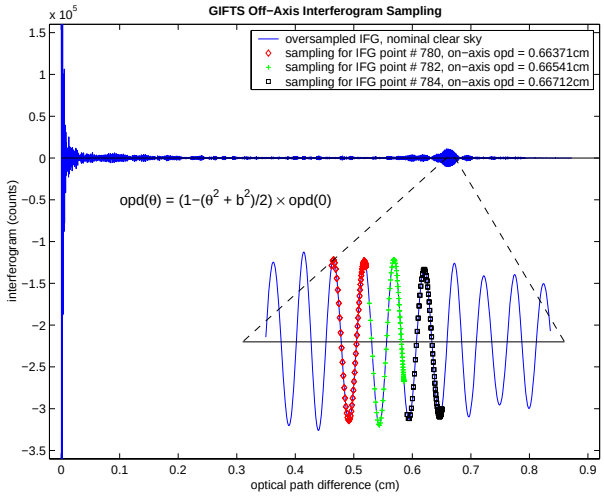

Figure 5. Illustration of the OPD sampling variations due to off-axis beams. The off-axis pixels sample the interferogram at smaller OPDs (compared to the on-axis beams), according to the given equation for OPD(θ). For three different on-axis sample points, the range of off-axis sampling points (from the near-center pixels to the corner pixels of the focal plane array) are shown in the blowup.

Instrument Line Shape Correction

To first order, the ILS is a sinc function (sin(x)/x). However, for accurate radiometry, it is important to make sure that the FOV is carefully aligned about the central axis of the interferometer and that an effective b is determined. Again, we use comparisons with specific regions of calculated atmospheric spectra to refine our nominal values of b (based on optical design). The finite field-of-view effect on ILS for the AERI, Scanning HIS and NAST-I instruments is negligible for the longwave band, but can be significant in the shortwave band. Procedures to remove the relatively small effects of ILS are routinely applied to the data from AERI, Scanning HIS and NAST-I. A similar behavior is realized for the geostationary orbiting GIFTS because of the extremely small range of angles contributing to each individual detector pixel (<1 mrad in the interferometer). As a result, the variation of ILS across the array is extremely small and could even be ignored without introducing significant errors. The ILS is essentially a pure sinc function and exhibits extremely small ILS differences between the on-axis and extreme-diagonal pixels. In the GIFTS primary sounding mode, the self-apodization is very small—less than 1% over the array. In fact, because of the very small angles involved for GIFTS, the deviations from a pure sinc-function ILS are significantly smaller than for the aircraft and ground-based instruments discussed above. Figure 6 shows that the peak brightness temperature effect of ignoring ILS variations is less than 0.15 K for a typical earth scene.

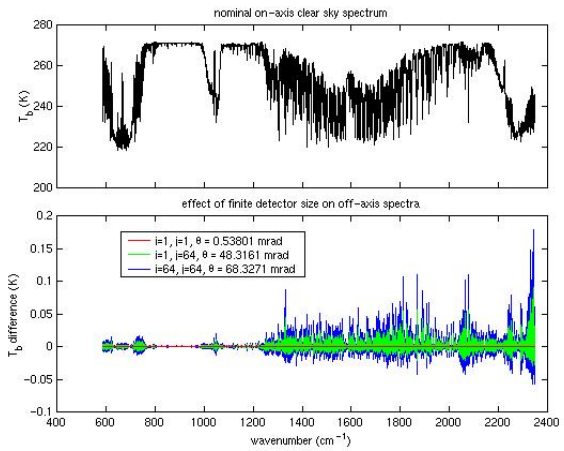

Figure 6. A nominal clear sky spectrum (top panel) and the magnitude of the finite detector size self-apodization effect in brightness temperature (bottom panel) for three FPA pixel locations. In the bottom panel, the i, j = (1,1) curve is the dark curve near zero, the i, j = (1,64) has a slightly larger magnitude, and the i, j = (64,64) curve has the largest magnitude.

Wavenumber Resampling (Off-axis Correction)

Once the spectral calibration is determined for each of the fields of view, the GIFTS radiance spectrum can be re-sampled from the original sampling interval to a standard reference wavenumber scale. The re-sampling can be performed in software using an FFT, "zero padding", and linear interpolation of an over-sampled spectrum. An alternative approach using a convolution rather than an FFT to resample the spectra will be evaluated for possible performance advantages. The result of the wavenumber resampling operation will be that all of the GIFTS spectra will have a common wavenumber scale independent of their location in the focal plane array. This is essential for the routine comparison of observations and radiative transfer calculations needed in the production of Level 2 products, e.g. temperature and humidity profiles.

Acknowledgements

This work was recently supported by NOAA federal grant NAO7EC0676 with previous support under NASA contract NAS1-00072.

References

Best, F. A., H. E. Revercomb, G. E. Bingham, R. O. Knuteson, D. C. Tobin, D. D. LaPorte, and W. L. Smith, 2000: Calibration of the Geostationary Imaging Fourier Transform Spectrometer (GIFTS), presented at SPIE's Second International Asia-Pacific Symposium on Remote Sensing of the Atmosphere, Environment, and Space, Sendai, Japan, 9–12 October 2000.

Best, F., H. Revercomb, D. LaPorte, R. Knuteson, and W. Smith, 1997: Accurately calibrated airborne and ground-based Fourier Transform Spectrometers II: HIS and AERI calibration techniques, traceability, and testing, presented at the Council for Optical Radiation Measurements (CORM) 1997 Annual Meeting, National Institute of Standards and Technology (NIST), Gaithersburg, MD, April 29, 1997.

Bingham, G. E., R. J. Huppi, H. E. Revercomb, W. L. Smith, F. W. Harrison, 2000: A Geostationary Imaging Fourier Transform Spectrometer (GIFTS) for hyperspectral atmospheric remote sensing,

presented at SPIE's Second International Asia-Pacific Symposium on Remote Sensing of the Atmosphere, Environment, and Space, Sendai, Japan, 9–12 October 2000.

Cousins, D., and W. L. Smith, 1997: National Polar-Orbiting Operational Environmental Satellite System (NPOESS) Airborne Sounder Testbed-Interferometer (NAST-I), Proceedings of SPIE, 3127, 323-331.

Dittberner, G. J., James J. Gurka, and Roger W. Heymann, 2003: NOAA's GOES satellite program—status and plans, 19th Conference on IIPS, 83rd Annual Meeting, 8–13 February 2003, Long Beach, CA. Published by the American Meteorological Society, Boston, Mass.

Gurka, J. J., Gerald J. Dittberner, Pamela Taylor, and Timothy J. Schmit, 2003: Specifying the requirements for imaging and sounding capabilities on the GOES-R series, 12th Conference on Satellite Meteorology and Oceanography, 83rd Annual Meeting, 8-13 February 2003, Long Beach, CA. Published by the American Meteorological Society, Boston, Mass.

Huang, H-L., J. Li, E. Weisz, K. Baggett, J. E. Davies, J. R. Mecikalski, B. Huang, C. S. Velden, R. Dengel, S. A. Ackerman, E. R. Olson, R. O. Knuteson, D. Tobin, L. Moy, D. J. Posselt, H. E. Revercomb, and W. L. Smith, 2004: Infrared hyperspectral sounding modeling and processing, 20th Conference on IIPS, 84th AMS Annual Meeting, 11-15 January 2004, Seattle, WA. Published by the American Meteorological Society, Boston, Mass.

Limaye, S. S., T. Smith, R. O. Knuteson, H. E. Revercomb, 2004: Geolocation of the Geosynchronous Imaging Fourier Transform Spectrometer (GIFTS) data, 20th Conference on IIPS, 84th AMS Annual Meeting, 11-15 January 2004, Seattle, WA. Published by the American Meteorological Society, Boston, Mass.

Revercomb, H.E., V.P. Walden, D.C. Tobin, J. Anderson, F.A. Best, N.C. Ciganovich, R.G. Dedecker, T. Dirkx, S.C. Ellington, R.K. Garcia, R. Herbsleb, R.O. Knuteson, D. LaPorte, D. McRae, and M. Werner, 1998: Recent results from two new aircraft-based Fourier transform interferometers: The Scanning High-resolution Interferometer Sounder and the NPOESS Atmospheric Sounder Testbed Interferometer, 8th International Workshop on Atmospheric Science from Space using Fourier Transform Spectrometry (ASSFTS), Toulouse, France, 16-18 November 1998.

Revercomb, H. E., F. A. Best, R. G. Dedecker, T. P. Dirkx, R. A. Herbsleb, R. O. Knuteson, J. F. Short, and W. L. Smith, 1993: Atmospheric Emitted Radiance Interferometer (AERI) for ARM. In Fourth Symposium on Global Change Studies, January 17–22, 1993, Anaheim, California. Published by the American Meteorological Society, Boston, Mass.

Revercomb, H. E., H. Buijs, H. B. Howell, D.D. LaPorte, W. L. Smith, and L. A. Sromovsky, 1988: Radiometric calibration of IR Fourier Transform Spectrometers: solution to a problem with the High Resolution Interferometer Sounder", Appl. Opt., 27, 3210–3218.

Rothman, L. S., et al., 1998: The HITRAN Molecular Spectroscopic Database and HAWKS: 1996 Edition, Journal of Quantitative Spectroscopy and Radiative Transfer, 60, pp. 665-710.

Smith, W. L., D. K. Zhou, F. W. Harrison, H. E. Revercomb, A. M. Larar, A. H. Huang, B. Huang, 2000: Hyperspectral remote sensing of atmospheric profiles from satellites and aircraft, presented at SPIE's Second International Asia-Pacific Symposium on Remote Sensing of the Atmosphere, Environment, and Space, Sendai, Japan, 9–12 October 2000.

Tobin, D. C., H. E. Revercomb, R. O. Knuteson, 2003: On-orbit Spectral Calibration of the Geosynchronous Imaging Fourier Transform Spectrometer (GIFTS), in Proceedings of CALCON 2003, Characterization and Radiometric Calibration for Remote Sensing, Space Dynamics Laboratory / Utah State University, Logan, Utah, 15-18 September 2003.

Appendix 2: The GIFTS On-Board Blackbody Calibration System – F. Best et al. 2004

Fred A. Best[a], Henry E. Revercomb[a], Robert O. Knuteson[a], David C. Tobin[a], Scott D. Ellington[a],

Mark W. Werner[a], Douglas P. Adler[a], Raymond K. Garcia[a], Joseph K. Taylor[a], Nick N. Ciganovich[a], Willliam L. Smith[b], Gail E. Bingham[c], John D. Elwell[c], and Deron K. Scott[c]

[a]University of Wisconsin-Madison, Madison, WI
[b]Hampton University, Hampton, VA
[c]Utah State University, Logan, UT

The NASA New Millennium Program's Geosynchronous Imaging Fourier Transform Spectrometer (GIFTS) instrument provides enormous advances in water vapor, wind, temperature, and trace gas profiling from geostationary orbit. The top-level instrument calibration requirement is to measure brightness temperature to better than 1 K (3 sigma) over a broad range of atmospheric brightness temperatures, with a reproducibility of ±0.2 K. For in-flight radiometric calibration, GIFTS uses views of two on-board blackbody sources (290 K and 255 K) along with cold space, sequenced at regular programmable intervals. The blackbody references are cavities that follow the UW Atmospheric Emitted Radiance Interferometer (AERI) design, scaled to the GIFTS beam size. The cavity spectral emissivity is better than 0.998 with an absolute uncertainty of less than 0.001. Absolute blackbody temperature uncertainties are estimated at 0.07 K. This paper describes the detailed design of the GIFTS on-board calibration system that recently underwent its Critical Design Review. The blackbody cavities use ultra-stable thermistors to measure temperature, and are coated with high emissivity black paint. Monte Carlo modeling has been performed to calculate the cavity emissivity. Both absolute temperature and emissivity measurements are traceable to NIST, and detailed uncertainty budgets have been developed and used to show the overall system meets accuracy requirements. The blackbody controller is housed on a single electronics board and provides precise selectable set point temperature control, thermistor resistance measurement, and the digital interface to the GIFTS instrument. Plans for the NIST traceable ground calibration of the on-board blackbody system have also been developed and are presented in this paper.

Introduction

The Geosynchronous Imaging Fourier Transform Spectrometer (GIFTS) instrument requires highly accurate radiometric calibration in order to provide its enormous advances in water vapor, wind, temperature, and trace gas profiling from geostationary orbit.[1,2,3] The unique GIFTS radiometric calibration scheme[4-7] uses two internal blackbody sources located behind the instrument telescope, combined with a space view, to provide end-to-end instrument calibration accuracy better than 1 K (3-sigma). The reproducibility is better than ±0.2 K. The calibration scheme builds on well-established general techniques for calibrating interferometer instruments.[8-10] There is a significant advantage to the internal blackbody approach used by GIFTS[4], in large part because it is practical to achieve a high emissivity with a small size blackbody. Because the blackbodies are small and internally located, they also provide significant immunity from solar forcing. The blackbodies are periodically viewed via a flip-in mirror that is located near the field stop behind the instrument telescope. The blackbodies, which

are independently controlled to different temperatures, are located on a translating table that positions either the ambient (255 K) or hot (290 K) blackbody into the view of the flip-in mirror. An instrument-level GIFTS calibration model involving blackbody temperature and temperature uncertainty, blackbody emissivity and emissivity uncertainty, telescope and flat mirror element temperatures, and structural temperatures has been developed and used to assess and budget various blackbody parameter uncertainties. The budget allocation for the blackbody subsystem is ≤ 0.5 K. Figure 1 illustrates how this top-level blackbody requirement is flowed down to the key parameters of the blackbody subsystem. This paper deals with the first four boxes involving blackbody temperature and emissivity. The structural temperature box deals with the blackbody radiance reflected from the surroundings. This paper describes the design and calibration of the GIFTS blackbody subsystem that consists of two nearly identical blackbodies and the associated controller that provides temperature readout and control. Table 1 presents the top-level requirements for the blackbody subsystem along with the current best estimate for each parameter. In all cases the design meets the requirements. An engineering model of all the hardware has been fabricated and is currently undergoing testing and calibration.

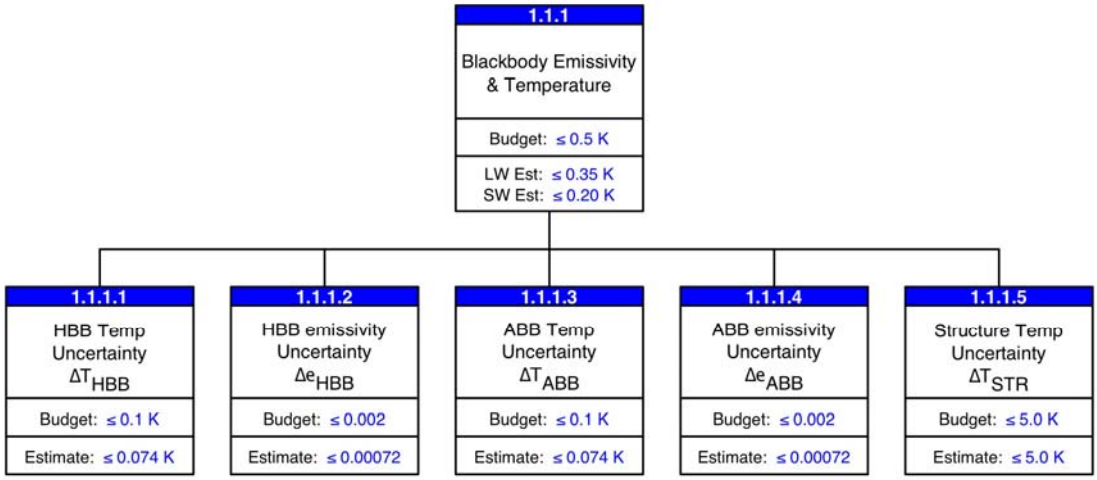

Figure 1. Top-level blackbody calibration error tree showing uncertainties associated with important subsystem parameters.

Parameter	Specification	Current Best Estimate
Ambient Blackbody Nominal Set Point	255 K	255 K
Hot Blackbody Nominal Set Point	290 K	290 K
Temperature Measurement Uncertainty	< 0.1 K (3 sigma)	< 0.074 K (3 sigma)
Ambient Blackbody Emissivity	> 0.996	> 0.998
Hot Blackbody Emissivity	> 0.996	> 0.998
Emissivity Uncertainty	< 0.002	< 0.00072 (3 sigma)
Wavelength	680 - 2,300 cm-1	680 - 2,300 cm-1
Source Aperture	2.54 cm	2.54 cm
Source FOV (full angle)	> 10°	> 10°
Mass (two blackbodies plus controller)	< 2.4 kg	< 2.1 kg
Power: average/max	< 2.2/5.2 W	< 2.2/5.2 W
Envelope	< 8 x 8 x 15.5 cm	< 8 x 8 x 15.4 cm

Table 1. Top-level blackbody subsystem specifications with current best estimates.

Blackbody Mechanical and Thermal Design

The key objective of the blackbody design is to provide an isothermal emissivity-enhancing cavity, that uses minimal power to maintain stable temperatures above the surrounding environment. In addition, the design must be structurally sound in order for the blackbody to survive the launch environment. The mechanical design of the blackbody is illustrated in Figure 2. The two blackbodies (hot and ambient) are nearly identical – the main difference being the thermistor nominal resistance that was selected to optimize temperature measurement resolution.

Mechanical Design

The cavity is machined from aluminum and has an entrance aperture of 1.0 inch. The cavity shape is a scaled down version of the design used in the University of Wisconsin (UW) developed Atmospheric Emitted Radiance Interferometer (AERI).11,12,13 The inner wall of the cavity is painted with Aeroglaze Z306 – a popular diffuse, high emissivity (0.94 to 0.97), and low outgassing black polyurethane. A Minco thermofoil heater, used for temperature control, is located on the outer cylindrical section of the cavity. The cavity is mounted to a thin wall support tube and mounting base constructed of Noryl GFN3, a glass reinforced plastic from GE. The material was chosen for its high strength, low thermal conductivity, and low thermal expansion mismatch compared to aluminum (the survival temperature of the blackbody is 180 K). Four holes in corners of the mounting base (not visible in Figure 2) are used for attachment of the blackbody to the translating table of the GIFTS instrument. The outer enclosure is constructed of aluminum, which minimizes temperature gradients in the cavity. The enclosure has a load path to the mounting base through a flange located mid-way up the support tube. This configuration uses the Noryl support tube to provide thermal isolation from both the cavity and the mounting base.

The structural design of the blackbody provides the needed strength and stiffness to survive the launch environment. The quasi-static design limit load is 50 G, and the random vibration environment is 8 Grms. To minimize vibration coupling with GIFTS instrument the minimum natural frequency requirement for the blackbody is specified at 150 Hz. The lowest natural frequency measured after random vibration and thermal cycling tests is 180 Hz.

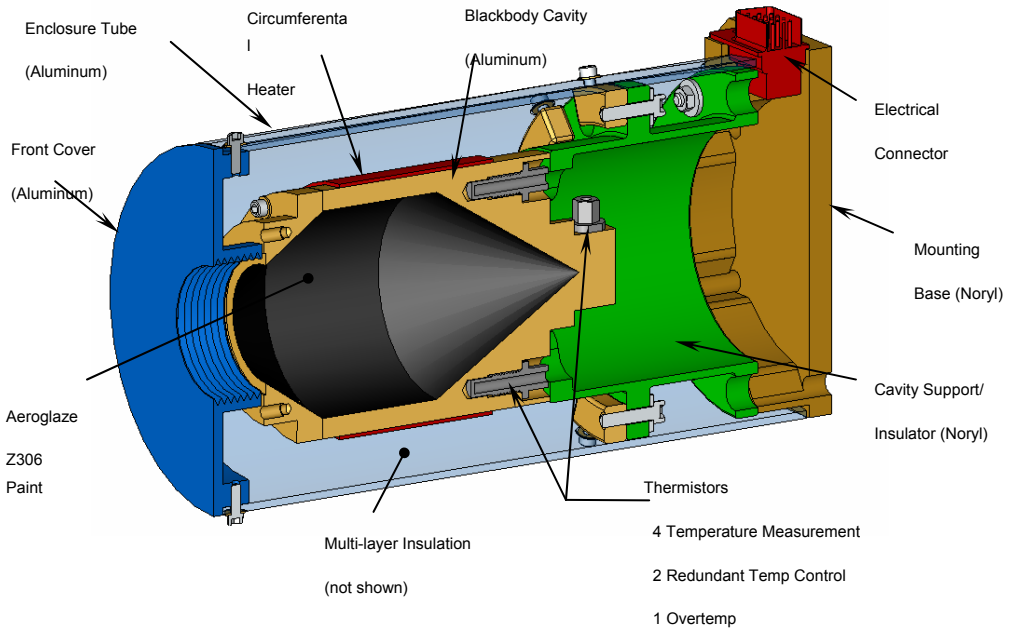

Figure 2. Blackbody section view illustrating key elements of the mechanical and thermal design. The heated isothermal cavity is supported structurally and isolated thermally via the Cavity Support Tube. Multi-layer insulation minimizes radiation heat transfer. The cavity entrance aperture (left side of figure) is 1.0 inch in diameter.

Thermal Design

In addition to withstanding payload launch loads, the blackbody structure provides robust thermal performance in a demanding environment. The blackbodies are mounted to a platform 60-110 K colder than the 255-290 K cavity operating temperatures, while the surroundings fluctuate from 140 to 300 K. The cavity temperatures must be extremely uniform (goal for maximum gradient is less than 0.2 K) and stable (goal for stability is within 10 mK over 10 minutes under maximum expected instrument thermal perturbation), therefore the cavity must be well insulated from the surrounding environment. To minimize radiant heat transfer Multi-Layer Insulation (MLI) is installed on the outside of the enclosure and between the enclosure and cavity. Due to the high temperature surroundings radiating heat into the black cavity, there is a risk of the ABB cavity temperature being driven above its set point. As a result the amount of insulation between the base and the cavity must be limited, requiring a tradeoff with heater power. In spite of this compromise the blackbodies are able to provide the set point temperatures with less than 0.5 W total heater power. The current estimate of the maximum temperature gradient within the cavity for the worst-case on-orbit condition is less than 0.09 K.

Thermistor Implementation

There are seven Thermometrics Ultra-stable SP-60 thermistors mounted into the cavity as detailed in Figure 3. Four of these sensors are used for reporting cavity temperature, two redundant sensors are used for temperature control, and one is dedicated to over-temperature protection. The thermistors were potted at Thermometrics into UW provided threaded aluminum housings, using methods similar to those used in

their off-the-shelf probe assemblies. The housing approach allows acceptance testing (including thermal cycling) and selection to be conducted on a thermistor assembly that is unlikely to change after being bonded with conductive epoxy into the cavity. The same thermistor type and similar mounting scheme were used successfully in the SABER (Sounding of the Atmosphere using Broadband Emission Radiometry) instrument, developed by the Utah State University Space Dynamics Laboratory. The SP-60 thermistor is expected to provide long-term stability better than 50 mK over a period of 10 years. This includes effects of atomic diffusion of the metal oxide matrix material, and any thermally or mechanically induced micro crack migration to grain boundaries.

An important aspect of the thermistor mounting configuration is that it provides a minimal temperature bias from heat leaking out the thermistor lead wires. Modeling and testing predict that this bias will be less than 8 mK in the worst case on-orbit thermal environment (blackbody at 313 K, radiative environment at 140 K, and mounting interface at 190 K). This conservatively assumes that the planned additional thermal heat-sinking of the leads to the flat portion at the cavity apex is totally ineffectual.

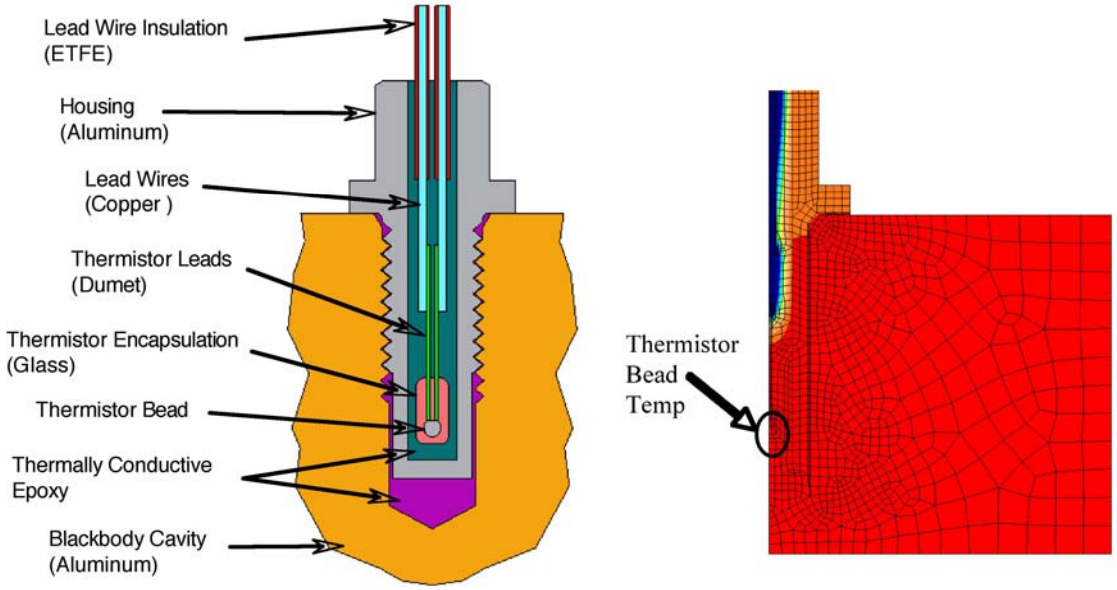

Figure 3. Section view of the thermistor mounting scheme, designed to provide a high degree of thermal coupling of the thermistor sensor to the aluminum cavity (left). Axisymmetric finite element thermal model (right) used to show a less than 8 mK gradient exists between the thermistor bead and surrounding cavity aluminum, due to the thermistor lead wire heat leak.

Blackbody Emissivity Modeling and Uncertainty Budget

Monte Carlo ray tracing methods were used to calculate the cavity emissivity. The inputs to this modeling include, cavity geometry and paint reflection and diffusity as a function of wavelength. An emissivity error budget was developed that takes into account paint characteristics and modeling uncertainties.

Black Paint Properties

The blackbody cavity is painted with Aeroglaze Z306 diffuse black polyurethane. The left plot in Figure 4 presents the emissivity verses wavelength for up to three coats of this paint. The GIFTS blackbody will be painted with three coats providing a total thickness of 0.003 inches. The emissivity measurements shown were made by Labsphere on blackbody witness samples from a lot of AERI blackbodies. These measurements of Z306 emissivity agree, to within the stated uncertainty of < 0.004, with measurements

by NIST of a sample they painted for a different application. The diffusity characteristics shown on the right plot in Figure 4 were estimated from data published by Persky[14], using a cosine angular dependence to fit measurements of Z306 made at 20° and 60°. No direct measurements of paint emissivity are made on the painted cavity because the testing apparatus is not physically compatible with this geometry. For this reason witness samples that are painted along with the cavities are used to characterize paint emissivity. During spray painting, a fixture is used to hold the witness samples in a configuration that mimics the cavity cone section. This helps make the paint application on the witness samples better represent the actual cavity paint. NIST will measure the emissivity of the blackbody witness samples to within 0.4%.

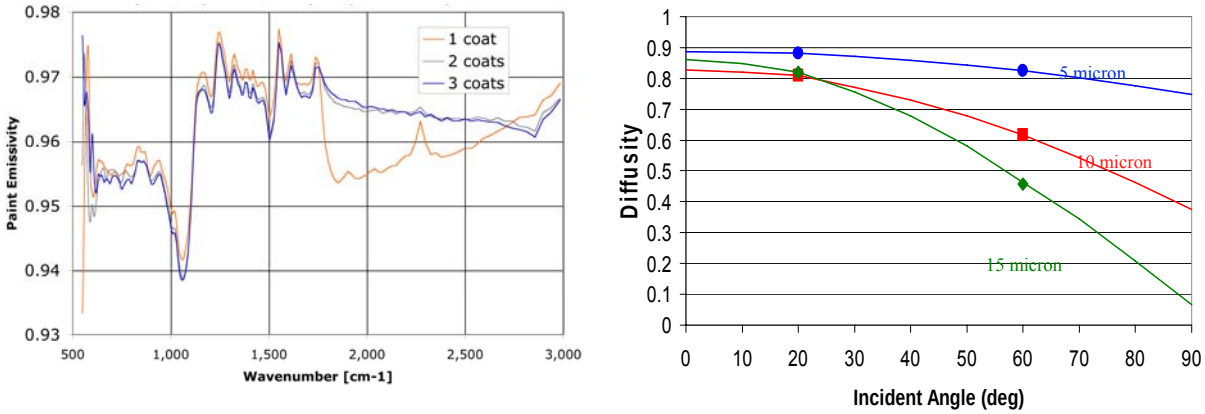

Figure 4. Aeroglaze Z306 emissivity (left) and diffusity (right) characteristics used in the Monte Carlo emissivity ray trace modeling. Three coats of paint are applied for a total thickness of 0.003 inches.

Monte Carlo Ray Tracing to Determine Cavity Emissivity

The GIFTS blackbody emissivity model uses a unique algorithm of the Monte Carlo method described in Prokhorov.[15] The algorithm is implemented for a wide class of axially symmetric cavities formed by rotation of polygonal line around the axis. The algorithm allows simulation of real radiometric systems containing radiating cavity with arbitrary axially symmetric temperature distribution, flat detector with circular sensitive element, and up to two apertures with arbitrary displacement of centers relative to the cavity axis. The cavity geometry used to simulate the GIFTS blackbodies is given in Figure 5.

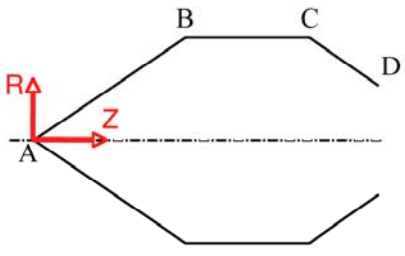

GIFTS blackbody internal cavity cross-section (dimensions in inches)

	Z	R
A	0	0.01
B	1.39	0.88
C	2.50	0.88
D	3.06	0.50

Figure 5. GIFTS blackbody cavity geometry used in Monte Carlo emissivity analysis.

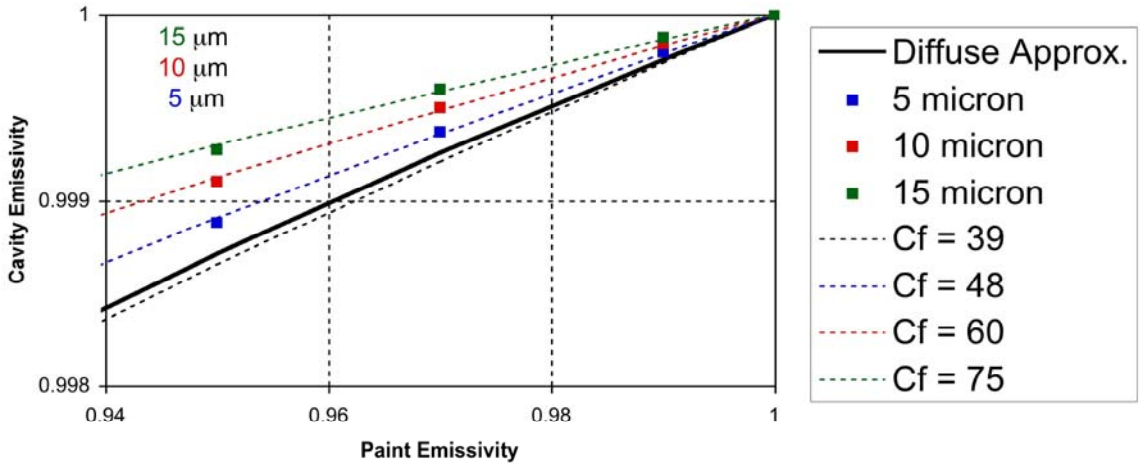

Figure 6. GIFTS blackbody isothermal cavity emissivity (average normal) computed using the STEEP3 model. The results for the diffusivity ratios shown in Fig. 4, for Aeroglaze Z306 are shown as symbols and a fit to the cavity factor approximation is shown as dashed lines. The solid line is the STEEP3 computation assuming the paint was entirely diffuse.

The GIFTS blackbody cavity is a relatively simple geometry with rotational symmetry about the central axis. The commercially available numerical model STEEP3 (Virial, Inc.) was used to compute the average normal emissivity using diffusity versus angle data from Persky (1999) at three wavelengths spanning the thermal infrared. The results are shown in Figure 6 compared with a fit to an approximate analytic equation that parameterizes the effective blackbody emissivity in terms a cavity factor. The analytic approximation to the GIFTS blackbody emissivity is given by: Cf = (1-E-1paint)/(1-E-1cavity). This analytic formula is useful in the propagation of errors because it can be easily differentiated. The formula also is convenient to implement in data processing software. Figure 6 shows that the GIFTS cavity shape leads to an isothermal emissivity greater than 0.998 for all wavelengths.

Emissivity Uncertainty Budget

A budget has been developed for the uncertainty in the estimate of the GIFTS blackbody emissivity. This budget estimate takes into account four items; uncertainty in the paint witness sample measurement, uncertainty in the paint application variation, an estimate of the long-term paint stability, and an estimate of the error arising from using an approximate cavity factor to represent the Monte Carlo model calculations. The equation for cavity factor given in the previous subsection is used to propagate the sources of the errors into the final emissivity uncertainty. Three sigma errors are used throughout. The results of the budget analysis are given in Table 2.

	Uncertainty (3 sigma)	Note	for Ep=0.94 f=39	²Ec	²Ec (3 sigma)
Paint Witness Sample Measurement	0.4% Ep	[1]	²Ep=0.0038	(1/f)*²Ep	0.00010
Paint Application Variation	1.0% Ep	[2]	²Ep=0.0094	(1/f)*²Ep	0.00024
Long-term Paint Stability	2.0% Ep	[3]	²Ep=0.0188	(1/f)*²Ep	0.00048
Cavity Factor	30% f	[4]	²f=11.7	(1-Ep)/f^2*²f	0.00046
				RSS	0.00072

Notes:
[1] Factor of 1.5 times NIST* Stated Accuracy for 2 sigma
[2] Worst case difference between 1 and 3 coats
[3] 2 x above
[4] Accounts of Cavity Model Uncertainty
* NIST Stated accuracy is 4% of Reflectivity (2 sigma)

Table 2. GIFTS blackbody emissivity error budget.

Blackbody Controller

The blackbody controller measures and controls the temperature of both blackbodies. The controller has two modes: Constant Temperature and Constant Power. Mode may be selected independently for each blackbody. In the Constant Temperature mode, heater power is controlled to hold the blackbody temperature very close to the set point. In the Constant Power mode, the heater duty cycle is held constant at the commanded value. Heater power may be set to zero, in which case the blackbody temperature closely tracks the ambient temperature. A functional block diagram of the blackbody controller is shown in Figure 7. The controller communicates with the instrument Command and Data Handler through the SDL Bus interface. Commands may be sent to the controller to change operating modes and parameters.

Data is also sent to the C&DH through this interface. Thermistors are used to measure temperature of the blackbody cavity. Internal calibration resistors are measured during each sampling cycle to minimize measurement error. Dedicated redundant blackbody thermistors are used to control temperature. The temperature set point is set via the data interface.

Temperature Control

In the constant temperature mode, the blackbody temperature is maintained at a set point determined by the set point integer. One of the two dedicated redundant control thermistors on each blackbody is used to control its temperature. The difference between the thermistor resistance and the set point is processed by an analog Proportional-Integral-Derivative (PID) circuit to determine the required heater power. A pulse width modulator (PWM) drives the blackbody heater. The heater switch operates at approximately 10 Hz, with low output slew rates to minimize EMI. PID parameters are determined by component values and are selected to match the characteristics of the blackbody. Figure 8 shows that blackbody temperature disturbances less than 2 mK result from the expected on-orbit changes in radiated power (140 mW) that arises from the re-positioning of the flip-in mirror for the GIFTS instrument calibration (presenting a view of the cold aft end of the instrument to the blackbody). In the Constant Power mode, the set point integer controls the heater duty cycle. In both modes, over-temperature protection is provided using a dedicated thermistor.

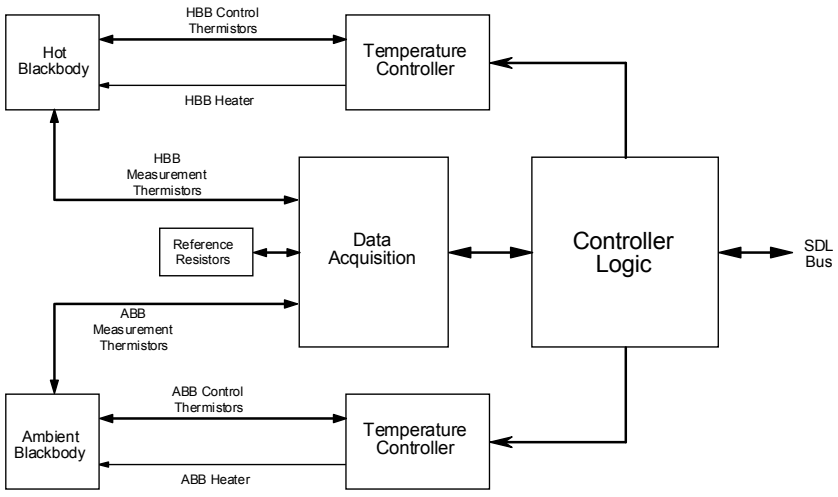

Figure 7. Functional block diagram of the blackbody controller. Each of the blackbodies is independently controlled. Communication to and from the instrument bus is through the controller logic block.

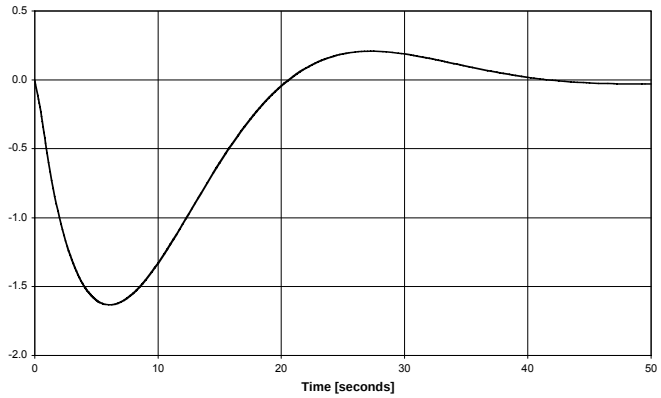

Figure 8. The blackbody response to a worse-case on-orbit perturbation leads to minimal temperature error. The plot shows the simulated response of the blackbody when the flip-in mirror is activated to present the view of the cold back of the instrument.

Temperature Measurement

The temperature measurement scheme is self-calibrating, based on continuous measurements of internal reference resistors. As a result, measurement accuracy is largely independent of offset and gain drift. Each thermistor and reference resistor is connected to a precision resistor and voltage source in a half-bridge configuration. The fixed excitation voltage setting is common to all 16 channels. The thermistor and reference resistors are measured sequentially. To improve resolution, 5 measurement ranges are used. Autoranging can be selected as a mode of operation.

The worst-case temperature measurement error due to reference resistor drift is less than 1 mK. Total measurement uncertainty due to the Blackbody Controller electronics at delivery is 14 mK. The additional uncertainty due to long-term electronics drift is less than 12 mK.

Table 3 lists the available blackbody controller control commands and data output information.

Control Commands
Blackbody Modes (Constant Temp. or Constant Power)
Set Points
Control Thermistor Select
Temperature Measurement Range
Autorange On/Off
Reset Mode

Data Output
Thermistor Data
Calibration Resistor Data
Range Data
Set Points
Blackbody Modes
Control Thermistor Selected
Autorange On/Off
Overtemperature Indicators
Fail Indicators
Frame Count

Table 3 lists the available blackbody controller control commands and data output information.

Blackbody Controller Implementation

Where possible, radiation hardened components were selected to tolerate the expected total incident dose (TID) of 61 kRad (Si) with at 2:1 safety factor. Where such components were not available, spot shielding was added to reduce the TID to an acceptable value. All parts were de-rated according to PPL-21.

The Blackbody Controller is constructed on a board approximately 10.2 by 6.3 inches (25.9 by 16.0 cm). The board plugs into a mother board (that is part of the GIFTS instrument electronics) and is secured by wedgelocks along the shorter sides, which provide a thermal path as well as structural support. The two blackbody connectors are located on the edge of the board opposite the motherboard connector. The left side of Figure 9 is a photograph of the board.

A thermal model of the board was developed (right side of Figure 9) and used to show that the warmest spot on the board is 54 C for the maximum dissipation case of 1.2 Watts, and assuming the worst case on-orbit warm environment and only conductive heat transfer (no radiative transfer). The board thermal design provides a worst case part junction temperature margin of better than 20 C.

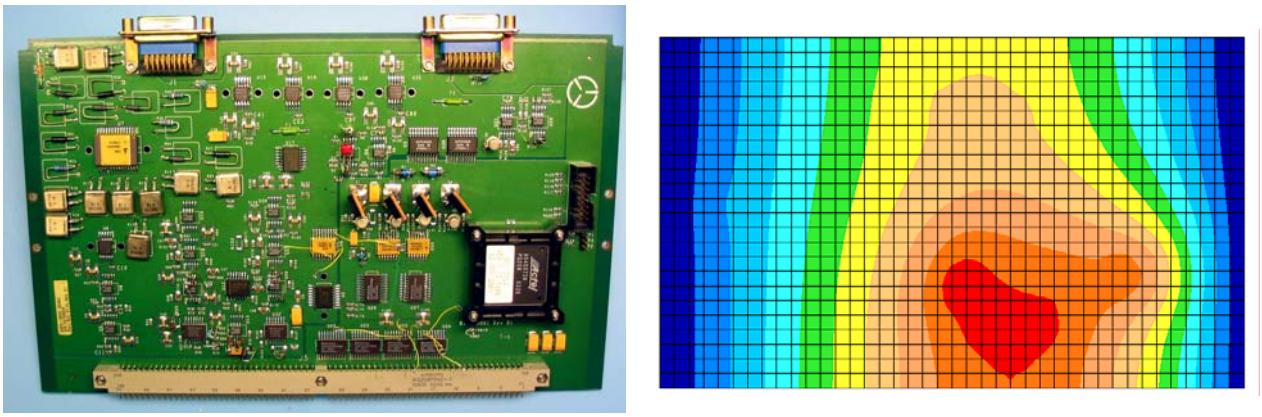

Figure 9. Engineering model blackbody controller board measuring 10.2 by 6.3 inches (left). Thermal model results of the board (right) indicate that the warmest part of the board will run at a 54 C, assuming warmest environment and no radiative transfer.

Temperature Uncertainty Budget and Calibration

The temperature calibration of the blackbody is conducted end-to-end using a dedicated pair of blackbodies and a controller. A temperature uncertainty budget was developed that includes thermistor calibration errors, temperature gradients, electronics uncertainty, and long-term stability of both the thermistors and electronics.

Blackbody Temperature Calibration

This section describes the plans for the temperature calibration of the GIFTS blackbody subsystem and follows from previous work at UW on similar systems, including the Atmospheric Emitted Radiance Interferometer (AERI), Scanning High-resolution Interferometer (S-HIS), and NPOESS Atmospheric Sounder Testbed (NAST).[16-20] The functional block diagram of the calibration test configuration is shown in Figure 10. The calibration configuration consists of an ambient and hot blackbody connected to the blackbody controller that communicates with the calibration computer. Coupled to each blackbody cavity is a specially made Thermometrics SP-60 temperature calibration standard. These probes are connected to a Hart Scientific 2564 Thermistor Scanner Module and a Hart 3560 Extended Communications Module that communicates with the calibration computer. The Thermometrics temperature calibration standard with associated Hart electronics was calibrated as a combined system at Hart Scientific to an accuracy of better than 5 mK (3 sigma), over the temperature range from -40 to +40 C.

During calibration the blackbodies are located inside an insulated box that resides within a temperature chamber that can be controlled to the different calibration temperatures. Gradients between the blackbody thermistors and the temperature standard are expected to be less than 20 mK, based on previous experience with AERI and Scanning HIS blackbody calibrations. The controller can be independently brought to different operating temperatures as well, but for the engineering model testing it will be maintained at room temperature. At each calibration temperature the temperature reported from each of the calibration standards is combined with the resistance read from the blackbody controller electronics. For each excitation current range, there will be at least four calibration temperatures. For each thermistor at each current range, the temperature and resistance data will be regression fit to the standard 3-term Steinhart and Hart thermistor relationship. Previous experience with AERI and Scanning HIS blackbody systems and modeling of the potential GIFTS blackbody subsystem non-linearities has indicated that there will be less than 5 mK residual error in the calibration fitting equation.

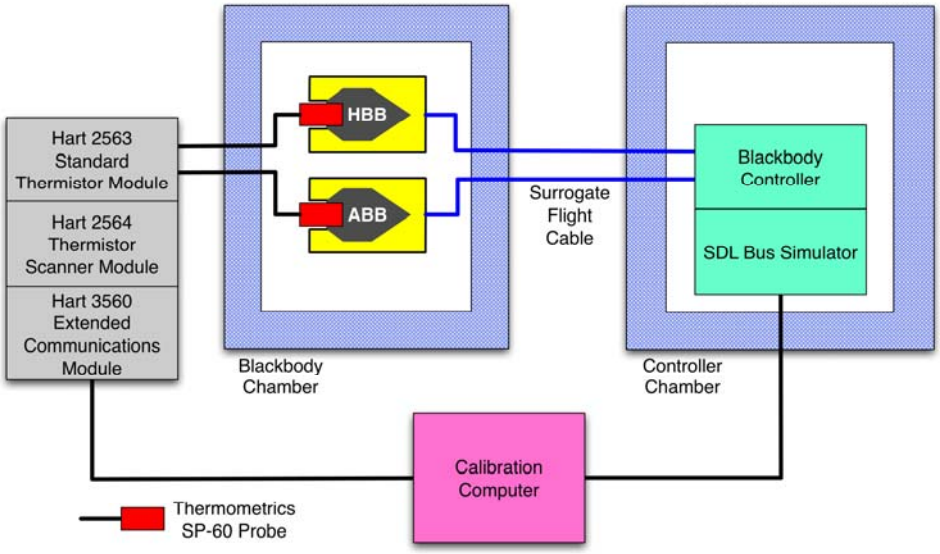

Figure 10. Blackbody thermistor calibration scheme functional block diagram.

Temperature Error Budget Summary

Table 3 summarizes the temperature uncertainty budget for the GIFTS blackbody subsystem. This budget shows the combined uncertainty due to all significant contributors is 0.074 K (3 sigma), compared to the allowable budget of 0.1 K. Most of the uncertainties have been described in earlier sections and will not be discussed further here. The cavity to thermistor gradient uncertainty is conservatively assumed to be 1/3 of the total predicted cavity gradient in the worst-case thermal environment. The temperature gradient uncertainty due to the thermistor wire heat leak is conservatively assumed to be the full value calculated for this effect in the worse case thermal environment and making conservative thermal coupling assumptions. The paint gradient arises from power lost by radiation out the blackbody aperture and is proportional to the ratio of paint thickness (76 μm) to paint conductivity (0.25 W m^{-1} K^{-1}). The value in the table for paint gradient uncertainty is the full predicted gradient assuming a 290 K blackbody radiating to the cold aft end to the instrument (assumed be 60 K). The effective radiometric temperature weighting factor uncertainty is conservatively assumed to be 1/3 of the total predicted cavity gradient in the worst-case thermal environment. The weighting factors are applied to each measurement thermistor to best represent the radiometric temperature of the cavity. The weighting factors are computed from Monte Carlo ray trace modeling that uses the cavity geometry with the expected cavity temperature distribution.

Temperature Uncertainty	3 sigma error [K]	RSS [K]
Temperature Calibration Standard (Thermometrics SP60 Probe with Hart Scientific 2560 Thermistor Module)	0.005	
		0.005
Blackbody Readout Electronics Uncertainty		
Readout Electronics Uncertainty (at delivery)	0.014	
		0.014
Blackbody Thermistor Temperature Transfer Uncertainty		
Gradient Between Temperature Standard and Cavity Thermistors *	0.020	
Calibration Fitting Equation Residual Error *	0.005	
		0.021
Cavity Temperature Uniformity Uncertainty		
Cavity to Thermistor Gradient Uncertainty *(1/3 of total max expected gradient)*	0.030	
Thermistor Wire Heat Leak Temperature Bias Uncertainty	0.008	
Paint Gradient *(assumes nominal HBB Temp and conservative viewing geometry)*	0.018	
		0.036
Long-term Stability		
Blackbody Thermistor *(10 years of drift assuming 105 C)*	0.050	
Blackbody Controller Readout Electronics	0.012	
		0.051
Effective Radiometric Temperature Weighting Factor Uncertainty		
Monte Carlo Ray Trace Model Uncertainty in Determining Teff *(1/3 of total max expected gradient)*	0.030	
		0.030
*Based on experience with UW AERI Blackbodies		0.074

Table 3. Temperature Uncertainty Budget Summary

Summary

A calibration blackbody subsystem suitable for space flight has been developed to meet the demanding requirements for the GIFTS instrument. This subsystem builds on the strong heritage of ground and aircraft based FTS instruments that have been developed at the University of Wisconsin. The engineering model of this subsystem has been fabricated and tested to show that requirements have been met. Further testing and temperature calibration are planned for the engineering model blackbody subsystem before it is delivered to the Utah State University Space Dynamics Laboratory for integration into GIFTS instrument Engineering Model cold test and calibration.

Acknowlegements

The GIFTS Blackbody development effort conducted at the University of Wisconsin was conducted under a contract (C922185) from the Utah State University, Space Dynamics Laboratory.

References

Smith, W.L., F. Harrison, D. Hinton, J. Miller, M. Bythe, D. Zhou, H. Revercomb, F. Best, H. Huang, R. Knuteson, D. Tobin, C. Velden, G. Bingham, R. Huppi, A. Thurgood, L. Zollinger, R. Epslin, and R. Petersen: "The Geosynchronous Imaging Fourier Transform Spectrometer (GIFTS)" In: Conference on Satellite Meteorology and Oceanography, 11th, Madison, WI, 15-18 October 2001. Boston, American Meteorological Society, 2001. Pp700-707.

Bingham, G.E., R.J. Huppi, H.E. Revercomb, W.L. Smith, F.W. Harrison: "A Geostationary Imaging Fourier Transform Spectrometer (GIFTS) for hyperspectral atmospheric remote sensing" Second SPIE International Asia-Pacific Symposium on Remote Sensing of the Atmosphere, Environment, and Space, Sendai, Japan, 9–12 October 2000.

Smith, W.L., D.K. Zhou, F.W. Harrison, H.E. Revercomb, A.M. Larar, A.H. Huang, B. Huang: "Hyperspectral remote sensing of atmospheric profiles from satellites and aircraft" Second SEPI International Asia-Pacific Symposium on Remote Sensing of the Atmosphere, Environment, and Space, Sendai, Japan, 9–12 October 2000.

Knuteson R.O., F.A. Best, G.E. Bingham, J.D. Elwell, H.E. Revercomb, D.C. Tobin, D.K. Scott, W.L. Smith: "On-orbit Calibration of the Geosynchronous Imaging Fourier Transform Spectrometer (GIFTS)" In: Proceedings of the SPIE, Fourth International Asia-Pacific Environmental Remote Sensing Symposium, 8 November 2004, Honolulu, Hawaii.

Elwell, J.D., D.K. Scott, H.E. Revercomb, F.A. Best, R.O. Knuteson, "An Overview of Ground and On-orbit Infrared Characterization and Calibration of the Geosynchronous Imaging Fourier Transform Spectrometer (GIFTS)" In: Proceedings of the Year 2003 Conference on Characterization and Radiometric Calibration for Remote Sensing, September 15 to 18, 2003, Utah State University, Space Dynamics Laboratory, Logan, Utah.

Revercomb, H.E., F.A. Best, D.C. Tobin, R.O. Knuteson, R.K. Garcia, D.D. LaPorte, G.E. Bingham, and W.L. Smith: "On-orbit calibration of the Geostationary Imaging Fourier Transform Spectrometer (GIFTS)" In: Proceedings of the Year 2002 Conference on Characterization and Radiometric Calibration for Remote Sensing, April 29 to May 2, 2002, Utah State University, Space Dynamics Laboratory, Logan, Utah.

Best, F.A., H.E. Revercomb, G.E. Bingham, R.O. Knuteson, D.C. Tobin, D.D. LaPorte, and W.L. Smith: "Calibration of the Geostationary Imaging Fourier Transform Spectrometer (GIFTS)" In: Proceedings of the SPIE, Remote Sensing of the Atmosphere, Environment, and Space Symposium, 9 October 2000, Sendai, Japan.

Goody, R. and R. Haskins: "Calibration of Radiances from Space" J. Climate, 11, 754–758, 1998.

Revercomb, H.E., H. Buijs, H.B. Howell, D.D. LaPorte, W.L. Smith, and L.A. Sromovsky: "Radiometric Calibration of IR Fourier Transform Spectrometers, Solution to a Problem with the High Resolution Interferometer Sounder" Appl. Opt., 27, 3210–3218, 1988.

Bingham, G.E., D.K. Zhou, B.Y. Bartschi, G.P. Anderson, D.R. Smith, J.H. Chetwynd, and R.M. Nadile: "Cryogenic Infrared Radiance Instrumentation for Shuttle (CIRRIS 1A) Earth limb spectral measurements, calibration, and atmospheric O3, HNO3, CFC-12, and CFC-11 profile retrieval" J. Geophys. Res., 102, D3, 3547–3558, 1997.

Knuteson R.O., H.E. Revercomb, F.A. Best, N.N. Ciganovich, R.G. Dedecker, T.P. Dirkx, S.D. Ellington, W.F. Feltz, R.K. Garcia, H.B. Howell, W.L. Smith, J.F. Short, D.C. Tobin: "Atmospheric Emitted Radiance Interferometer (AERI) Part I: Instrument Design" manuscript submitted to J. Atmospheric and Oceanic Technology on 31 December 2003.

Knuteson R.O., H.E. Revercomb, F.A. Best, N.N. Ciganovich, R.G. Dedecker, T.P. Dirkx, S.D. Ellington, W.F. Feltz, R.K. Garcia, H.B. Howell, W.L. Smith, J.F. Short, D.C. Tobin: "Atmospheric Emitted Radiance Interferometer (AERI) Part II: Instrument Performance" manuscript submitted to J. Atmospheric and Oceanic Technology on 31 December 2003.

Best, F.A., H.E. Revercomb, R.O. Knuteson, D.C. Tobin, R.G. Dedecker, T.P. Dirkx, M.P. Mulligan, N.N. Ciganovich, and Te, Y.: "Traceability of Absolute Radiometric Calibration for the Atmospheric Emitted Radiance Interferometer (AERI)" In: Proceedings of the Year 2003 Conference on Characterization and Radiometric Calibration for Remote Sensing, September 15 to 18, 2003, Utah State University, Space Dynamics Laboratory, Logan, Utah.

Persky, M.J.: "Review of black surfaces for space-borne infrared systems" Rev. Sci. Instrum., Vol 70, No. 5, pp 2193-2217, 1999.

Prokhorov, A.V.: “Monte Carlo Method in Optical Radiometry” Metrologia, Vol 35, No. 4, pp. 465-471, 1998.

Revercomb, H.E., et al.: “Scanning HIS Aircraft Instrument Calibration and AIRS Validation” In: Proceedings of the Year 2003 Conference on Characterization and Radiometric Calibration for Remote Sensing, September 15 to 18, 2003, Utah State University, Space Dynamics Laboratory, Logan, Utah.

Revercomb, H.E., et al.: “Applications of high spectral resolution FTIR observations demonstrated by the radiometrically accurate ground-based AERI and the Scanning HIS aircraft instruments” In: Proceedings of the SPIE 3rd International Asia-Pacific Environmental Remote Sensing Symposium 2002, Remote Sensing of the Atmosphere, Ocean, Environment, and Space, Hangzhou, China, 23-27 October 2002, SPIE, The International Society for Optical Engineering, Bellingham, WA, 2002.

Cousins, D., and W.L. Smith: “National Polar-Orbiting Operational Environmental Satellite System (NPOESS) Airborne Sounder Testbed-Interferometer (NAST-I)” Proceedings of SPIE, 3127, 323–331, 1997.

Minnett, P.J., R.O. Knuteson, F.A. Best, B.J. Osborne, J.A. Hanafin, and O.B. Brown: “The Marine-Atmospheric Emitted Radiance Interferometer (M-AERI), a high-accuracy, sea-going infrared spectroradiometer” In: Journal of Atmospheric and Oceanic Technology, vol 18, 2001, 994-1013.

Fowler, J.B.: “A Third Generation Water Bath Based Blackbody Source” J. Res. Nat. Inst. Stand. Technol., 100, 591–599, 1995.

Appendix 3: On-board Blackbody Calibration System of GIFTS – R. Knuteson et al. 2004

R. O. Knuteson[1], F. A. Best[1], G. E. Bingham[2], J. D. Elwell[2], H. E. Revercomb[1], D. C. Tobin[1], D. K. Scott[2], J. Taylor[1], and W. L. Smith[3]

[1]University of Wisconsin-Madison, Madison, WI
[2]Utah State University, Logan, UT
[3]Hampton University, Hampton, VA

Abstract
The Geosynchronous Imaging Fourier Transform Spectrometer (GIFTS) sensor has been designed to provide highly accurate radiometric and spectral radiances in order to meet the requirements of remote sensing of atmospheric motion from a geostationary orbit. The GIFTS sensor was developed under NASA New Millenium Program funding to demonstrate the tracking of infrared water vapor features in the atmosphere with high vertical resolution. A calibration concept has been developed for the GIFTS instrument design which meets the top level requirement to measure brightness temperature to better than 1 K. The in-flight radiometric calibration is performed using views of two on-board blackbody sources along with cold space. For the GIFTS design, the spectral calibration is established by the highly stable diode laser used as the reference for interferogram sampling, and verified with comparisons to atmospheric absorption line positions. The status of the GIFTS on-orbit calibration approach is described and accuracy estimates are provided. GIFTS is a collaborative activity among NASA Langley Research Center, Utah State Space Dynamics Laboratory, and the University of Wisconsin Space Science and Engineering Center.

The U.S. National Oceanic and Atmospheric Administration (NOAA) operates geostationary operational environmental satellites (GOES) for short-range warning and nowcasting, and polar-orbiting environmental satellites (POES) for longer term forecasting. GOES satellites provide continuous monitoring from space in a geosynchronous orbit about 35,800 km (22,300 miles) above the Earth. A new generation of sensors is under development that will greatly increase the horizontal, vertical, and temporal sampling of the GOES sounder and provide a truly four-dimensional view of the Earth's atmosphere. NOAA's plan for a Hyperspectral Environmental Suite (HES) calls for the replacement of the current GOES instrumentation starting as early as 2013 (Dittberner et al. 2003; Gurka et al. 2003). NASA's Geosynchronous Imaging Fourier Transform Spectrometer (GIFTS) sensor, under fabrication at the Utah State Space Dynamics Laboratory (SDL), will serve as a valuable test bed for the evaluation of approaches to flight hardware and ground data processing in the years leading up to NOAA's operational Hyperspectral Environmental Suite. The GIFTS sensor makes use of a 2-D array of detectors to increase area coverage rates while providing dramatically higher vertical resolution by measuring the thermal infrared upwelling emission spectrum at high spectral resolution. The sensor calibration makes use of two internal high precision blackbody references in addition to an external view to space. The GIFTS ground data processing algorithms used to convert from instrument values (Level 0 data) to geo-located, calibrated radiances (Level 1 data) are under development at the University of Wisconsin Space Science and Engineering Center (UW-SSEC).

The UW-SSEC has a long history of development in support of the meteorological application of geostationary observations with an emphasis on the determination of atmospheric winds by the tracking

of radiance features caused by the motion of clouds and water vapor. The development of the spin scan cloud camera in the early 1960s lead to the first global images from geostationary orbit as shown in Fig. 1. The UW-SSEC also developed the science algorithms and software for the processing of this geostationary satellite data stream (see Fig. 2). The animation of a time series of geostationary images was used to track the motion of atmospheric features. The Man-computer Interactive Data Access System (McIDAS) was developed at UW-SSEC in the 1970s and 1980s and has been used ever since in operational data processing of GOES satellites by NOAA. The GIFTS/HES concept is the natural next step in the increasingly sophisticated exploitation of weather observations from geostationary orbit by providing enhanced vertical resolving capability to complement the high spatial and temporal sampling.

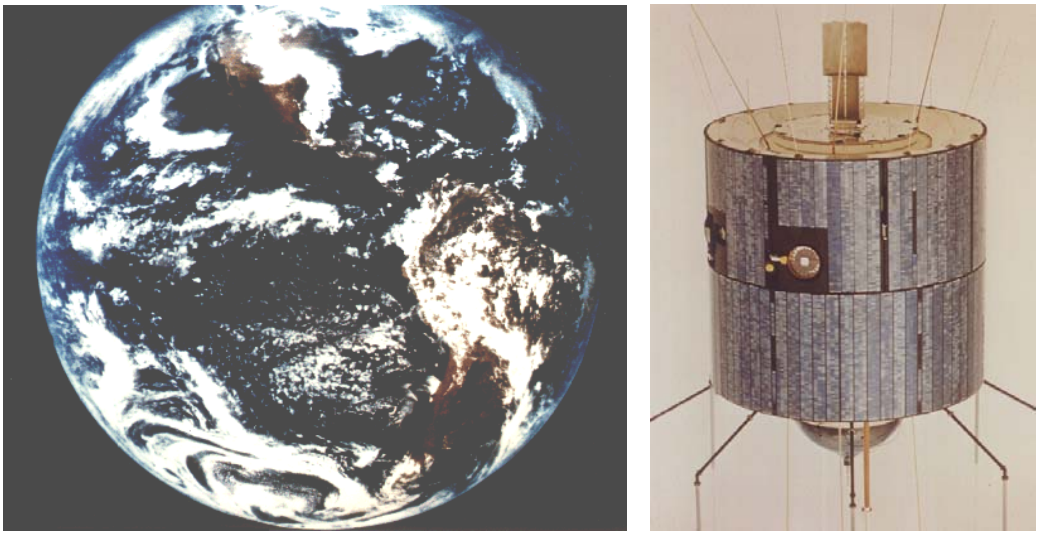

Figure 1. University of Wisconsin involvement in geostationary weather satellites dates back to the invention of the "spin scan cloud camera" by the founding director of the Space Science and Engineering Center, Prof. Verner Suomi, in collaboration with Prof. Robert Parent. The color full disk Earth image (left) shown was taken by ATS-3 (right) in 1966. Prof. Suomi's promotion of the use of geosynchronous orbit for tracking the motion of clouds to obtain winds was captured in his famous phrase, "The clouds move, not the satellite!" The GIFTS/HES concept is the natural technological follow-on to this goal by allowing the time dependent motion tracking of atmospheric constituents, e.g. water vapor, at many more atmospheric levels in the vertical than was previously possible.

Figure 2. University of Wisconsin involvement in the development of the hardware and software required to make images of the spin scan camera data lead to the development of the Man-computer Interactive Data Access System (McIDAS) which, after many generations, is still used extensively by NOAA in the processing of geostationary satellite imagery. Prof. Robert Parent (left) and Prof. Verner Suomi (right) are shown analyzing meteorological data using an early ground processing system (circa 1959). The processing of large amounts of satellite data continue to pose a challenge for the future hyper-spectral sounders which have both high spatial and high temporal resolution.

Background

The UW-SSEC pioneered the development of absolute radiometric and spectral calibration for "warm" InfraRed Fourier Transform Spectrometers (FTIR) with an accuracy and reproducibility that is sufficient for the use of the observations in atmospheric remote sensing (Revercomb, 1988). Even though the GIFTS is a "cold" instrument, the same physical principles developed for the UW-SSEC instruments (and adopted by the NPOESS Crosstrack IR Sounder program) will be applied to the calibration of the GIFTS radiances in order to take into account gain and offset changes in the instrument during normal operation. The GIFTS spectral coverage indicated in Fig. 3 illustrates that the dynamic range of signals from terrestrial thermal infrared radiation spans hundreds of degreees. However, the demands of remote sensing of atmospheric effects are high since the signal of subtle changes in temperature and atmospheric humidity from the mean atmospheric state are only tenths of degrees (Smith, 2000). Achieving absolute calibration at the tenth of degree accuracy level is a goal that is within the reach of high spectral resolution IR remote sensing using precision on-board blackbody references with NIST traceability. This approach has been demonstrated at the UW-SSEC in both the groundbased Atmospheric Emitted Radiance Interferometer (AERI) program and the aircraft-based High-resolution Interferometer Sounder (HIS) program (Knuteson, 2004a,b; Revercomb, 1998).

In both the AERI and HIS programs, FTIR spectrometers have been used in order to take advantage of the very high spectral frequency knowledge that is inherent in the FTS design. At the relatively high spectral resolutions (resolving power > 1000) in the thermal infrared, the wavenumber sampling and instrument line shapes must be known to better than 1% accuracy or errors will be introduced in the comparison with forward model calculations that exceed the radiometric requirement. With an FTIR sensor, a single parameter determines the wavenumber sampling of each spectral band and all the spectral elements see the same field of view on the Earth. The FTS spectral parameter can be determined pre-launch but also in-flight by comparison to known spectral absorption lines across the spectral band of interest. In contrast, a grating spectrometer that uses individual detector elements at each spectral element requires extensive pre-launch testing to characterize the many individual unique spectral response function (SRF) shapes. Unfortunately the grating SRFs are impossible to confirm on-orbit to the desired accuracy. The excellent spectral knowledge and stability of the FTIR system was the primary motivation for the selection of FTS for the GIFTS sensor. The grating spectrometer implemented on the NASA Atmospheric InfraRed Sounder (AIRS) sensor has the further disadvantage that each detector has a slightly different field of view to the ground. This leads to spectral "artifacts" when viewing scenes that are not uniform temperature (over a 15 km region). This is illustrated in Fig. 4 where spectral discontinuities are obvious in observations from the NASA AIRS grating spectrometer over tropical storm Isador, rendering the data effectively unusable near the eye of the storm. The GIFTS sensor avoids this problem by using a single detector to measure all the wavelengths of a spectral band simultaneously for each individual field of view to the Earth.

The ability to accurately calibrate high spectral resolution infrared observations is also important for the future of detecting global change from space-borne observations (Goody & Haskins, 1998). The technology exists with precision blackbodies and FTS laser spectral sampling to approach the tenth of degree accuracy and stability desired for the detection of global climate change on decadal scales. Although this is outside the scope of the GIFTS sensor requirements, the GIFTS design shows the feasibility of high absolute accuracy in a practical implementation for sensors in geostationary orbit. The design makes use of two high precision cavity radiometers with high absolute emissivity (>0.998) and good long term stability (diffuse paints). The cavity blackbodies used for GIFTS are built and calibrated at the UW-SSEC based upon heritage with the AERI and HIS programs. The unique approach for GIFTS is to place these reference cavities aft of the Earth viewing telescope with an "on-demand" flip in mirror to direct the IR emission from the blackbodies into the sensor. The main advantage of this approach is that the IR beam is much smaller after the telescope so that a true high emissivity cavity design can be used for the blackbodies while keeping the volume, weight, and power requirements to a minimum. The successful design of these blackbodies for the GIFTS sensor is described in Best, et al., 2004. The high absolute accuracy of the onboard reference blackbodies compensates for the additional uncertainty from degradation of the telescope optics over time. A scheme for monitoring this telescope degradation over time that makes use of the internal reference views and views to deep space has been devised for the GIFTS sensor by the Space Dynamics Laboratory (Elwell et al., 2003).

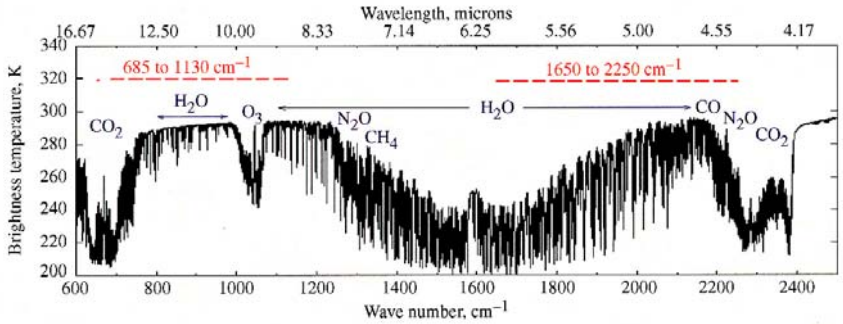

Figure 3. A calculation of the top of atmosphere radiance emitted by the standard atmosphere in units of equivalent brightness temperature (Kelvin). The dashed lines indicate the two spectral bands selected for the NASA GIFTS sensor. The longwave (LW) band covers the traditional "temperature sounding" region for the characterization of atmospheric temperature from the top of the atmosphere to the surface and includes the 8-12 μm IR window for the characterization of land surface and cloud top temperature and emissivity. The shortwave/midwave (SWM) band includes a non-traditional coverage of the shortwave side of the "6.3 μm water vapor sounding" region. The short-midwave band coverage (1650-2250 cm^{-1}) was shown by analysis to be optimal for three reasons; 1) this region avoids the interference of "fixed" gases N_2O and CH_4 which degrade the water vapor sounding performance, 2) the shorter wavelength (fewer thermal photons) leads to better signal to noise performance for the detectors chosen, 3) provides coverage of carbon monoxide thereby allowing the tracking of air pollution plumes from source to sink.

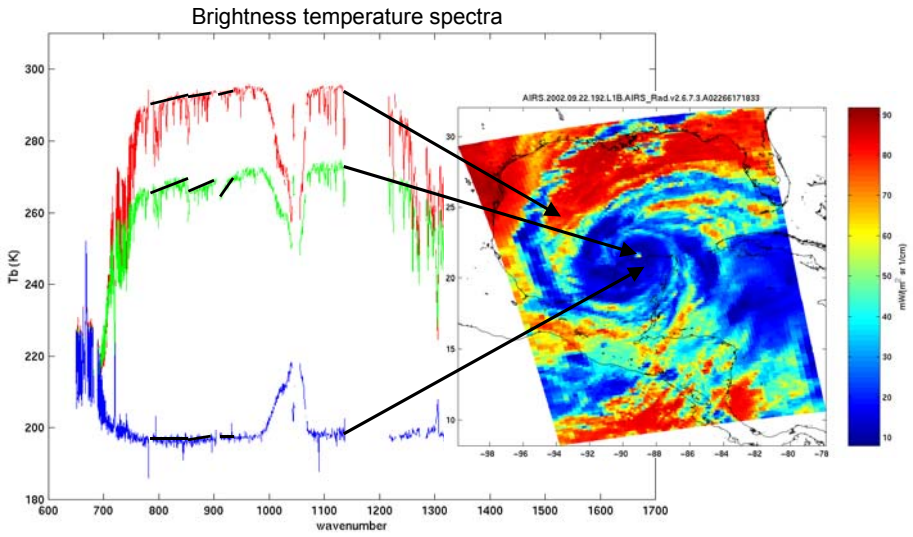

Figure 4. Spectral artifacts in the 8-12 μm window region from a grating spectrometer are obvious from this observation from the NASA AIRS sensor on the Aqua platform. The AIRS observation that includes the eye of tropical storm Isadore (22 Sept 2002 @ ~19:12-19:18 UTC) has large discontinuities (indicated by the black bars). This is not a physical atmospheric effect, rather it is caused by the fact that the thousands of individual AIRS detectors that record each spectral element have thousands of different fields of view to the earth. This is a serious problem for the use of this data in scenes of mixed cloudiness. Notice that this spectral artifact disappears for fields of view that have little temperature contrast (either entirely warm or entirely cold). The FTIR design avoids this problem by using a single detector to record all the wavelengths in a spectral band simultaneously and an on-board metrology laser sampling system to provide a consistent wavenumber scale across each spectral band.

GIFTS Radiometric Calibration

The GIFTS radiometric calibration is designed to use two small reference blackbodies located behind the telescope, combined with a space view (Best et al.,2000). Figure 5 is a schematic of the GIFTS optical design showing the location of the two internal blackbody reference sources between the optical elements labeled M2 and M3 (Bingham et al., 2000). This is also the location of an image of the aperture stop for each detector in the focal plane arrays. Figure 6 illustrates the "flip mirror" mechanism with a linear slide to position either the warm or cold blackbody into the instrument beam. The blackbody design is scaled from the UW ground-based design used on AERI and S-HIS aircraft instruments. Constraints on the original spacecraft envelope prevented a traditional external large aperture blackbody implementation. The advantages of using two internal blackbodies compared to one large external blackbody include;

(1) higher emissivity is practical with small size,
(2) effective temperature of the body easier to characterize, and
(3) protection from solar forcing gradients.

A photo of the GIFTS engineering model blackbody cavity built by UW-SSEC is shown in Figure 6 (Best et al., 2004).

Radiometric calibration of the GIFTS spectrometer has the same considerations as that of any radiometer. Key factors include the accuracy of onboard references, thermal stability over calibration cycles, and linearity after correction. This approach was proven 15 years ago with a warm interferometer by UW-SSEC using the HIS aircraft instrument as described in Revercomb, et al., 1988 and is being used for processing the CrIS data for NPOESS. The cold spectrometer design places a tight constraint on blackbody emissivity uncertainty since the energy reflected from a cold instrument is very small compared to an instrument that is close to the blackbody temperature. This, coupled with volume and mass constraints for GIFTS led to using small high-emissivity internal blackbody references, plus a space view. The broad spectral coverage from a single detector (inherent to FTS) prevents detector-to-detector FOV variations from altering spectral radiance shapes (greatly simplifying FOV co-alignment and testing requirements). The calibration method is summarized in Eq. 1. This is a modified version of the Revercomb et al., 1988 equation to include the ratio of the transmission of the flip in mirror (labeled "m") to the fore optics telescope (labeled "t").

(1)

$$N = \left(\frac{\tau_m}{\tau_t}\right)(B_H - B_C)Re\left(\frac{C_E - C_S}{C_H - C_C}\right) + B_S$$

The radiance N is derived from raw spectra of Earth (C_E), Space (C_S), and the internal Hot (C_H) and Cold (C_C) blackbodies where B_i is the predicted radiance from the Hot, Cold, and Space references including the effective emissivity of the blackbody cavity and the energy reflected off the blackbody from the environment.

The GIFTS calibration requirement has been flown down to requirements on the subsystem components, in particular to the blackbody subsystem. Figure 7 is a block diagram showing the top level GIFTS calibration error budget broken into two main contributions; radiometric and spectral calibration contributions. Each box in these charts contains three pieces of information; the requirement (either from the GIFTS Instrument Requirements Document or an equivalent implied requirement), the budget allocation for that box, and the engineering current best estimate for that item. For example the Radiometric Requirement (labeled 1.1 in Fig. 7) has a requirement of < 1K, a budget allocation of < 0.9 K, and an engineering best estimate of < 0.73K (LW) and < 0.54K (SMW). The engineering best estimate for the Radiometric Requirement flows up from the lower level contributions shown in Figure 8. In particular, the calibration budget contribution from uncertainties in the blackbodies is shown as box 1.1.1. The blackbody calibration contribution budget allocation is < 0.5K and the engineering best estimates are <0.35K (LW) and <0.20K (SMW). The uncertainty estimates of the UW-SSEC blackbodies are described in much greater detail in Best et al., 2004. The uncertainty estimates in the calibrated radiance are obtained through a perturbation analysis of Eq. 1 where the uncertainties of the blackbody emissivity and temperature are taken into account. The result of this analysis for the LW and SMW bands is shown in Figs. 9 and 10 as a function of scene temperature. Also shown are the overall GIFTS requirement and an estimate assuming an external blackbody reference with lower emissivity and larger temperature uncertainty. The parameter values used in the uncertainty analysis can be

found in Table 1. A similar analysis showing the contribution of spectral calibration uncertainties to the overall calibration budget is included in the next section.

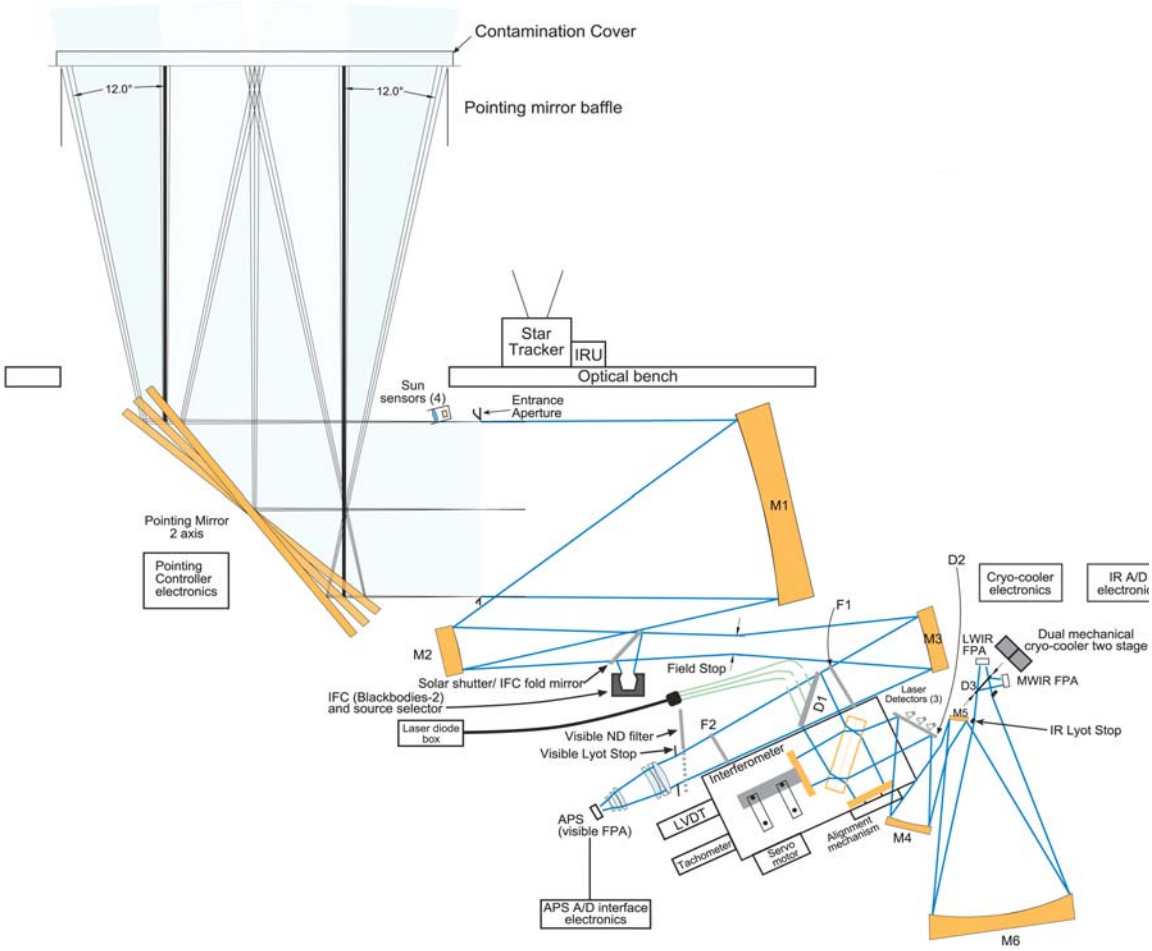

Figure 5. GIFTS sensor module electro-optical functional diagram showing the location of the two UW-SSEC blackbodies (labeled IFC in the diagram) aft of the Earth viewing telescope and the IFC fold mirror which directs energy from the blackbodies into the instrument upon command. Since the beam diameter at this location is small, the internal blackbodies can have high emissivity while remaining relatively compact and lightweight. The blackbodies were designed, built, and calibrated at the UW-SSEC using standards traceable to NIST.

Figure 6. The left-hand panel illustrates two blackbodies and a visible flood source mounted on the same linear slide. One source at a time is correctly positioned under the flip-in mirror. The right-hand illustration is a photo of the UW-SSEC engineering model of the GIFTS blackbody. The blackbody aperture is 1.00 inches in diameter, the width of the cylindrical body is 1.76 inches in diameter, and the total cavity depth is 3.06 inches.

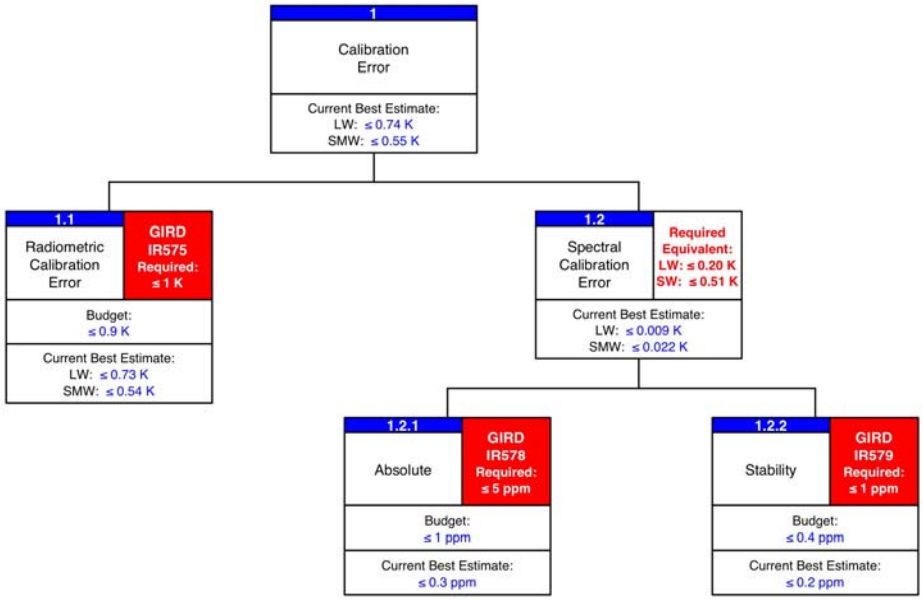

Figure 7. GIFTS top-level absolute calibration budget stating the radiometric and spectral requirements, the error budget allocation, and the current engineering best estimates.

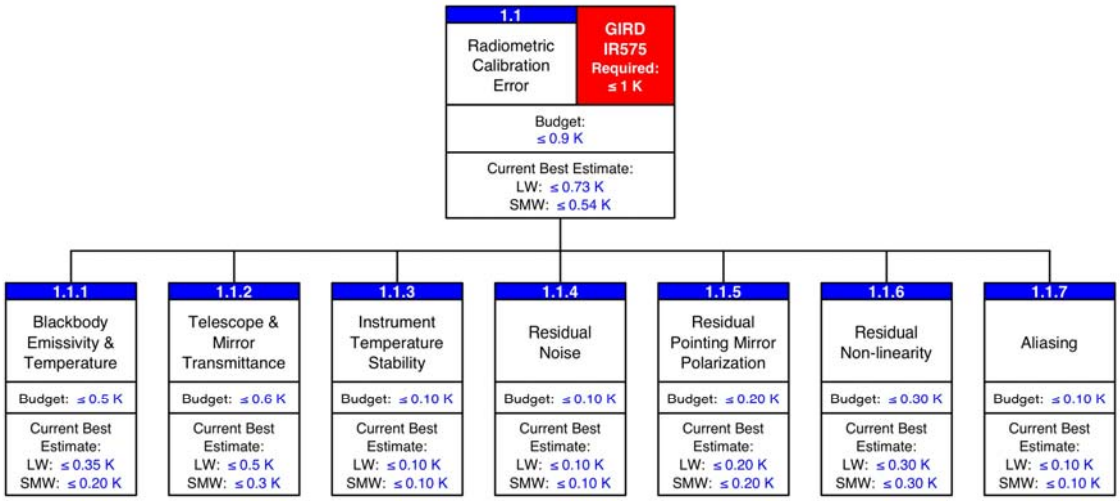

Figure 8. GIFTS radiometric calibration budget. The engineering estimates of the individual error contributors are combined (RSS) to obtain the total 3-sigma calibration error estimate.

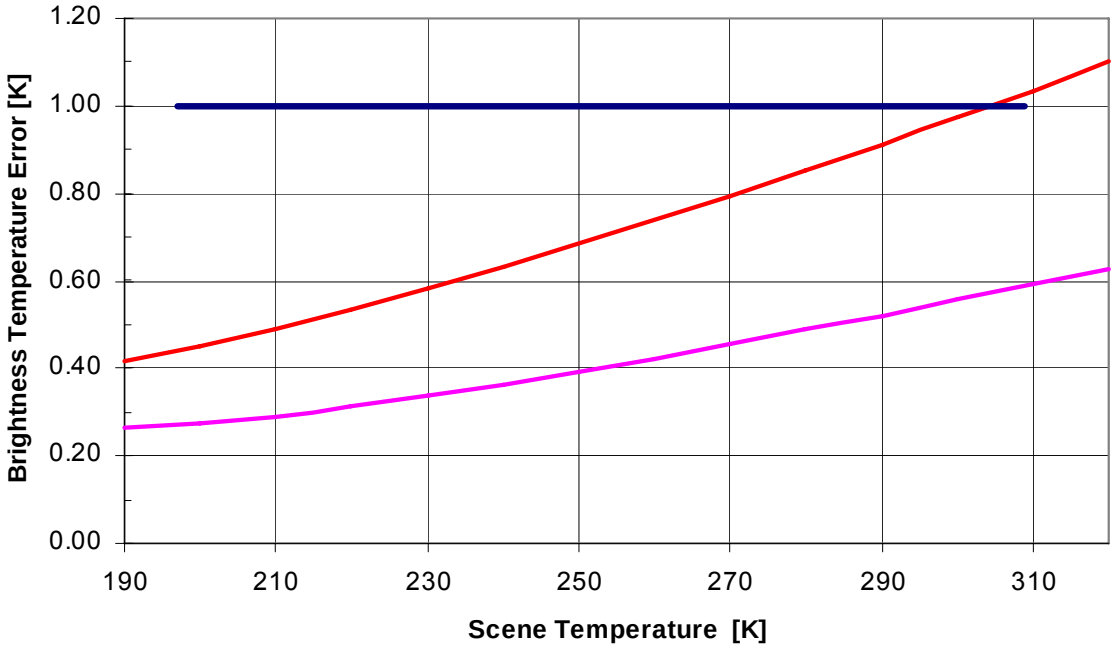

Figure 9. Uncertainty estimate (3-sigma) for the GIFTS radiometric calibration at 10 μm for the blackbody contribution only (lower magenta curve) and compared to that of a lower emissivity external blackbody (middle red curve). The GIFTS requirement is 1 K. This result shows the potential advantage of using internal high emissivity reference sources with well characterized temperature gradients over a large aperture external blackbody that is subject to large temperature forcing.

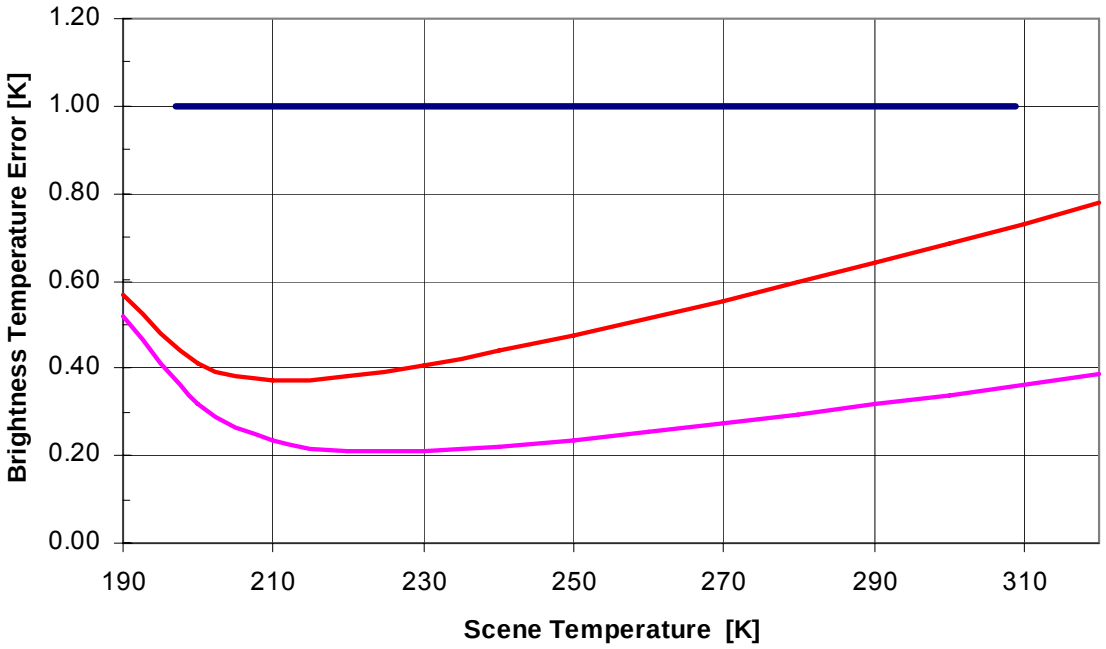

Figure 10. Same as Fig. 9 but for 5 μm.

GIFTS Spectral Calibration

The GIFTS itself is a fundamental spectral standard, due to the use of a stable laser reference coupled with the FTS design (i.e. independent of hard to characterize optical properties like blur that mandate extensive Instrument Line Shape, ILS, testing in T/V). An onboard stable laser reference makes spectral calibration essentially independent of instrument temperature (simplifies T/V testing). The GIFTS Instrument Line Shape has no significant dependence on scene content (cloud non-uniformity), for the small angles involved from geo orbit (simplifies T/V testing, applications, and improves accuracy). A single-footprint grating instrument designed like AIRS has this property too, but not an imaging grating that must use the detector array as the exit slit. The short and long term geometric and laser frequency stability, and the resulting spectral calibration, of GIFTS are expected to be very good by design (better than requirement). Spectral calibrations with Earth scene data will be used to establish and monitor the on-orbit calibration (consistency with T/V characterization is expected) (Tobin et al., 2003). Spectral positions of selected atmospheric lines are known with high accuracy and are used to determine the calibration (Rothman et al., 1998). For a given clear sky Earth spectrum, the effective laser wavenumber and resulting wavenumber scale of the observed spectrum is varied to produce best agreement with a calculated spectrum (1 ppm capability has been proven with S-HIS observations and coincident in situ observations of temperature and water vapor).

The contribution to the total calibration budget caused by spectral calibration uncertainties is given in Fig. 11. The requirement for absolute calibration is < 5 ppm (parts per million). Since we believe this requirement is too loose we have assigned an error budget of < 1 ppm and have made an engineering best estimate on the absolute knowledge that is better than 0.3 ppm. The

contributions to this absolute error estimate have been identified as coming mainly from the on-orbit determination using the positions of known atmospheric absorption lines, e.g. carbon dioxide.

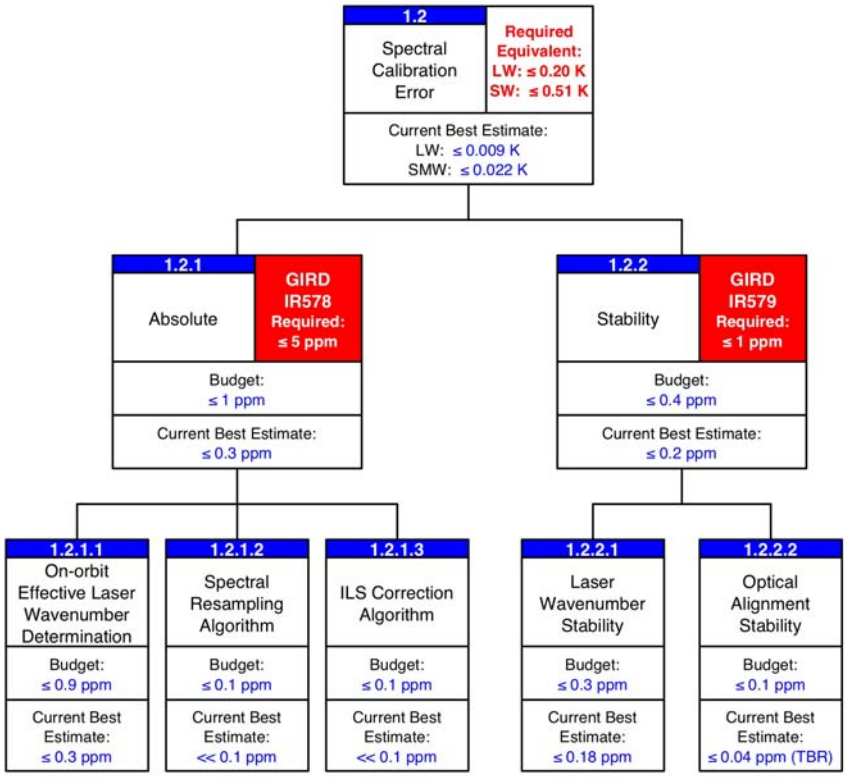

Figure 11. GIFTS spectral calibration budget and engineering best estimates. The spectral error budget is much tighter than the requirement in order to prevent errors in spectral knowledge from providing a significant contribution to the total calibration error budget. This is possible since the GIFTS makes use of a stable on-board laser combined with the FTS design which makes determination of the absolute spectral knowledge possible during flight using atmospheric absorption lines as a spectral reference. This approach has been demonstrated with the UW-SSEC Scanning-HIS aircraft instrument.

Input Parameters		
wn	Wavenumber	See figures.
tau	Telescope (2) elements and blackbody mirror transmission	0.913
Thbb	Hot blackbody temperature	300 K
Tcbb	Cold blackbody temperature	265 K
Tspace	Temperature of space	4 K
Ttel	Telescope temperature	265 K
Tstr	Temperature of structure reflecting into BB's	265

Ehbb	Emissivity of hot blackbody	0.996
Ecbb	Emissivity of cold blackbody	0.996
Parameters Used For Temperature Stability		
Etel	Telescope emissivity	0.087
TauTot	Total transmission through instrument	0.205
TtelΔ	Change in telescope temp between earth and space views	0.5 K
Uncertainty Magnitudes		
ΔThbb	0.07 K	
ΔTcbb	0.07 K	
ΔEhbb	0.002 K	
ΔEcbb	0.002 K	
ΔTstr	5 K	
Δtau	0.0086 RSS	
ΔTtel	2 K	

Table 1. Calibration uncertainty analysis parameters.

Summary

This paper represents the state of the GIFTS radiometric and spectral calibration at the time of the sensor critical design review. The on-orbit calibration approach using two internal calibration references sources and a space view are estimated to meet the GIFTS requirements and to show superior performance to a single external large aperture blackbody reference. Similarly, the on-orbit absolute spectral calibration and stability is estimated to meet the design goal of minimizing the contribution of spectral calibration error to the overall calibration budget. Future work will include the verification of the engineering best estimates to the maximum extent possible during GIFTS thermal vacuum testing.

Acknowledgements

This work was supported by federal grant NAS1-00072.

References

Best, F. A., H. E. Revercomb, R. O. Knuteson, D. C. Tobin, S. D. Ellington, M. W. Werner, D. P. Adler, R. K. Garcia, J. K. Taylor, N. N. Ciganovich, W. L. Smith, G. E. Bingham, J. D. Elwell, and D. K. Scott, 2004: The Geosynchronous Imaging Fourier Transform Spectrometer (GIFTS) On-board Blackbody Calibration System. In: Proceedings of the SPIE, Fourth International Asia-Pacific Environmental Remote Sensing Symposium, 8 November 2004, Honolulu, Hawaii.

Best, F. A., H. E. Revercomb, G. E. Bingham, R. O. Knuteson, D. C. Tobin, D. D. LaPorte, and W. L. Smith, 2000: Calibration of the Geostationary Imaging Fourier Transform Spectrometer (GIFTS), presented at SPIE's Second International Asia-Pacific Symposium on Remote Sensing of the Atmosphere, Environment, and Space, Sendai, Japan, 9–12 October 2000.

Bingham, G. E., R. J. Huppi, H. E. Revercomb, W. L. Smith, F. W. Harrison, 2000: A Geostationary Imaging Fourier Transform Spectrometer (GIFTS) for hyperspectral atmospheric remote sensing, presented at SPIE's Second International Asia-Pacific Symposium on Remote Sensing of the Atmosphere, Environment, and Space, Sendai, Japan, 9–12 October 2000.

Dittberner, G. J., James J. Gurka, and Roger W. Heymann, 2003: NOAA's GOES satellite program—status and plans, 19th Conference on IIPS, 83rd Annual Meeting, 8–13 February 2003, Long Beach, CA. Published by the American Meteorological Society, Boston, Mass.

Elwell, J. D., D. K. Scott, H. E. Revercomb, F. A. Best, R. O. Knuteson, 2003 : An overview of Ground and On-orbit Characterization and Calibration of the Geosynchronous Imaging Fourier Transform Spectrometer (GIFTS) in Proceedings of CALCON 2003, Characterization and Radiometric Calibration for Remote Sensing, Space Dynamics Laboratory / Utah State University, Logan, Utah, 15-18 September 2003.

Gurka, J. J., Gerald J. Dittberner, Pamela Taylor, and Timothy J. Schmit, 2003: Specifying the requirements for imaging and sounding capabilities on the GOES-R series, 12th Conference on Satellite Meteorology and Oceanography, 83rd Annual Meeting, 8-13 February 2003, Long Beach, CA. Published by the American Meteorological Society, Boston, Mass.

Goody, R. and R. Haskins, 1998: Calibration of Radiances from Space, J Climate, 11, 754-758, 1998.

Knuteson R. O., H. E. Revercomb, F. A. Best, N. C. Ciganovich, R. G. Dedecker, T. P. Dirkx, S. C. Ellington, W. F. Feltz, R. K. Garcia, H. B. Howell, W. L. Smith, J. F. Short, D. C. Tobin, 2004: Atmospheric Emitted Radiance Interferometer (AERI) Part I: Instrument Design, J. Atmos. Oceanic Technol (in press).

Knuteson R. O., H. E. Revercomb, F. A. Best, N. C. Ciganovich, R. G. Dedecker, T. P. Dirkx, S. C. Ellington, W. F. Feltz, R. K. Garcia, H. B. Howell, W. L. Smith, J. F. Short, D. C. Tobin, 2004: Atmospheric Emitted Radiance Interferometer (AERI) Part II: Instrument Performance, J. Atmos. Oceanic Technol (in press).

Revercomb, H.E., V.P. Walden, D.C. Tobin, J. Anderson, F.A. Best, N.C. Ciganovich, R.G. Dedecker, T. Dirkx, S.C. Ellington, R.K. Garcia, R. Herbsleb, R.O. Knuteson, D. LaPorte, D. McRae, and M. Werner, 1998: Recent results from two new aircraft-based Fourier transform interferometers: The Scanning High-resolution Interferometer Sounder and the NPOESS Atmospheric Sounder Testbed Interferometer, 8th International Workshop on Atmospheric Science from Space using Fourier Transform Spectrometry (ASSFTS), Toulouse, France, 16-18 November 1998.

Revercomb, H. E., H. Buijs, H. B. Howell, D.D. LaPorte, W. L. Smith, and L. A. Sromovsky, 1988: Radiometric calibration of IR Fourier Transform Spectrometers: solution to a problem with the High Resolution Interferometer Sounder", Appl. Opt., 27, 3210–3218.

Rothman, L. S., et al., 1998: The HITRAN Molecular Spectroscopic Database and HAWKS: 1996 Edition, Journal of Quantitative Spectroscopy and Radiative Transfer, 60, pp. 665-710.

Smith, W. L., D. K. Zhou, F. W. Harrison, H. E. Revercomb, A. M. Larar, A. H. Huang, B. Huang, 2000: Hyperspectral remote sensing of atmospheric profiles from satellites and aircraft, presented at SPIE's Second International Asia-Pacific Symposium on Remote Sensing of the Atmosphere, Environment, and Space, Sendai, Japan, 9–12 October 2000.

Tobin, D. C., H. E. Revercomb, R. O. Knuteson, 2003: On-orbit Spectral Calibration of the Geosynchronous Imaging Fourier Transform Spectrometer (GIFTS), in Proceedings of CALCON 2003, Characterization and Radiometric Calibration for Remote Sensing, Space Dynamics Laboratory / Utah State University, Logan, Utah, 15-18 September 2003.

Appendix 3: Geostationary Interferometer 24-Hour Simulated Dataset for Test Processing and Calibration

Erik R. Olson, Jason Otkin, Robert Knuteson, Maciek Smuga-Otto, Raymond K. Garcia, Wayne Feltz, Hung-Lung Huang, Christopher Velden, and Leslie Moy

Cooperative Institute for Meteorological Satellite Studies (CIMSS)

University of Wisconsin-Madison

The UW-Madison CIMSS is producing simulation datasets as a part of the risk reduction effort in the NOAA GOES-R program. One of the potential baseline sounder designs for the GOES-R Hyperspectral Environmental Suite (HES) is a geostationary imaging Fourier transform spectrometer. This paper describes a simulation based on the specifications of the existing NASA GIFTS instrument, which is currently undergoing thermal vacuum testing. The initial step of the preparation uses a Weather Research and Forecasting (WRF) model simulation covering most of the North and South American continents to provide internally consistent atmospheric profiles over a potential geostationary imaging area. Next, the GIFTS forward radiative transfer model calculates the outgoing radiance spectra at the top of the atmosphere. Finally, a detailed mathematical model of the instrument is used to calculate the resulting raw signal sent down from the satellite. The intended use of this 24 hour dataset is to test science algorithms and data processing software.

Introduction

The GOES-R program specifications include a requirement for a baseline sounding instrument capable of approximately 1 cm-1 resolution in a number of possible wavenumber regions. An imaging Michelson interferometer is one of the two primary sounder technologies which can meet this need. This paper focuses on simulation data synthesis for the GIFTS instrument, which is currently in thermal vacuum testing at the Utah Space Dynamics Laboratory. A considerable amount of the detailed design work, fast forward model development, instrument model refinement, and science algorithm testing has already been achieved by the sounding community for the GIFTS instrument. This makes the imaging interferometer design an attractive choice for a potential component of a complete next generation geostationary meteorological suite.

While deciding on the parameters of this dataset we solicited input from various research groups representing a range of interests in the meteorological and atmospheric science communities. The large spatial coverage of the dataset will provide a sufficient number of

cases for testing the pattern matching algorithms used in the wind vector determination program. Large variations in surface conditions and a broad latitude range provides a variety of conditions for profile retrieval algorithm testing.

While the quantity of data contained in our 24 hour datasets dataset is more than sufficient for science algorithm testing, the size of the dataset is necessary for testing prototype software for science and environment data processing. Exercising the modules that make up this processing system with a self-consistent 24-hour dataset will help identify problems posed by large datasets in general.

Throughout the creation of this test dataset we strived to produce data that is representative of what an operational imaging interferometer will produce. The numerical weather model is unlikely to reproduce the exact atmospheric and cloud conditions that happened in the real world on the chosen day, but we feel the profiles are a good example of potential conditions. The subsequent radiative transfer and instrument modeling steps were designed to give our best estimate of GIFTS instrument data output for the given atmosphere and cloud property profiles. Further refinements to this modeling can be made as the GIFTS instrument ground-test data is analyzed.

The creation of the simulated datasets is comprised of three steps. After the numerical weather model produces atmosphere and cloud profiles (described in section 2), a regression analysis-based fast radiative transfer model produces top of atmosphere (TOA) radiance spectra (sections 3 and 4). The final step is to model the GIFTS optics and detectors to produce interferograms, which are described in sections 5 and 6.

Cloud Particle and Atmospheric Profile Modeling with WRF

The Weather Research and Forecasting (WRF) model is used to generate realistic high-resolution temperature and water vapor profiles covering a large geographical domain. Post processing of the model simulated data is performed in order to provide climatological ozone estimates and also to calculate effective particle diameters for each microphysical species.

Due to inaccuracies inherent in all numerical weather modeling systems, the primary objective of this work is to produce realistic simulated datasets that contain mesoscale cloud, temperature, and water vapor structures representative of a real atmosphere. The ability to reproduce the exact atmospheric state for a given situation is constrained by several model limitations. For example, even the most sophisticated bulk microphysics schemes in the WRF models contain numerous assumptions that simplify cloud morphology and cloudy radiative transfer processes. Another serious limitation is the observation that model grid spacing (□x) is not synonymous with grid resolution (Grasso 2000).

The ability of a model to resolve small scale structure effectively (relative to the grid spacing) is limited by the dissipation mechanisms used by that model, including both

explicit smoothers and explicit and implicit dissipation inherent to a given integration scheme. It should be noted, however, that even with these limitations, sophisticated numerical models still represent an excellent method to generate physically realistic atmospheric datasets with fine spatial and temporal resolution.

Version 2.1 of the WRF model was used to produce a realistic simulation of atmospheric conditions on the chosen day. The simulation was initialized at 00 UTC on 24 June 2003 with 1º Global Forecasting System (GFS) analyses and then run for 30 hours on a single 1580 x 1830 grid point domain with 8-km horizontal grid spacing and 50 vertical levels. The simulation employed the WRF Single-Moment 6-class microphysics scheme (Hong et al. 2004), the Yonsei University PBL scheme, the RRTM longwave and Dudhia shortwave radiation schemes, and the Noah LSM. No cumulus parameterization scheme was used so only explicitly resolved convection was modeled during the simulation.

The domain chosen for this simulation encompasses a very large geographical area that contains regions of clear and cloudy-sky conditions. Fig. 1 shows the WRF-simulated vertically-integrated cloud microphysical content at 1400 UTC on June 24, 2003. Inspection of this figure reveals the presence of substantial cloud-cover over a large portion of the ocean while large regions of clear sky conditions are present over North and South America. It is also interesting to note the well-defined Intertropical Convergence Zone (ITCZ) extending across the domain at approximately 10° N. In figure 2, colored isosurfaces are plotted for a total cloud microphysical content (summation of the cloud water, rain water, ice, snow, and graupel mixing ratios) of .01 g kg-1. The color is a function of temperature, ranging from warm (yellow) to cold (blue).

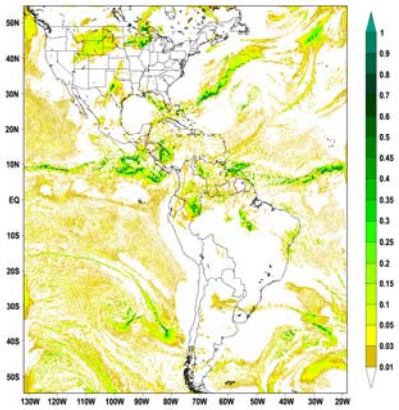

Fig. 1: WRF simulated vertically integrated cloud microphysical content valid at 1400 UTC on 24 June 2003.

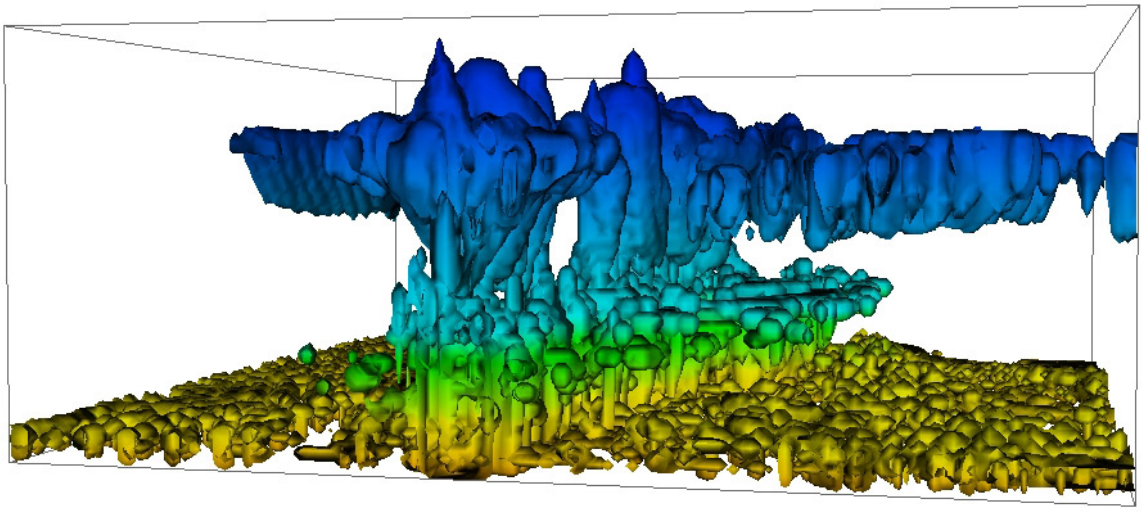

Figure 2: 3-D representation of the simulated cloud profile for structure along the ITCZ over the eastern Pacific. Ocean at 1400 UTC on 24 June 2003.

Although the 8-km horizontal resolution of this simulation is not sufficient to fully resolve the atmospheric detail that the GIFTS instrument's 4-km pixel footprint will be able to reveal, it is clear that this simulation still contains a substantial amount of fine-scale atmospheric structure. Future versions of the 24-hour dataset will include sub-domains with substantially finer horizontal resolution (< 2 km).

The last part of the WRF simulation breaks up the full domain outputs into a horizontal grid of 128 by 128 "cubes". This represents the number of detectors in the GIFTS detector arrays, but has four times the ground coverage due to the GIFTS 4 kilometer spatial resolution and the WRF grid spacing of 8 kilometers. The GIFTS cubes are aligned side by side, and their edges match up exactly. This arrangement differs from the actual viewing pattern of GIFTS, which will have overlapping cubes to improve the quality of the spatially resampled image mosaics. When more details about the telescope pointing mechanism on GIFTS are known a simulation study of the optimum overlap amount can be performed.

Clear Sky Model

The GIFTS clear sky forward model is a LBLRTM based Pressure Layer Optical Depth (PLOD) fast model. At fixed pressure layers, regressions are made to line-by-line transmittance calculations obtained with LBLRTM. The line-by-line transmittance data are monochromatic values, and need to be mapped to the GIFTS spectral domain. The

mapping has an effective spectral resolution of 0.6 cm-1, and the results are apodized prior to performing the regression analysis.

We use 32 training profiles from a NOAA database. Each profile has 100 vertical layers and is calculated at 6 satellite view angles. The predictors generated from the profiles are the same ones used for the AIRS instrument.

Three regressions are made at every layer for 3073 channels between 587 and 2347 cm-1: one for fixed gases, one for H2O, and one for O3. Each gas type has its own set of predictors, and therefore, its own regression coefficients.

Figure 3 displays the current planned spectral coverage of GIFTS measurements with clear-sky brightness temperature calculated from the U.S standard atmosphere.

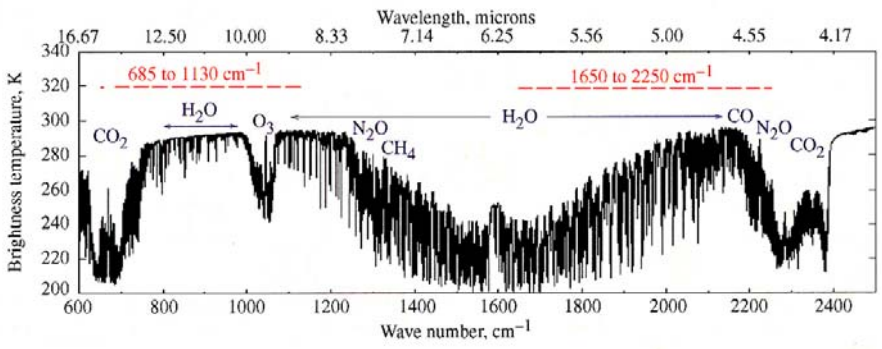

Fig. 3: GIFTS spectral coverage and its brightness temperature spectrum.

The clear sky top of atmosphere radiance is currently broken down into three terms: the atmospheric contribution, the surface emissions, and the surface reflected contribution. As our modeling of the surface emissivity becomes more sophisticated, we need to include a more accurate calculation of the reflected term. The downwelling flux at the surface is now calculated via a two point Gaussian quadrature approximation with the assumption of a Lambertian surface.

The surface reflected term requires knowledge of the downwelling flux, upwelling transmittance and reflectance of the surface. It would be too time consuming to run a dedicated fast model for the downwelling calculations so the existing fast model is used instead. Three sources of potential error arise from this computational shortcut. First, the fast model has a built-in directionality - the model is designed for TOA radiances, and is based on a level to space regressions rather than independent layer terms. Depending on the application (micro-window or on/off line), using upwelling transmissivity for downwelling radiance may be reasonable. Second, the fast model calculations are made at the instrument resolution, whereas preferably it should be the product of the flux and

transmissivity terms that are convolved to instrument resolution. Without creating a separate model with downward directionality, these errors cannot be further reduced. A third, smaller, source of error comes from using a low order Gaussian Quadrature approximation. They have decided that the two point approximation is a good trade-off between error and computational resources.

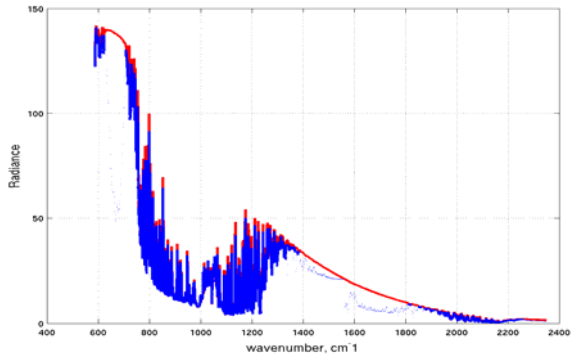

Fig. 4: Comparison of downwelling clear sky model (blue) and LBLRTM calculations (red).

Cloudy Sky Model

For the two layer cloudy sky GIFTS forward model, the standard 100 layers of the atmosphere are divided into five groups. These groups are the layers below the lower cloud base, the lower cloud, the layers between the clouds, the upper cloud, and the remaining layers above the upper cloud.

Output from the WRF models includes profiles of mixing ratios for rain water, ice, cloud water, snow, and graupel. To determine the phase at each layer the following quantity is calculated:

$$\text{phase \#} = \frac{\sum_{habit} category * mixing\ ratio}{\sum_{habit} mixing\ ratio}$$

where the category number is 2.0 for ice, snow, and graupel, and 1.0 for water mixing ratios. If the phase number is greater than 1.5, then the cloud group layer is modeled as ice. All other cloud group layers are modeled as water clouds. The mixing ratio profiles are also used to calculate the visible optical depth and effective particle size.

The cloud upper and lower boundaries are determined by grouping cloudy atmospheric layers into one or two cloud layer groups. Adjacent atmospheric layers containing clouds

of similar phase are grouped together. Only the two cloud groups with the largest optical depths are considered. The two layer model also ignores any cloudy layers that have visible optical depths less than 0.5 for water and 0.01 for ice. Total visible optical depth and effective size for both of the clouds (if two exist) are calculated from the individual layer properties.

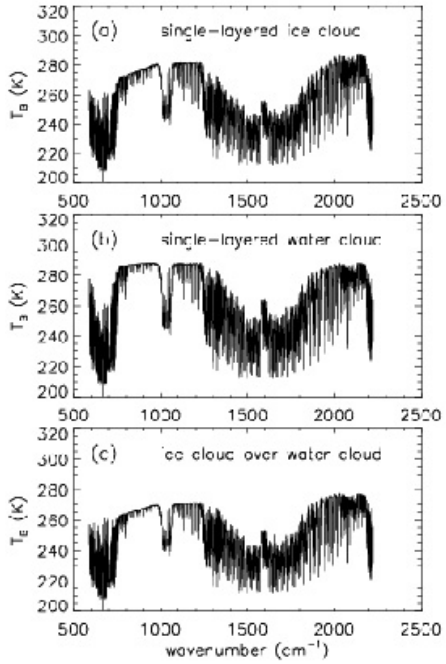

Fig. 5: Sample brightness temperature spectra for three cloud combinations.

The final optical depths and particle effective sizes are used to determine the radiative properties of the cloud. A multi-dimensional look up table (LUT) of the spectral transmittance and reflectance values is provided by Ping Yang (Yang et. al. in press). The ice cloud table covers an optical depth range of 0.04 to 100 and an effective size range of 10 – 157 microns. For water clouds the ranges are 0.06 – 150 and 2 – 100 microns. Multiplying the cloudy transmittance values by the clear sky transmittance values yields a transmittance profile for the TOA radiance calculations. For cloudy conditions, the surface reflection term is much smaller than for clear sky, so we approximate the downwelling radiance to be the same as the upwelling radiance for the pertinent layers. Figure 5 shows TOA radiances computed for three different atmospheric conditions. Panel a is for a single layer ice cloud at a height of 12 km with an optical depth of 1 and effective size of 40 μm. Panel b represents a water cloud at a height of 2 km, optical depth of 5 and effective particle size of 10μm. The last panel (c) is a two layer cloud combination, with a 50 μm effective particle size ice cloud layer like panel a overlying a water cloud layer with the same properties as the cloud in panel b.

Surface Emissivity Model

In order to increase the realism of the infrared emission spectrum over land, a global emissivity database developed at UW-SSEC is used to characterize the surface infrared properties below each of the NWP profiles prior to computing top of atmosphere radiance. The latitude and longitude of each profile is used to select from the gridded emissivity database. The database is derived from a combination of high spectral resolution laboratory measurements of selected materials, and multiple years of MODIS (MOD11) observed land surface emissivities at 3.7, 3.9, 4.0, 8.5, 11.0 and 12.0 micron wavelengths. For a given month, a continuous spectrum of emissivity from 3.7 to 14.3 microns is available from this database for every latitude/longitude point globally at 0.05 degree resolution (Wetzel-Seemann et al., 2006).

Instrument Model

The modeling of the instrument and the data that is output from the instrument is broken into two parts. The first part models how the optics of the instrument will affect the observations. The second half of the instrument model covers most of the detector related effects. The model for the GIFTS instrument developed at the UW-CIMSS represents an abstraction of the actual instrument to represent the key features of an imaging FTS sensor but is not intended to capture all the technical details of the sensor under development at Utah State Space Dynamics Laboratory.

The TOA radiances produced from the GIFTS fast model are used as a starting point. The optics model then adds the instrument background contribution, a phase shift, a spectral smearing, and a spectral shift. The spectral smearing and shift are due to self apodization by the instrument optics. We also apply the detector responsivity and numerical filter effects at this point, but in the future we plan to move these steps to the detector part of the instrument model. The final product is a group of raw instrument interferograms.

The data from the GIFTS instrument is sent to the ground processing system as interferogram counts. The main function of the calibration software is to convert the interferograms to spectra in physical units and use the blackbody observations to remove the instrument background contribution. The temperature of the instrument optics follows a diurnal pattern as the amount of solar illumination on instrument components changes over the orbital path. The change in the optics temperature is used to vary the background contribution to the interferogram signal. Figure 6 shows a model estimate of how the optics temperatures might change over 24 hours. A simple lookup table for the optics temperature is used to vary the instrument background term of the output signal.

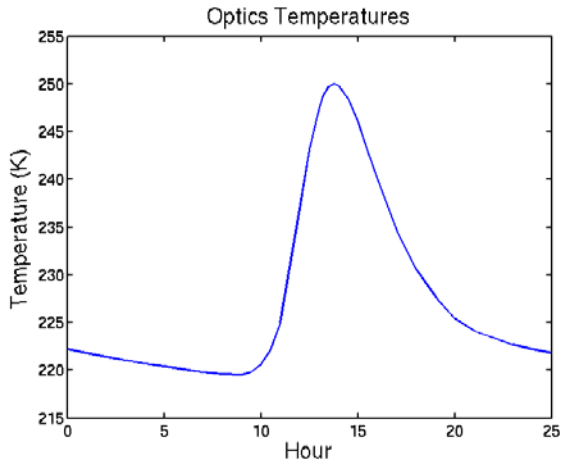

Fig. 6: Change in instrument optics temperatures over 24 hours. The temperatures over the last hour are just a repeat of the first hour.

We also we simulate the off-axis effect common to imaging interferometers in the data. Calculation of the off-axis effect involves very large Fourier transforms, so we perform this step for only part of the dataset. For the rest of the data a smaller FFT is done to produce real interferograms.

The final part of the instrument model simulates the effects of the detectors. Since the responsivity and numerical filter have already been applied, the main procedure is to apply the variations in gains and offsets throughout the detector array. This is done with Gaussian distribution gain factors, from 0.5 to 1.5 randomly spread across the detector array. The detector signal offsets are also random values between zero and 50. For each individual detector in the array, the gain and offset values remain constant throughout the 24 hour dataset.

The last two steps in the detector model are to add the noise inherent in the detector and simulate the quantization of the interferometer converting the analog signal to a digital stream. The noise added is a Gaussian distribution of noise equivalent radiance multiplied by the square root of the number of interferogram points.

The blackbody view data is an integral part of the simulated dataset. The GIFTS instrument is designed to have three in-flight calibration sources. These are two heated cavities that bound typical atmosphere temperatures as well as a deep space viewing option. The viewing schedule for a geostationary interferometer is likely to include blocks of blackbody views once about every 30 minutes. To provide the ability to test a variety of calibration schedules as well as predictive calibration algorithms, a series of 4 hot, 4 warm, and 4 space views are simulated to occur every 10 minutes for the 24 hour dataset.

Conclusions

The 24 hour GIFTS simulation dataset represents our efforts to provide realistic idea of what data from a geostationary interferometer as part of the GOES-R program would give to research efforts. The data is designed to help advance wind vector determination research as well as a range of single field of view retrieval algorithms. The size of the dataset also provides the groups working on design of data processing systems with a realistic volume of data.

In subsequent versions of the test dataset we hope to add some more detail to the simulations. A higher spatial resolution WRF simulation for a small subsection would complement the full disk data well. With the higher resolution data, we can simulate the effect of viewing geometry on the data for larger viewing angles.

Acknowledgement

This work was supported by NOAA federal grant NAO7EC0676.

References

Baum B. A., Harkey M. K., Frey R. A., Mace G. G., and Yang P., Nighttime Multilayered could detection using MODIS and ARM data, J. Appl. Meteor. 2003; 42: 905-919.

Grasso, L. D., 2000: The Differentiation Between Grid Spacing and Resolution and Their Application to Numerical Modeling. Bull. Amer. Meteor. Soc., 81, 579-580.

Hong, S.-Y., J. Dudhia, and S.-H. Chen, 2004: A revised approach to ice microphysical processes for the bulk parameterization of clouds and precipitation. Mon. Wea. Rev., 132, 103-120.

Hung-Lung Huang, Chris Velden, Jun Li, Elisabeth Weisz, Kevin Baggett, Jim Davies, John Mecikalski, Bormin Huang, Russ Dengel, Steven A. Ackerman, Erik R. Olson, Robert O. Knuteson, Dave Tobin, Leslie Moy, Jason Otkin, Hank E. Revercomb, and William L. Smith+, "Infrared Hyperspectral Sounding Modeling and Processing – An Overview," in 20th International Conference on Interactive Information and Processing Systems (IIPS) for Meteorology, Oceanography, and Hydrology, 2003.

Huang, H.-L., H. E. Revercomb, J. Thom, P. B. Antonelli, B. Osborne, D. Tobin, R. Knuteson, R. Garcia, S. Dutcher, J. Li, and W. L. Smith, "Geostationary Imaging FTS (GIFTS) Data Processing: Measurement Simulation and Compression, 2000. Proceedings of SPIE, William L. Smith and Yoshifumi Yasuoka, editors. Hyperspectral Remote Sensing of the Land and Atmosphere. 9-12 Oct. 2000, 103-114.

Knuteson, Robert, Ackerman, Steve, Best, Fred, Dedecker, Ralph, Garcia, Ray, Olson, Erik, Revercomb, Hank, Smuga-Otto, Maciek, and Tobin, D., 2005: Calibration

algorithm accuracy versus efficiency tradeoffs for a geosynchronous imaging Fourier transform spectrometer. International Conference on Interactive Information and Processing Systems (IIPS) for Meteorology, Oceanography, and Hydrology, 21st, San Diego, CA, 8-13 January 2005 (preprints). American Meteorological Society, Boston, MA, 2005.

Knuteson, R., Best, F., Dedecker, R., Garcia, R., Limaye, S., Olson, E., Revercomb, H., and Tobin D., 2004a: LEVEL 0-1 Algorithm Description For The Geosynchronous Imaging Fourier Transform Spectrometer, AMS annual meeting, Seattle, WA, January 2004, American Meteorological Society.

Knuteson, R. O., F. A. Best, G. E. Bingham, J. D. Elwell, H. E. Revercomb, D. K. Scott, J. K. Taylor, D. C. Tobin, W. L. Smith, 2004b: On-orbit calibration of the Geosynchronous Imaging Fourier Transform Spectrometer (GIFTS). In: Proceedings of the SPIE, Fourth International Asia-Pacific Environmental Remote Sensing Symposium, 8 November 2004, Honolulu, Hawaii.

Moy, Leslie, Dave Tobin, Paul van Delst, Hal Woolf, "Clear Sky Forward Model Development for GIFTS", AMS Annual Meeting, Seattle, WA, January 2004.

Strow L. L., Motteler H. E., Benson R. G., Hannon S. E., and Souza Machado S., Fast computation of monochromatic infrared atmospheric transmittances using compressed look-up tables, J. Quant. Spectrosc. Radiat. Transf., 1998; 59: 481-493.

Wetzel Seeman, S., Borbas, E., Knuteson, R., Huang, H.-L., Menzel, W., 2006: A Global Infrared Land Surface Emissivity Database, AMS Annual Meeting, Atlanta, GA, January 2006.

Yang, P., H. Wei, H.-L. Huang, B. A. Baum, Y. X. Hu, G. W. Kattawar, M. I. Mishchenko, and Q. Fu, 2004: Scattering and absorption property database for nonspherical ice particles in the near-through far-infrared spectral region, Appl. Opt. (accepted).

Appendix 4: Preliminary Evaluation of the GIFTS Calibration Algorithm Using the GIPS

Robert Knuteson, Ray Garcia, Erik Olson, Hank Revercomb, Maciek Smuga-Otto, and Dave Tobin

Cooperative Institute for Meteorological Satellite Studies (CIMSS)

Space Science and Engineering Center, University of Wisconsin-Madison

Ground calibration algorithms for a Geosynchronous Imaging FTS (GIFTS) are being developed at the University of Wisconsin-Madison Space Science and Engineering Center. This development is being conducted in support of NOAA's GOES-R Risk Reduction program with a focus on the hyperspectral sounder that is anticipated to be a part of the GOES-R Hyperspectral Environmental Suite (HES). The near term objective is to develop calibration algorithms that can be evaluated using thermal vacuum test data from NASA's Geosynchronous Imaging Fourier Transform Spectrometer (GIFTS). The GIFTS is designed to produce 128x128 interferograms in two spectral bands every 11 seconds using a Michelson interferometer and two detector focal plane arrays. In preparation for the thermal vacuum test data, simulated data has been used in the GIFTS Information Processing System (GIPS) to illustrate expected accuracy of a unique on-orbit calibration approach using two high emissivity internal reference cavities plus a space view.

Introduction

The geostationary imaging weather satellites play a vital role in the global system of operational observing platforms by providing the high temporal and spatial resolution needed for severe storm nowcasting as well as the large scale motion fields that influence events such as tropical cyclone intensity and path prediction. The next generation geostationary satellites is expected to take a revolutionary advance toward improving the determination of atmospheric stability and clear air convective initiation as well as the height assignment of wind vectors derived from putting retrieved water vapor fields in motion (Dittberner et al., 2003). The timely availability of this information will greatly enhance the mesoscale and synoptic information available for Numerical Weather Prediction (NWP) data assimilation. The Geostationary Imaging Fourier Transform Spectrometer (GIFTS) is an instrument development project under the NASA New Millenium Program initiative that addresses the technological needs of the next generation geostationary sounders. The GIFTS instrument was designed as a research prototype and proof of concept demonstration of how new detector focal plane technology can be combined with a mature spectrometer design to accomplish the goals of a future advanced geostationary sounder. The GIFTS instrument has been designed and fabricated under the management of NASA Langley Research Center with Utah State University Space Dynamics Laboratory as prime contractor (Smith et al., 2000; Bingham et al., 2000). At the time of writing, the GIFTS is in

thermal vacuum testing to verify the instrument performance characteristics and to validate the new technologies used in the design.

One of the concepts unique to GIFTS is the use of two high emissivity cavity blackbodies internal to the instrument and behind the scene mirror in addition to a view to deep space. These onboard reference cavities were designed and built at the UW-SSEC (Best et al, 2000, 2004). The expected accuracy of this calibration approach is illustrated in this paper through the use of simulated GIFTS data and the algorithms that make up the GIFTS Information Processing System (GIPS) (Garcia et al., 2005; Knuteson 2004a, 2005).

Background

The UW-SSEC pioneered the development of absolute radiometric and spectral calibration for "warm" InfraRed Fourier Transform Spectrometers (FTIR) with an accuracy and reproducibility that is sufficient for the use in atmospheric remote sensing (Revercomb et al., 1988). Even though the GIFTS is a "cold" instrument, the same physical principles developed for the UW-SSEC instruments will be applied to the calibration of the GIFTS radiances in order to take into account gain and offset changes in the instrument during normal operation. The GIFTS spectral coverage indicated in Fig. 1 illustrates that the dynamic range of signals from terrestrial thermal infrared radiation spans hundreds of degreees. However, the demands of remote sensing of atmospheric effects are high since the signal of subtle changes in temperature and atmospheric humidity from the mean atmospheric state are only tenths of degrees (Smith, 2000). Achieving absolute calibration at the tenth of degree accuracy level is a goal that is within the reach of high spectral resolution IR remote sensing using precision on-board blackbody references with NIST traceability. This approach has been demonstrated at the UW-SSEC in both the groundbased Atmospheric Emitted Radiance Interferometer (AERI) program and the aircraft-based High-resolution Interferometer Sounder (HIS) program (Knuteson et al., 2004c,d; Revercomb et al., 1988).

In both the AERI and HIS programs, FTIR spectrometers have been used in order to take advantage of the very high spectral frequency knowledge that is inherent in the FTS design. At the relatively high spectral resolutions (resolving power > 1000) in the thermal infrared, the wavenumber sampling and instrument line shapes must be known to better than 1% accuracy or errors will be introduced in the comparison with forward model calculations that exceed the radiometric requirement. With an FTIR sensor, a single parameter determines the wavenumber sampling of each spectral band and all the spectral elements see the same field of view on the Earth. The FTS spectral parameter can be determined pre-launch but also in-flight by comparison to known spectral absorption lines across the spectral band of interest (Tobin et al., 2003). The excellent spectral knowledge and stability of the FTIR system was the primary motivation for the selection of FTS for the GIFTS sensor.

The ability to accurately calibrate high spectral resolution infrared observations is also important for the future of detecting global change from space-borne observations (Goody & Haskins, 1998). The technology exists with precision blackbodies and FTS laser spectral sampling to approach the tenth of degree accuracy and stability desired for the detection of global climate change on decadal scales. Although this is outside the scope of the GIFTS sensor requirements, the GIFTS design shows the feasibility of high absolute accuracy in a practical implementation for sensors in geostationary orbit. The design makes use of two high precision cavity radiometers

with high absolute emissivity (>0.998) and good long term stability (diffuse paints). The cavity blackbodies used for GIFTS are built and calibrated at the UW-SSEC based upon heritage with the AERI and HIS programs. The unique approach for GIFTS is to place these reference cavities aft of the Earth viewing telescope with an "on-demand" flip in mirror to direct the IR emission from the blackbodies into the sensor. The main advantage of this approach is that the IR beam is much smaller after the telescope so that a true high emissivity cavity design can be used for the blackbodies while keeping the volume, weight, and power requirements to a minimum. The successful design of these blackbodies for the GIFTS sensor is described in Best, et al., 2004. The high absolute accuracy of the onboard reference blackbodies compensates for the additional uncertainty from degradation of the telescope optics over time. A scheme for monitoring this telescope degradation over time that makes use of the internal reference views and views to deep space has been devised for the GIFTS sensor by the Space Dynamics Laboratory (Elwell et al., 2003).

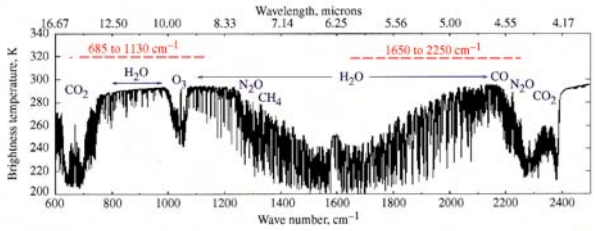

Figure 1. A calculation of the top of atmosphere radiance emitted by the standard atmosphere in units of equivalent brightness temperature (Kelvin). The dashed lines indicate the two spectral bands selected for the NASA GIFTS sensor. The longwave (LW) band covers the traditional "temperature sounding" region for the characterization of atmospheric temperature from the top of the atmosphere to the surface and includes the 8-12 mm IR window for the characterization of land surface and cloud top temperature and emissivity. The shortwave/midwave (SWM) band includes a non-traditional coverage of the shortwave side of the "6.3 mm water vapor sounding" region. The short-midwave band coverage (1650-2250 cm-1) was shown by analysis to be optimal for three reasons; 1) this region avoids the interference of "fixed" gases N2O and CH4 which degrade the water vapor sounding performance, 2) the shorter wavelength (fewer thermal photons) leads to better signal to noise performance for the detectors chosen, 3) provides coverage of carbon monoxide thereby allowing the tracking of air pollution plumes from source to sink.

Instrumentation

The GIFTS radiometric calibration is designed to use two small reference blackbodies located behind the telescope, combined with a space view (Best et al., 2000; Bingham et al., 2000). This is also the location of an image of the aperture stop for each detector in the focal plane arrays. Figure 2 illustrates the "flip mirror" mechanism with a linear slide to position either the warm or cold blackbody into the instrument beam. The blackbody design is scaled from the UW ground-based design used on AERI and S-HIS aircraft instruments. Constraints on the original spacecraft envelope prevented a traditional external large aperture blackbody implementation. The advantages of using two internal blackbodies compared to one large external blackbody include; (1) higher emissivity is practical with small size, (2) effective temperature of the body easier to characterize, and (3) protection from solar forcing gradients. A photo of the GIFTS engineering model blackbody cavity built by UW-SSEC is shown in Figure 2 (Best et al., 2004).

A Monte Carlo ray trace analysis has been performed that makes use of the internal cavity paint reflectivity and the detailed cavity geometry to estimate the cavity normal isothermal emissivity. A spectrum of the cavity emissivity is shown in Figure 3.

The GIFTS calibration requirement has been traced to requirements on the subsystem components, in particular to the blackbody subsystem. The blackbody calibration contribution budget allocation is < 0.5K and the engineering best estimates are <0.35K (LW) and <0.20K (SMW). The uncertainty estimates of the UW-SSEC blackbodies are described in much greater detail in Best et al., 2004.

Figure 2. The top panel illustrates two blackbodies and a visible flood source mounted on the same linear slide. One source at a time is correctly positioned under the flip-in mirror. The bottom panel is a photo of the UW-SSEC engineering model of the GIFTS blackbody. The blackbody aperture is 1.00 inches in diameter, the width of the cylindrical body is 1.76 inches in diameter, and the total cavity depth is 3.06 inches. GIFTS sensor module electro-optical design provides for two internal reference cavities aft of the Earth viewing telescope and a fold mirror which directs energy from the blackbodies into the instrument upon command. Since the beam diameter at this location is small, the internal blackbodies can have high emissivity while remaining relatively compact and lightweight. The blackbodies were designed, built, and calibrated at the UW-SSEC using standards traceable to NIST.

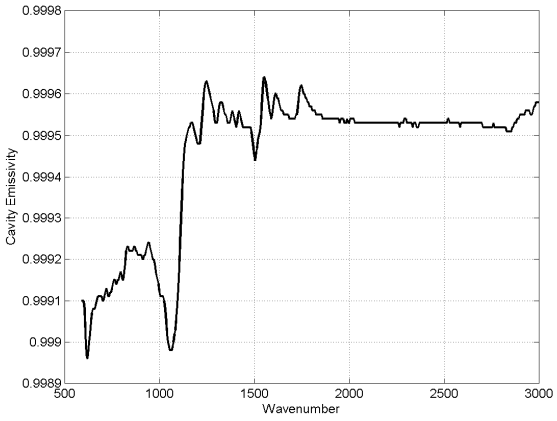

Figure 3. Isothermal normal cavity emissivity estimate for the UW-SSEC blackbodies used as the GIFTS internal calibration references. This estimate is based upon a Monte Carlo ray trace using the cavity geometry and the measured and modeled reflectance properties of the paint used to coat the inner surfaces of the cavity. This estimate includes a wavelength cavity factor due to the spectral variation of specular and diffuse reflection across the wavenumber range of interest.

Theory

Radiometric calibration of the GIFTS spectrometer has the same considerations as that of any radiometer. Key factors include the accuracy of onboard references, thermal stability over calibration cycles, and linearity after correction. The GIFTS's cold spectrometer design places a tight constraint on blackbody emissivity uncertainty since the energy reflected from a cold instrument is very small compared to an instrument that is close to the blackbody temperature. This, coupled with volume and mass constraints for GIFTS led to using small high-emissivity internal blackbody references, plus a space view. The broad spectral coverage from a single detector (inherent to FTS) prevents detector-to-detector FOV variations from altering spectral radiance shapes (greatly simplifying FOV co-alignment and testing requirements). The calibration method is summarized in Eq. 1. This is a modified version of the Revercomb et al., 1988 equation to include the ratio of the transmission of the flip in mirror (labeled "m") to the fore optics telescope (labeled "t") (Knuteson et al., 2004b).

(1)

$$N = \left(\frac{\tau_m}{\tau_t}\right)\left(B_H - B_C\right) Re\left(\frac{C_E - C_S}{C_H - C_C}\right) + B_S$$

The radiance N is derived from raw spectra of Earth (C_E), Space (C_S), and the internal Hot (C_H) and Cold (C_C) blackbodies where $B_{H,C,S}$ is the predicted Planck radiance from the Hot, Cold, and Space references including the effective emissivity of the blackbody cavity and the energy reflected off the blackbody from the environment, assumed here to be at 265 K.

Uncertainty in the knowledge of the reference source temperature and emissivity will lead to uncertainty in the calibrated radiances. The space view is assumed to be known exactly so no

error is introduced. However, measured characteristics of the UW-SSEC blackbody can be used to estimate a 3-sigma (not-to-exceed) error bound. These parameter uncertainties are summarized in Table 1. The uncertainty estimates in the calibrated radiance are obtained through a perturbation analysis of Eq. 1 where the uncertainties of the blackbody emissivity and temperature are taken into account.

On-orbit Calibration Parameter	Nominal value	Assumed Uncertainty
Hot BB Temperature	300 K	0.1 K
Cold BB Temperature	265 K	0.1 K
Hot BB Emissivity	(see Fig. 3)	0.001
Cold BB Emissivity	(see Fig. 3)	0.001
Space View Temperature	2.76 K	0.0
Space View Emissivity	1.0	0.0

Table 1. On-orbit calibration parameter uncertainties assumed in this analysis. (3-sigma)

Results

Simulated GIFTS interferograms were used as input to the modified Revercomb et al calibration equation given in Eq. 1. Details of the GIFTS simulation model have been previously described in Huang, et al. (2000). The complex spectra resulting from the Fast Fourier Transform of the simulated interferograms is shown in Figure 4 as magnitude and phase spectra for each of the four scene views; Earth, hot blackbody, cold blackbody, and deep space. A linearly varying phase has been included in the simulation to force the FFT of the interferograms to have both a real and imaginary component. The responsivity, which is the inverse of the calibration slope, is shown in Figure 5 for each of the two simulated GIFTS spectral bands and illustrates the cutoff assumed for the simulated GIFTS optical pass bands. The GIFTS simulation is not intended to be completely realistic but merely serves as an example of the type of data that will be available from the instrument in flight. The simulation is suitable for illustrating the expected radiometric calibration accuracy of a typical Earth scene. Figure 6 shows the result of application of the calibration equation to the raw complex spectra; the real part of the equation is shown as a brightness temperature spectrum while the imaginary part (not shown) is zero to within the noise level.

A perturbation analysis has been performed using these simulated GIFTS observations to illustrate the uncertainty in the calibration error expected in this typical clear sky scene due to uncertainties in the knowledge of the internal calibration reference sources. Figure 7 shows the brightness temperature error as a function of wavenumber induced by varying the blackbody temperature and emissivity by the amounts shown in Table 1. The label, RSS, indicates the root sum square of the error contributions which represents a 3-sigma estimate of the expected absolute calibration uncertainty. Figure 8 shows the same perturbation analysis as a function of scene brightness temperature.

To illustrate the imaging capability of the GIFTS sensor, an Earth scene data cube (128x128 fields of view) was simulated and the same calibration error analysis was applied to each field of view. The result is shown in Figure 9 as images of the scene brightness temperature in the

longwave window and the estimated calibration error at the same wavelength. Note that the colder scenes have slightly smaller errors than the warmer scene pixels. This is further illustrated in the 3-D plot of Figure 10 where the error closely follows the cloud scene temperature.

Conclusions

The GIFTS error budget for the contribution of the internal calibration errors is 0.5 K (3-sigma) out of a total requirement of <1K for all radiometric calibration errors. The current engineering best estimate is < 0.35 K in the longwave and < 0.20 K in the short/midwave bands. The examples shown here are consistent with those previous estimates. Moreover, the analysis shown in this paper for a specific simulation dataset is consistent with the general perturbation analysis described in Knuteson, et al. (2004b)

Acknowledgements

This work was supported by NOAA federal grant NAO7EC0676.

References

Best, F. A., H. E. Revercomb, G. E. Bingham, R. O. Knuteson, D. C. Tobin, D. D. LaPorte, and W. L. Smith, 2000: Calibration of the Geostationary Imaging Fourier Transform Spectrometer (GIFTS), presented at SPIE's Second International Asia-Pacific Symposium on Remote Sensing of the Atmosphere, Environment, and Space, Sendai, Japan, 9–12 October 2000.

Best, F. A., H. E. Revercomb, R. O. Knuteson, D. C. Tobin, S. D. Ellington, M. W. Werner, D. P. Adler, R. K. Garcia, J. K. Taylor, N. N. Ciganovich, W. L. Smith, G. E. Bingham, J. D. Elwell, and D. K. Scott, 2004: The Geosynchronous Imaging Fourier Transform Spectrometer (GIFTS) On-board Blackbody Calibration System. In: Proceedings of the SPIE, Fourth International Asia-Pacific Environmental Remote Sensing Symposium, 8 November 2004, Honolulu, Hawaii.

Bingham, G. E., R. J. Huppi, H. E. Revercomb, W. L. Smith, F. W. Harrison, 2000: A Geostationary Imaging Fourier Transform Spectrometer (GIFTS) for hyperspectral atmospheric remote sensing, presented at SPIE's Second International Asia-Pacific Symposium on Remote Sensing of the Atmosphere, Environment, and Space, Sendai, Japan, 9–12 October 2000.

Dittberner, G. J., James J. Gurka, and Roger W. Heymann, 2003: NOAA's GOES satellite program—status and plans, 19th Conference on IIPS, 83rd Annual Meeting, 8–13 February 2003, Long Beach, CA. Published by the American Meteorological Society, Boston, Mass.

Elwell, J. D., D. K. Scott, H. E. Revercomb, F. A. Best, R. O. Knuteson, 2003 : An overview of Ground and On-orbit Characterization and Calibration of the Geosynchronous Imaging Fourier Transform Spectrometer (GIFTS) in Proceedings of CALCON 2003, Characterization and Radiometric Calibration for Remote Sensing, Space Dynamics Laboratory / Utah State University, Logan, Utah, 15-18 September 2003.

Garcia, Raymond K., Ackerman, Steven A., Antonelli, Paolo, Dedecker, Ralph G., Dutcher, Steven, Howell, H. Ben, Huang, Hung-Lung, Knuteson, Robert O., Olson, Erik R., Revercomb, Henry E., Smuga-Otto, Maciej J., and Tobin, David, 2005: A prototype for the GIFTS information processing system. International Conference on Interactive Information and Processing Systems (IIPS) for Meteorology, Oceanography, and Hydrology, 21st, San Diego, CA, 8-13 January 2005 (preprints). American Meteorological Society, Boston, MA, 2005.

Goody, R. and R. Haskins, 1998: Calibration of Radiances from Space, J Climate, 11, 754-758, 1998.

Huang, Jung-Lung; Revercomb, H. E.; Thom, J.; Antonelli, P. B.; Osborne, B.; Tobin, D.; Knuteson, R.; Garcia, R.; Cutcher, S.; Li, J., and Smith, W. L., 2000: Geostationary Imaging FTS (GIFTS) data processing: Measurement simulation and compression. Hyperspectral Remote Sensing of the Land and Atmosphere, Sendai, Japan, 9-12 October 2000. Bellingham, WA, International Society for Optical Engineering, (SPIE), 2001, pp103-114.

Knuteson, Robert, Ackerman, Steve, Best, Fred, Dedecker, Ralph, Garcia, Ray, Olson, Erik, Revercomb, Hank, Smuga-Otto, Maciek, and Tobin, D., 2005: Calibration algorithm accuracy versus efficiency tradeoffs for a geosynchronous imaging Fourier transform spectrometer. International Conference on Interactive Information and Processing Systems (IIPS) for Meteorology, Oceanography, and Hydrology, 21st, San Diego, CA, 8-13 January 2005 (preprints). American Meteorological Society, Boston, MA, 2005.

Knuteson, R., Best, F., Dedecker, R., Garcia, R., Limaye, S., Olson, E., Revercomb, H., and Tobin D., 2004a: LEVEL 0-1 Algorithm Description For The Geosynchronous Imaging Fourier Transform Spectrometer, AMS annual meeting, Seattle, WA, 12-16 January 2004, American Meteorological Society.

Knuteson, R. O., F. A. Best, G. E. Bingham, J. D. Elwell, H. E. Revercomb, D. K. Scott, J. K. Taylor, D. C. Tobin, W. L. Smith, 2004b: On-orbit calibration of the Geosynchronous Imaging Fourier Transform Spectrometer (GIFTS). In: Proceedings of the SPIE, Fourth International Asia-Pacific Environmental Remote Sensing Symposium, 8 November 2004, Honolulu, Hawaii.

Knuteson R. O., H. E. Revercomb, F. A. Best, N. C. Ciganovich, R. G. Dedecker, T. P. Dirkx, S. C. Ellington, W. F. Feltz, R. K. Garcia, H. B. Howell, W. L. Smith, J. F. Short, D. C. Tobin: Atmospheric Emitted Radiance Interferometer (AERI) Part I: Instrument Design, Journal of Atmospheric and Oceanic Technology, Volume 21 (2004), Issue 12, 1763-1776.

Knuteson R. O., H. E. Revercomb, F. A. Best, N. C. Ciganovich, R. G. Dedecker, T. P. Dirkx, S. C. Ellington, W. F. Feltz, R. K. Garcia, H. B. Howell, W. L. Smith, J. F. Short, D. C. Tobin: Atmospheric Emitted Radiance Interferometer (AERI) Part II: Instrument Performance, Journal of Atmospheric and Oceanic Technology, Volume 21 (2004), Issue 12, 1777-1789.

Revercomb, H. E., H. Buijs, H. B. Howell, D.D. LaPorte, W. L. Smith, and L. A. Sromovsky, 1988: Radiometric calibration of IR Fourier Transform Spectrometers: solution to a problem with the High Resolution Interferometer Sounder", Appl. Opt., 27, 3210–3218.

Smith, W. L., D. K. Zhou, F. W. Harrison, H. E. Revercomb, A. M. Larar, A. H. Huang, B. Huang, 2000: Hyperspectral remote sensing of atmospheric profiles from satellites and aircraft, presented at SPIE's Second International Asia-Pacific Symposium on Remote Sensing of the Atmosphere, Environment, and Space, Sendai, Japan, 9–12 October 2000.

Tobin, D. C., H. E. Revercomb, R. O. Knuteson, 2003: On-orbit Spectral Calibration of the Geosynchronous Imaging Fourier Transform Spectrometer (GIFTS), in Proceedings of CALCON 2003, Characterization and Radiometric Calibration for Remote Sensing, Space Dynamics Laboratory / Utah State University, Logan, Utah, 15-18 September 2003.

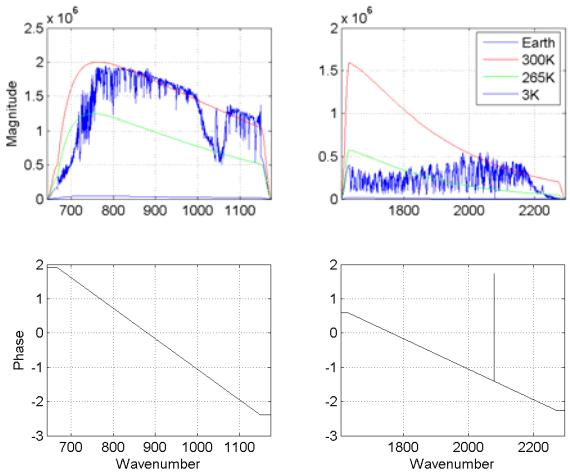

Figure 4. Simulated GIFTS interferograms have been Fourier transformed to show the magnitude and phase of the uncalibrated complex spectra used in this noise analysis.

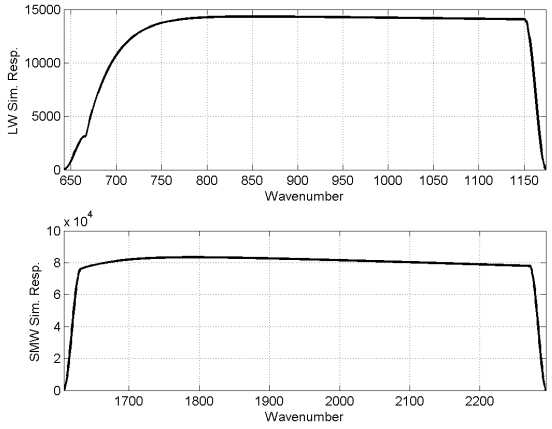

Figure 5. Simulated GIFTS responsivity magnitudes computed from the ratio of the difference of simulated internal blackbody views to the difference of planck radiances at 300 K and 265 K. These simulated responsivities are not intended to mimic the real GIFTS instrument except in defining the approximate spectral cutoffs for the longwave and short/midwave bands.

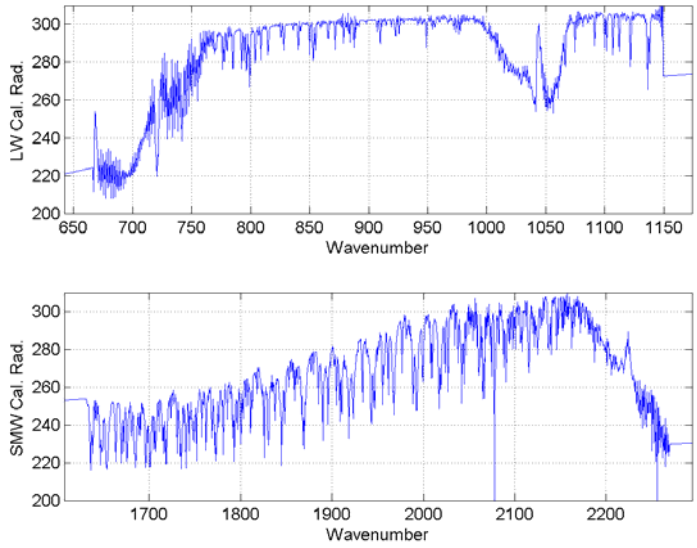

Figure 6. Calibrated GIFTS radiance obtained after applying Eq. 1 to simulated GIFTS interferograms for a warm scene (Central Oklahoma, IHOP case) and simulated views of internal (Hot and Cold) and external (Space) views. Telescope transmission is assumed known in this simulation.

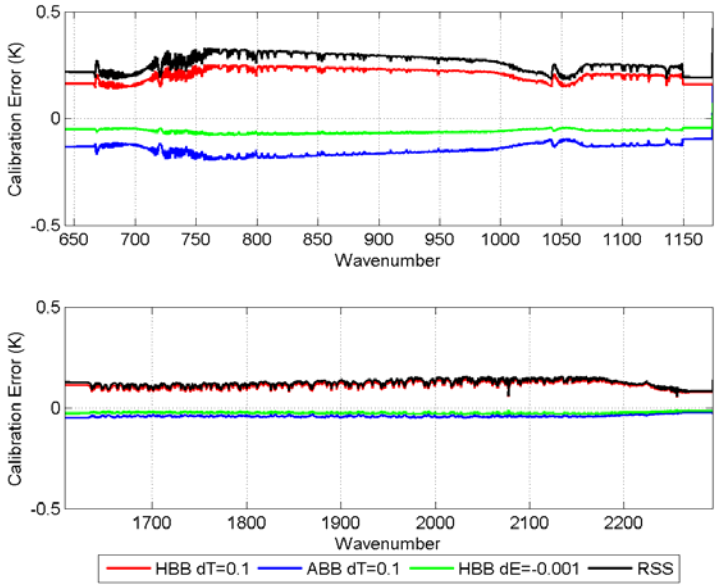

Figure 7. The internal blackbody calibration error of LW and SWM GIFTS bands are shown as an error spectrum for the calibrated scene shown in Fig. 6 and using the uncertainties shown in the figure legend. The GIFTS error budget for the contribution of the internal calibration errors is 0.5 K (3-sigma).

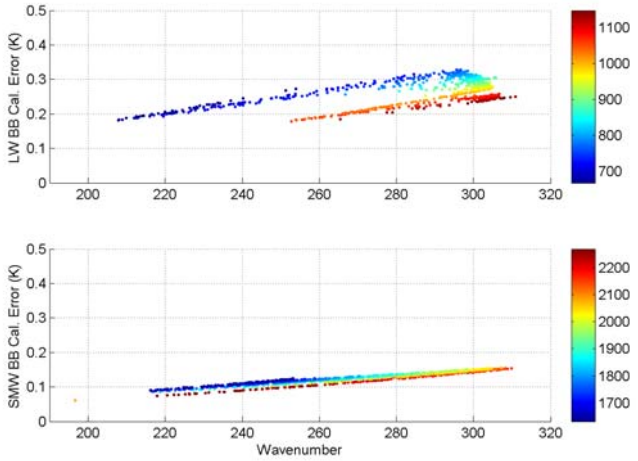

Figure 8. The internal blackbody calibration error of LW and SWM GIFTS bands are shown as scatterplot for the calibrated scene shown in Fig. 6 and using the uncertainties given in Table 1. The points are color coded based upon the wavenumber scale as indicated in the colorbar to the right of each panel. The GIFTS error budget for the contribution of the internal calibration errors is 0.5 K (3-sigma) out of a total requirement of <1K for all radiometric calibration errors. The current engineering best estimate is < 0.35 K in the longwave and < 0.20 K in the short/midwave bands. This example is consistent with those estimates.

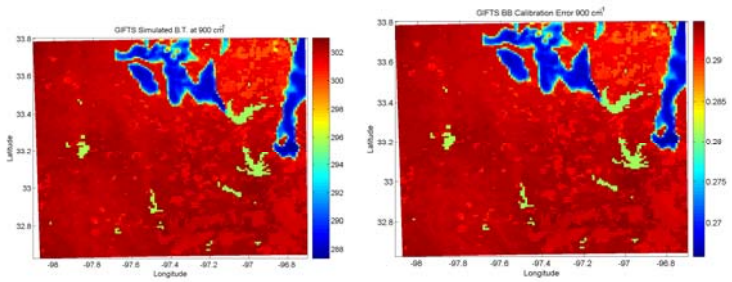

Figure 9. A brightness temperature image of a simulated GIFTS Earth scene (left panel) is shown for the center of the longwave band (900 cm-1). The internal blackbody calibration error at 900 cm-1 is shown in the right hand panel as an image using the uncertainties given in Table 1. The variation in window scene temperature is caused by presence of clouds in the simulation. All units are in Kelvin.

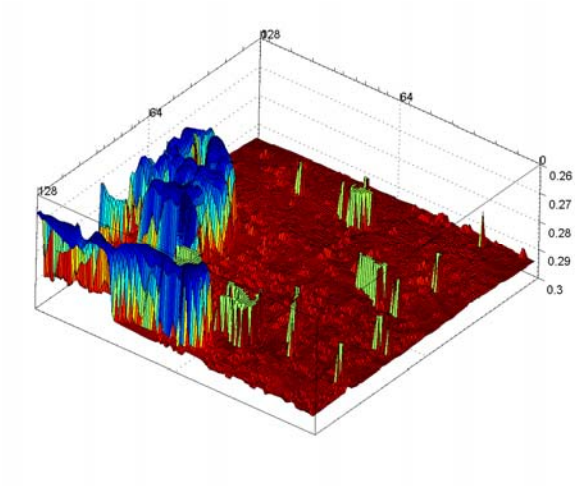

Figure 10. Same blackbody calibration error data as the right hand panel of Fig. 9, but shown here as a three-dimensional surface plot. The internal blackbody calibration error at 900 cm-1 varies across the scene due to the presence of clouds in the simulation. The "peaks" in the surface represent a decrease in the error in the absolute calibration of the GIFTS radiances for the colder cloudy scenes. All units are in Kelvin.

Appendix 5: Calibration Algorithm Accuracy Versus Efficiency Tradeoffs for GIFTS

Ground calibration algorithms for a geosynchronous imaging FTS are being developed at the Uni. of Wisconsin-Madison Space Science and Engineering Center. This development is being conducted in support of NOAA's GOES-R Risk Reduction program with a focus on the hyperspectral sounder that is anticipated to be a part of the GOES-R Hyperspectral Environmental Suite (HES). The near term objective is to develop calibration algorithms that can be evaluated using thermal vacuum test data from NASA's Geosynchronous Imaging Fourier Transform Spectrometer (GIFTS). The GIFTS is designed to produce 128x128 interferograms in two spectral bands every 11 seconds using a Michelson interferometer and two detector focal plane arrays. Data rates pose a special challenge to the design of the GIFTS ground data processing system which will need to convert the interferograms into radiometrically and spectrally calibrated radiances. This paper will address tradeoffs in accuracy versus processing efficiency for the science algorithms that are under consideration for achieving the desired ground data processing throughput for the GIFTS sensor.

The U.S. National Oceanic and Atmospheric Administration (NOAA) operates geostationary operational environmental satellites (GOES) for short-range warning and nowcasting, and polar-orbiting environmental satellites (POES) for longer term forecasting. GOES satellites provide continuous monitoring from space in a geosynchronous orbit about 35,800 km (22,300 miles) above the Earth. The current generation of GOES satellites contain separate imager and sounder instruments. The sounder is used to remotely sense the atmospheric thermodynamic state, e.g. atmospheric stability and total column water vapor. A new generation of sensors are under development that will greatly increase the horizontal, vertical, and temporal sampling of the GOES sounder and provide a truly four-dimensional view of the Earth's atmosphere. NOAA's plan for a Hyperspectral Environmental Suite (HES) calls for the replacement of the current GOES instrumentation starting as early as 2013 (Dittberner et al. 2003; Gurka et al. 2003). Meanwhile, NASA's New Millennium Program Earth Observing 3 (NMP EO3) mission is the first step in improving the U.S. geostationary weather observing system. The NMP EO3 mission features the Geosynchronous Imaging Fourier Transform Spectrometer (GIFTS), an instrument that incorporates new technologies to implement an innovative atmospheric measuring concept proposed by NASA's Langley Research Center (Smith et al. 2000).

The NASA GIFTS research instrument will serve as a valuable test bed for the evaluation of approaches to flight hardware and ground data processing in the years preceding the implementation of NOAA's operational Hyperspectral Environmental Suite.

An overview of the algorithm theoretical basis document (ATBD) that is being written by the University of Wisconsin Cooperative Institute for Meteorological Satellite Studies (UW-CIMSS) describing the science algorithms required in the ground processing of GIFTS data was presented in Knuteson et al. (2004a). The scope of that document was limited to the algorithms needed for the conversion of raw instrument counts (Level 0 data) to calibrated radiances (Level 1 data). The geo-location approach was described in Limaye et al. (2004) while the science algorithms for higher level products (2+) were described in Huang et al. (2004). This paper will provide more

detail on the algorithms being developed for the GIFTS ground data processing with an emphasis on tradeoffs between algorithm accuracy and computational efficiency.

Instrument Description

The GIFTS instrument is an imaging Fourier Transform Spectrometer (FTS) designed to provide significant advances in water vapor, wind, temperature, and trace gas profiling from geostationary orbit. Imaging FTS offers an instrument approach that can satisfy the demanding radiometric and spectral accuracy requirements for remote sensing and climate applications, while providing the massively parallel spatial sampling needed for rapid coverage of the Earth disk, as well as more frequent coverage of selected regions. The GIFTS baseline design uses focal plane detector arrays to cover two broad spectral regions; a longwave infrared band (685–1129 cm^{-1}) and a midwave/shortwave band (1650–2250 cm^{-1}). Each focal plane array contains a grid of 128 × 128 elements for a total of 16,384 fields of view with a nominal field of view diameter of 4 km at the sub-satellite point. Details of the initial instrument design are described elsewhere (Bingham et al., 2000; Best et al., 2000, 2004; Knuteson et al., 2004b). Figure 1 shows the spectral coverage of the GIFTS sensor. The longwave (LW) band covers the traditional "temperature sounding" region for the characterization of atmospheric temperature from the top of the atmosphere to the surface and includes the 8-12 μm IR window for the characterization of land surface and cloud top temperature and emissivity. The shortwave/midwave (SMW) band includes a non-traditional coverage of the shortwave side of the "6.3 μm water vapor sounding" region. The short-midwave band coverage (1650-2250 cm^{-1}) was shown by analysis to be optimal for three reasons; 1) this region avoids the interference of "fixed" gases N_2O and CH_4 which degrade the water vapor sounding performance, 2) the shorter wavelength leads to better signal to noise performance for the detectors chosen, 3) and it provides coverage of carbon monoxide thereby allowing the tracking of air pollution plumes from source to sink.

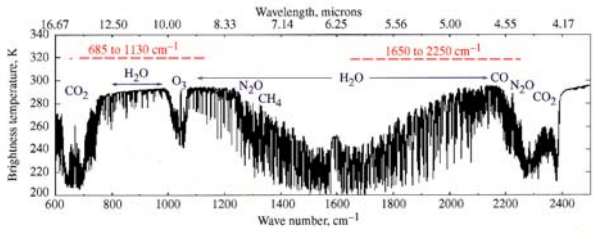

Figure 1. A calculation of the top of atmosphere radiance emitted by the standard atmosphere in units of equivalent brightness temperature (Kelvin). The dashed lines indicate the two spectral bands selected for the NASA GIFTS sensor.

Algorithm Overview

The GIFTS sensor will sample the interferogram from each detector as a function of optical path delay and numerically filter the data in real-time to reduce the data rate before transmission to the ground-based X-band receiver. The sensor will obtain views of the onboard calibration references and deep space at regular intervals interleaved with the observations of Earth scenes. The ground reception facility will decode the telemetry stream and pass the GIFTS sensor data in real-time to a ground data processing facility. The GIFTS Level 0 to 1 ground data processing is anticipated

to include the following tasks: i) Fourier transform of the GIFTS interferograms, ii) application of a non-linearity correction to the sensor data, iii) radiometric calibration, iv) spectral calibration, v) instrument line shape correction, and vi) spectral resampling to a common wavenumber grid. This paper will focus on two algorithms under consideration for the implementation of the spectral resampling. Tradeoffs between algorithm accuracy and computational performance will be described.

Wavenumber Resampling Methods

Once the spectral calibration (i.e. wavenumber sampling scale) is determined for each of the GIFTS fields of view, the calibrated radiance spectrum can be re-sampled from the original sampling interval to a pre-specified reference wavenumber scale (Tobin et al., 2003). The re-sampling can be performed in software using a double FFT and linear interpolation of an over-sampled spectrum. An alternative approach using a convolution rather than an FFT to resample the spectra is being evaluated for potential performance advantages. The result of the wavenumber resampling operation will be that all of the GIFTS spectra have a common wavenumber scale independent of their location in the focal plane array. This is essential for the routine comparison of observations and radiative transfer calculations needed in the production of Level 2 products, e.g. temperature and humidity profiles.

The double FFT method requires the fast fourier transform of the original spectrum (with a power of two number of points, N=2(n-1)) to the interferogram domain where additional zeros are added to the end of the interferogram ("zero padding"). For the GIFTS focal plane arrays used in this analysis, the number of points in the spectrum are taken to be n = 1025 (LW), and 2049 (SMW). Zeros are added to produce a symmetric interferogram containing M*N points where M*N is a power of two. Transforming this expanded interferogram back to the spectral domain provides an oversampled spectrum that can be used to interpolate to the desired spectral sampling. Equation 1 illustrates this method where the original radiance spectrum S is interpolated to the final resampled spectrum S'. In Eqn. 1, FFT and IFFT are the Fast Fourier Transform and its inverse, and L() is the linear interpolation operator from the oversampled wavenumber scale v'' to the desired final spectral scale v'. The double FFT method (with linear interpolation) is of order M'*N log (M'*N) + M*N floating point operations (FLOPs) where M' = M+1 to account for the original forward FFT. The FLOP estimate is valid only when a power of two is used in the inverse FFT. Powers of two are the most efficient use of FFTs, although prime factor algorithms are also an option.

(1)

$$
\begin{aligned}
I &= FFT(S, N) \\
I'(i) &= I(i), i = 1, n; \\
I'(j) &= 0,\ j = n+1, M*(n-1) \\
S'' &= IFFT(I', M*N) \\
S' &= L(S'', v'', v')
\end{aligned}
$$

The sinc resampling (or F-matrix) method can also be used to transform the original spectrum S to the desired resampled spectrum S' defined in Eqn. 2 as the matrix multiplication (from CrIS ATBD; BOM-CrIS-0067)

(2)

$$S' = F \cdot S,$$

where

$$F = \frac{dv}{dv'} \cdot \frac{\sin c((v - v')/dv')}{\sin c((v - v')/(Ndv'))}$$

In Eqn. 2, F is an nxn matrix, S and S' are 1xn column vectors, the sinc function is defined to be sin(x)/x, and N = 2(n-1). The generation of the F-matrix is computationally expensive, but it can be pre-computed and stored for later use as long as the GIFTS spectral calibration is stable over time. The application of the sinc resampling method is a simple matrix multiplication and has order n^2 floating point operations for a full rank matrix.

The GIFTS focal plane arrays contain 128x128 (16384) pixel elements each of which represents a complete GIFTS spectrum (one spectrum per spectral band). Due to the fact that the laser trigger is aligned with the interferometer optical axis, the spectral calibration of the GIFTS sensor varies as a function of off-axis pixel angle from near the center of the focal plane arrays. Correcting for this effect using the double FFT plus linear interpolation method requires only that the initial wavenumber sampling scale be known for each pixel element. Once this original scale is known the actual computational time required to perform the FFT method is independent of which pixel is being corrected. There is no preferred order of processing the pixel elements. In contrast, the F-matrix approach suggests that concentric "rings" of detector elements should be grouped together in the data processing to take advantage of pre-computed F-matrices. This is because the full F-Matrix is too expensive to generate for each of the individual 16384 pixel elements in each spectral band. Since the F-matrix approach will require a more sophisticated data management approach for efficient implementation, it is important to quantify the computational advantages (if any) of this approach over the double FFT method.

Conclusions

The UW-SSEC has performed timing tests using prototype implementations of two competing algorithms for the task of resampling the GIFTS spectra in each band to a common wavenumber scale. The conclusions of this analysis are given below:

(1) The computational performance of the FFT resampling method using a 16K FFT is roughly comparable to the full F-matrix sinc resampler for the GIFTS LW band. However, in the GIFTS SMW band the FFT 32K FFT is about 3 times faster than the full F-matrix method with similar accuracy.

(2) When the complications of the data management of the large F-matrices is taken in to account and the need to precompute the F-matrices, it would be hard to justify the use of sinc resampling using the full F-matrix approach for the GIFTS task.

(3) However, there is still the possibility that the F-matrix can be reduced in one dimension by zeroing out off-diagonal matrix elements while still meeting the accuracy requirements. Investigation of this "near diagonal" F-matrix approach is under evaluation.

Acknowledgements

This work was supported by NOAA federal grant NAO7EC0676.

References

Best, F. A., H. E. Revercomb, G. E. Bingham, R. O. Knuteson, D. C. Tobin, D. D. LaPorte, and W. L. Smith, 2000: Calibration of the Geostationary Imaging Fourier Transform Spectrometer (GIFTS), presented at SPIE's Second International Asia-Pacific Symposium on Remote Sensing of the Atmosphere, Environment, and Space, Sendai, Japan, 9–12 October 2000.

Best, F. A., H. E. Revercomb, R. O. Knuteson, D. C. Tobin, S. D. Ellington, M. W. Werner, D. P. Adler, R. K. Garcia, J. K. Taylor, N. N. Ciganovich, W. L. Smith, G. E. Bingham, J. D. Elwell, and D. K. Scott, 2004: The Geosynchronous Imaging Fourier Transform Spectrometer (GIFTS) On-board Blackbody Calibration System. In: Proceedings of the SPIE, Fourth International Asia-Pacific Environmental Remote Sensing Symposium, 8 November 2004, Honolulu, Hawaii.

Bingham, G. E., R. J. Huppi, H. E. Revercomb, W. L. Smith, F. W. Harrison, 2000: A Geostationary Imaging Fourier Transform Spectrometer (GIFTS) for hyperspectral atmospheric remote sensing, presented at SPIE's Second International Asia-Pacific Symposium on Remote Sensing of the Atmosphere, Environment, and Space, Sendai, Japan, 9–12 October 2000.

Dittberner, G. J., James J. Gurka, and Roger W. Heymann, 2003: NOAA's GOES satellite program—status and plans, 19th Conference on IIPS, 83rd Annual Meeting, 8–13 February 2003, Long Beach, CA. Published by the American Meteorological Society, Boston, Mass.

Gurka, J. J., Gerald J. Dittberner, Pamela Taylor, and Timothy J. Schmit, 2003: Specifying the requirements for imaging and sounding capabilities on the GOES-R series, 12th Conference on Satellite Meteorology and Oceanography, 83rd Annual Meeting, 8-13 February 2003, Long Beach, CA. Published by the American Meteorological Society, Boston, Mass.

Huang, H-L., J. Li, E. Weisz, K. Baggett, J. E. Davies, J. R. Mecikalski, B. Huang, C. S. Velden, R. Dengel, S. A. Ackerman, E. R. Olson, R. O. Knuteson, D. Tobin, L. Moy, D. J. Posselt, H. E. Revercomb, and W. L. Smith, 2004: Infrared hyperspectral sounding modeling and processing, 20th Conference on IIPS, 84th AMS Annual Meeting, 11-15 January 2004, Seattle, WA. Published by the American Meteorological Society, Boston, Mass.

Knuteson, R., Best, F., Dedecker, R., Garcia, R., Limaye, S., Olson, E., Revercomb, H., and Tobin D., 2004a: LEVEL 0-1 Algorithm Description For The Geosynchronous Imaging Fourier Transform Spectrometer, AMS annual meeting, Seattle, WA, 12-16 January 2004, American Meteorological Society.

Knuteson, R. O., F. A. Best, G. E. Bingham, J. D. Elwell, H. E. Revercomb, D. K. Scott, J. K. Taylor, D. C. Tobin, W. L. Smith, 2004b: On-orbit calibration of the Geosynchronous Imaging

Fourier Transform Spectrometer (GIFTS). In: Proceedings of the SPIE, Fourth International Asia-Pacific Environmental Remote Sensing Symposium, 8 November 2004, Honolulu, Hawaii.

Limaye, S. S., T. Smith, R. O. Knuteson, H. E. Revercomb, 2004: Geolocation of the Geosynchronous Imaging Fourier Transform Spectrometer (GIFTS) data, 20th Conference on IIPS, 84th AMS Annual Meeting, 11-15 January 2004, Seattle, WA. Published by the American Meteorological Society, Boston, Mass.

Smith, W. L., D. K. Zhou, F. W. Harrison, H. E. Revercomb, A. M. Larar, A. H. Huang, B. Huang, 2000: Hyperspectral remote sensing of atmospheric profiles from satellites and aircraft, presented at SPIE's Second International Asia-Pacific Symposium on Remote Sensing of the Atmosphere, Environment, and Space, Sendai, Japan, 9–12 October 2000.

Tobin, D. C., H. E. Revercomb, R. O. Knuteson, 2003: On-orbit Spectral Calibration of the Geosynchronous Imaging Fourier Transform Spectrometer (GIFTS), in Proceedings of CALCON 2003, Characterization and Radiometric Calibration for Remote Sensing, Space Dynamics Laboratory / Utah State University, Logan, Utah, 15-18 September 2003.

References

Baum B. A., Harkey M. K., Frey R. A., Mace G. G., and Yang P., "Nighttime Multilayered could detection using MODIS and ARM data", *Journal of Applied. Meteorology.* 2003; 42: 905-919.

Best, F. A., H. E. Revercomb, R. O. Knuteson, D. C. Tobin, S. D. Ellington, M. W. Werner, D. P. Adler, R. K. Garcia, J. K. Taylor, N. N. Ciganovich, W. L. Smith, G. E. Bingham, J. D. Elwell, and D. K. Scott, "The Geosynchronous Imaging Fourier Transform Spectrometer (GIFTS) On-board Blackbody Calibration System", *Proceedings of the SPIE*, Fourth International Asia-Pacific Environmental Remote Sensing Symposium, 8 November 2004, Honolulu, Hawaii.

Best, F. A., H. E. Revercomb, G. E. Bingham, R. O. Knuteson, D. C. Tobin, D. D. LaPorte, and W. L. Smith, "Calibration of the Geostationary Imaging Fourier Transform Spectrometer (GIFTS)", presented at SPIE's Second International Asia-Pacific Symposium on Remote Sensing of the Atmosphere, Environment, and Space, Sendai, Japan, 9–12 October 2000.

Bingham, G. E., R. J. Huppi, H. E. Revercomb, W. L. Smith, F. W. Harrison, "A Geostationary Imaging Fourier Transform Spectrometer (GIFTS) for hyperspectral atmospheric remote sensing", presented at SPIE's Second International Asia-Pacific Symposium on Remote Sensing of the Atmosphere, Environment, and Space, Sendai, Japan, 9–12 October 2000.

Bingham, G. E., D. K. Zhou, B. Y. Bartschi, G. P. Anderson, D. R. Smith, J. H. Chetwynd, and R. M. Nadile, "Cryogenic Infrared Radiance Instrumentation for Shuttle (CIRRIS 1A) Earth limb spectral measurements, calibration, and atmospheric O3, HNO3, CFC-12, and CFC-11 profile retrieval", *J. Geophys. Res.*, 102, D3, 3547-3558, 1997.

Cousins, D., and W. L. Smith, "National Polar-Orbiting Operational Environmental Satellite System (NPOESS) Airborne Sounder Testbed-Interferometer (NAST-I)", *Proceedings of SPIE*, 3127, 323-331, 1997.

Dittberner, G. J., J. J. Gurka, and R. W. Heymann, "NOAA's GOES satellite program—status and plans, 19th Conference on IIPS", 83rd Annual Meeting, 8–13 February

2003, Long Beach, CA. Published by the American Meteorological Society, Boston, Mass.

Elwell, J. D., D. K. Scott, H. E. Revercomb, F. A. Best, R. O. Knuteson. "An overview of Ground and On-orbit Characterization and Calibration of the Geosynchronous Imaging Fourier Transform Spectrometer (GIFTS)", *Proceedings of CALCON 2003*, Characterization and Radiometric Calibration for Remote Sensing, Space Dynamics Laboratory / Utah State University, Logan, Utah, 15-18 September 2003.

Garcia, R. K., Ackerman, S. A., Antonelli, P., Dedecker, R. G., Dutcher, S., Howell, H.B., Huang, H.-L., Knuteson, R. O., Olson, E. R., Revercomb, H. E., Smuga-Otto, M. J., and Tobin, D. "A prototype for the GIFTS information processing system," International Conference on Interactive Information and Processing Systems (IIPS) for Meteorology, Oceanography, and Hydrology, 21st, San Diego, CA, 8-13 January 2005 (preprints). American Meteorological Society, Boston, MA, 2005.

Goody, R. and R. Haskins, 1998: Calibration of Radiances from Space, *Journal of Climate*, 11, 754-758, 1998.

Grasso, L. D., 2000: The Differentiation Between Grid Spacing and Resolution and Their Application to Numerical Modeling. *Bull. Amer. Meteor. Soc.*, 81, 579-580.

Hong, S.-Y., J. Dudhia, and S.-H. Chen, 2004: A revised approach to ice microphysical processes for the bulk parameterization of clouds and precipitation. *Mon. Wea. Rev.*, 132, 103-120.

Huang H.-L., Velden C., Li J., Weisz E., Baggett K., Davies J., Mecikalski J., Huang B., Dengel R., Ackerman S., Olson E., Knuteson R., Tobin D., Moy L., Otkin J., Revercomb H., and Smith W., "Infrared Hyperspectral Sounding Modeling and Processing – An Overview," in *20th International Conference on Interactive Information and Processing Systems (IIPS) for Meteorology, Oceanography, and Hydrology,* 2003.

Huang, H.-L., H. E. Revercomb, J. Thom, P. B. Antonelli, B. Osborne, D. Tobin, R. Knuteson, R. Garcia, S. Dutcher, J. Li, and W. L. Smith, "Geostationary Imaging FTS (GIFTS) Data Processing: Measurement Simulation and Compression, 2000. Proceedings of SPIE, William L. Smith and Yoshifumi Yasuoka, editors. Hyperspectral Remote Sensing of the Land and Atmosphere. 9-12 Oct. 2000, 103-114.

Huang, Jung-Lung; Revercomb, H. E.; Thom, J.; Antonelli, P. B.; Osborne, B.; Tobin, D.; Knuteson, R.; Garcia, R.; Cutcher, S.; Li, J., and Smith, W. L., 2000: Geostationary Imaging FTS (GIFTS) data processing: Measurement simulation and compression. Hyperspectral Remote Sensing of the Land and Atmosphere, Sendai, Japan, 9-12 October 2000. Bellingham, WA, International Society for Optical Engineering, (SPIE), 2001, pp103-114.

Knuteson, R., Ackerman, S., Best, F., Dedecker, R., Garcia, R., Olson, E., Revercomb, H., Smuga-Otto, M., and Tobin, D., 2005: Calibration algorithm accuracy versus efficiency tradeoffs for a geosynchronous imaging Fourier transform spectrometer. *International Conference on Interactive Information and Processing Systems (IIPS) for Meteorology, Oceanography, and Hydrology*, 21st, San Diego, CA, 8-13 January 2005 (preprints). American Meteorological Society, Boston, MA, 2005.

Knuteson, R. O., F. A. Best, G. E. Bingham, J. D. Elwell, H. E. Revercomb, D. K. Scott, J. K. Taylor, D. C. Tobin, W. L. Smith, 2004b: On-orbit calibration of the Geosynchronous Imaging Fourier Transform Spectrometer (GIFTS). In: *Proceedings of the SPIE, Fourth International Asia-Pacific Environmental Remote Sensing Symposium*, 8 November 2004, Honolulu, Hawaii.

Knuteson, R., Best, F., Dedecker, R., Garcia, R., Limaye, S., Olson, E., Revercomb, H., and Tobin D., 2004a: LEVEL 0-1 Algorithm Description For The Geosynchronous Imaging Fourier Transform Spectrometer, AMS annual meeting, Seattle, WA, January 2004, American Meteorological Society.

Knuteson R. O., H. E. Revercomb, F. A. Best, N. C. Ciganovich, R. G. Dedecker, T. P. Dirkx, S. C. Ellington, W. F. Feltz, R. K. Garcia, H. B. Howell, W. L. Smith, J. F. Short, D. C. Tobin: Atmospheric Emitted Radiance Interferometer (AERI) Part I: Instrument Design, Journal of Atmospheric and Oceanic Technology, Volume 21 (2004), Issue 12, 1763-1776.

Knuteson R. O., H. E. Revercomb, F. A. Best, N. C. Ciganovich, R. G. Dedecker, T. P. Dirkx, S. C. Ellington, W. F. Feltz, R. K. Garcia, H. B. Howell, W. L. Smith, J. F. Short, D. C. Tobin: Atmospheric Emitted Radiance Interferometer (AERI) Part II: Instrument Performance, Journal of Atmospheric and Oceanic Technology, Volume 21 (2004), Issue 12, 1777-1789.

Menzel, W. P., W. L. Smith, and L. D. Herman, "Visible Infrared Spin-Scan Radiometer Atmospheric Sounder Radiometric Calibration: An inflight evaluation from intercomparisons with HIRS and radiosonde measurements", Appl. Opt., 20, 3641-3644, 1981.

Moy, Leslie, Dave Tobin, Paul van Delst, Hal Woolf, "Clear Sky Forward Model Development for GIFTS", AMS Annual Meeting, Seattle, WA, January 2004.

Revercomb, H. E., L. A. Sromovsky, P. M. Fry, F. A. Best, D. D. LaPorte, Demonstration of imaging Fourier Transform Spectrometer (FTS) performance for planetary and geostationary Earth observing, SPIE's Second International Asia-Pacific Symposium on Remote Sensing of the Atmosphere, Environment, and Space, Sendai, Japan, 9-12 October 2000.

Revercomb, H. E., H. Buijs, H. B. Howell, D.D. LaPorte, W. L. Smith, and L. A. Sromovsky, 1988: Radiometric calibration of IR Fourier Transform Spectrometers: solution to a problem with the High Resolution Interferometer Sounder", Appl. Opt., 27, 3210–3218.

Smith, W. L., D. K. Zhou, F. W. Harrison, H. E. Revercomb, A. M. Larar, A. H. Huang, B. Huang, 2000: Hyperspectral remote sensing of atmospheric profiles from satellites and aircraft, presented at SPIE's Second International Asia-Pacific Symposium on Remote Sensing of the Atmosphere, Environment, and Space, Sendai, Japan, 9–12 October 2000.

Strow L. L., Motteler H. E., Benson R. G., Hannon S. E., and Souza Machado S., Fast computation of monochromatic infrared atmospheric transmittances using compressed look-up tables, *J. Quant. Spectrosc. Radiat. Transf.*, 1998; 59: 481-493.

Tobin, D. C., H. E. Revercomb, R. O. Knuteson, 2003: On-orbit Spectral Calibration of the Geosynchronous Imaging Fourier Transform Spectrometer (GIFTS), in Proceedings of CALCON 2003, Characterization and Radiometric Calibration for Remote Sensing, Space Dynamics Laboratory / Utah State University, Logan, Utah, 15-18 September 2003.

Wetzel Seeman, S., Borbas, E., Knuteson, R., Huang, H.-L., Menzel, W., 2006: A Global Infrared Land Surface Emissivity Database, AMS Annual Meeting, Atlanta, GA, January 2006.

Yang, P., H. Wei, H.-L. Huang, B. A. Baum, Y. X. Hu, G. W. Kattawar, M. I. Mishchenko, and Q. Fu, 2004: Scattering and absorption property database for nonspherical ice particles in the near-through far-infrared spectral region, *Appl. Opt.* (accepted).